An Autonomous Structural Health Monitoring System for Waiau Interchange

David T. Ma, Associate Professor
Department of Civil & Environmental Engineering
University of Hawaii at Mānoa

Prepared in cooperation with the:
State of Hawaii Department of Transportation Highways Division
and U.S. Department of Transportation Federal Highway Administration [1]

March 2013

[1]The contents of this report reflect the view of the author, who is responsible for the facts and accuracy of the data presented herein. The contents do not necessarily reflect the official views or policies of the State of Hawaii, Department of Transportation or the Federal Highway Administration. This report does not constitute a standard, specification or regulation.

Technical Report Documentation Page

1. Report No.	2. Government Accession No.	3. Recipient's Catalog No.
TA-2008-2R		

4. Title and Subtitle	5. Report Date
An Autonomous Structural Health Monitoring System for Waiau Interchange	March 2013
	6. Performing Organization Code

7. Author(s)	8. Performing Organization Report No.
David T. Ma	

9. Performing Organization Name and Address	10. Work Unit No. (TRAIS)
University of Hawaii, Manoa 2540 Dole St. Honolulu, Hi 96822	11. Contract or Grant No. 2008-2R

12. Sponsoring Agency Name and Address	13. Type of Report and Period Covered
Hawaii Department of Transportation Highways Division 869 Punchbowl St. Honolulu, HI 96813	Technical (2008-2012)
	14. Sponsoring Agency Code

15. Supplementary Notes

Prepared in cooperation with the U.S. Department of Transportation, Federal Highway Administration

16. Abstract

Bridge infrastructure is a critical element of the transportation system which makes maintaining its safety and performance vital to a healthy society. However, the civil infrastructure systems in the United States are decaying at an accelerated rate due to factors such as aging, drastically increased traffic loads, insufficient funds for maintenance and management, along with many others. The collapse of the I-35W bridge in Minneapolis, Minnesota in 2007 has manifested the drawbacks of the maintenance and management efforts currently implemented. In the State of Hawaii, bridges are currently managed by the Bridge Section of the Hawaii Department of Transportation using Pontis, an AASHTO bridge and highway management software package. The data required for this approach is obtained through periodic visual inspections, which have been shown to be unreliable and subjective. This project develops an automatic structural health monitoring system that collects and analyzes realtime data so that structural behavior is continuously assessed. The system includes sensing instruments, a data acquisition subsystem, a power supply unit, a data transmission unit and a remote server for data processing and storage. The system is deployed on a highway bridge in Honolulu, HI. The detailed design and installation of the system are included in this report. Typical monitoring results are also presented to demonstrate the effectiveness of the system.

17. Key Words	18. Distribution Statement
BRIDGE MONITORING, CRACKING, WIRELESS DATA MANAGEMENT	No restriction. This document is available to the public from the sponsoring agency at the website http://www.cflhd.gov.

19. Security Classif. (of this report)	20. Security Classif. (of this page)	21. No. of Pages	22. Price
Unclassified	Unclassified	95	

Form DOT F 1700.7 (8-72) **Reproduction of completed page authorized**

ABSTRACT

Bridge infrastructure is a critical element of the transportation system which makes maintaining its safety and performance vital to a healthy society. However, the civil infrastructure systems in the United States are decaying at an accelerated rate due to factors such as aging, drastically increased traffic loads, insufficient funds for maintenance and management, along with many others. The collapse of the I-35W bridge in Minneapolis, Minnesota in 2007 has manifested the drawbacks of the maintenance and management efforts currently implemented. In the State of Hawaii, bridges are currently managed by the Bridge Section of the Hawaii Department of Transportation using Pontis, an AASHTO bridge and highway management software package. The data required for this approach is obtained through periodic visual inspections, which have been shown to be unreliable and subjective. This project develops an automatic structural health monitoring system that collects and analyzes realtime data so that structural behavior is continuously assessed. The system includes sensing instruments, a data acquisition subsystem, a power supply unit, a data transmission unit and a remote server for data processing and storage. The system is deployed on a highway bridge in Honolulu, HI. The detailed design and installation of the system are included in this report. Typical monitoring results are also presented to demonstrate the effectiveness of the system.

Contents

1 INTRODUCTION **8**
- 1.1 Background and motivation . . . 8
- 1.2 Objectives . . . 10
- 1.3 Overview of chapters . . . 11

2 BRIDGE MONITORING **12**
- 2.1 Structural Health Monitoring . . . 12
- 2.2 State-of-the-art Technologies . . . 13

3 BRIDGE SELECTION **15**
- 3.1 Bridges considered . . . 15
- 3.2 Findings . . . 16
- 3.3 Waiau Interchange . . . 16
- 3.4 Instrumentation plan . . . 17

4 SYSTEM DESIGN **20**
- 4.1 System architecture . . . 20
- 4.2 Sensors and substation . . . 23
  - 4.2.1 LVDT system . . . 27
  - 4.2.2 Strain measurements . . . 32
  - 4.2.3 Temperature measurements . . . 39

5 INSTALLATION **44**
- 5.1 Power and traffic control . . . 44
  - 5.1.1 Introduction . . . 44
  - 5.1.2 Power for BMS equipment . . . 44
  - 5.1.3 Traffic control for installation . . . 48
- 5.2 BMS installation . . . 48
  - 5.2.1 Wire/conduit . . . 48

5.2.2 Sensor system and substation 53
5.2.3 Wireless modem configuration 54

6 RESULTS **62**

7 CONCLUSIONS **66**

List of Figures

3.1 Geographical location of Waiau Interchange 18
3.2 Cracks observed on the bridge 19

4.1 Crack location 21
4.2 System architecture 22
4.3 Sensor layout 23
4.4 Substation layout 24
4.5 Substation configuration 25
4.6 LVDT sensor set 28
4.7 Connection details of LVDT sensors, conditioners and substation . . . 30
4.8 LVDT subsystem layout 31
4.9 Strain gauge (HBP-35-250-06-3VR) 32
4.10 A 1-RV91-6/120 strain gauge rosette 33
4.11 Orientation of the rectangular strain gage rosette 34
4.12 Strain gauge rosettes connection 35
4.13 Strain gauge rosette subsystem layout 36
4.14 Axial strain gauges connection 37
4.15 Axial strain gauge layout 38
4.16 Thermistor HBWTG-5V-AD22100-XTR 40
4.17 Wire connection and color coding of temperature sensors subsystem . 41
4.18 NTC thermistors R-T conversion tables 42
4.19 Temperature sensor subsystem layout 43

5.1 Electrical power supply site plan 45
5.2 Electrical panel equipment 46
5.3 Traffic Control: Phase 1 49
5.4 Traffic Control: Phase 2a 49
5.5 Traffic Control: Phase 2b 50
5.6 Traffic Control: Phase 3a 50

5.7 Traffic Control: Phase 3b 51
5.8 Traffic Control: Phase 4 51
5.9 Traffic Control: Phase 5 52
5.10 Traffic Control: Phase 6 52
5.11 Wire conduit layout (Overview) 53
5.12 Wire conduit layout (1) 54
5.13 Wire conduit layout (2) 55
5.14 Wire conduit layout (3) 56
5.15 Wire conduit layout (4) 56
5.16 Conduit connection 57
5.17 Conduit installation 58
5.18 LVDT zero setting circuit 59
5.19 LVDT installation 59
5.20 LVDT and strain rosette 60
5.21 Axial strain gauge installation 60
5.22 Temperature sensor installation 61

6.1 Original record of displacements from LVDT3 5 and LDVT8 10 . . . 63
6.2 Original record of strain gauge rosettes Sgr2, Sgr3 and Sgr4 63
6.3 Original record of temperatures Temp1, Temp2, Temp3 and Temp4 . 64
6.4 Principal strains converted from strain gauge rosettes Sgr2, Sgr3 and Sgr4 65

7.1 Calibration record for LVDT channels LT-01 $\tilde{\text{L}}$T-04 74
7.2 Calibration record for LVDT channels LT-05 $\tilde{\text{L}}$T-08 75
7.3 Calibration record for LVDT channels LT-09 $\tilde{\text{L}}$T-10 75
7.4 HBP series polyimide carrier strain gauges 76
7.5 HBP-12-2000-C series polyimide carrier strain gauges 77
7.6 Strain gauge rosettes DMSSerie Y 78
7.7 SCM5B38 input modules 79
7.8 SCM5B38 specifications 80
7.9 Calibration record for channel Strain gauge rosette, SGR-1-X 81
7.10 Calibration record for channel Strain gauge rosette, SGR-1-Y 82
7.11 Calibration record for channel Strain gauge rosette, SGR-1-Z 83
7.12 Calibration record for channel Strain gauge rosette, SGR-2-X 84
7.13 Calibration record for channel Strain gauge rosette, SGR-2-Y 85
7.14 Calibration record for channel Strain gauge rosette, SGR-2-Z 86
7.15 Calibration record for channel Strain gauge rosette, SGR-3-X 87
7.16 Calibration record for channel Strain gauge rosette, SGR-3-Y 88

7.17 Calibration record for channel Strain gauge rosette, SGR-3-Z 89
7.18 Calibration record for channel Strain gauge rosette, SGR-4-X 90
7.19 Calibration record for channel Strain gauge rosette, SGR-4-Y 91
7.20 Calibration record for strain gauge rosette, SGR in terms of temperature 92
7.21 Calibration record for channel axial strain gauge, SG-01 93
7.22 Calibration record for channel axial strain gauge, SG-02 94

List of Tables

3.1 Bridges considered as candidates of the project 16

4.1 Summary of 10 LVDT channels calibration result 29
4.2 Color code for LVDT terminals 31
4.3 Summary of calibration records for strain gauges 37
4.4 Temperature sensor assignments 39

Chapter 1

INTRODUCTION

1.1 Background and motivation

The deterioration of civil infrastructural systems in the United States has been well documented and publicized. Approximately 50 percent of all bridges in this country were built before the 1940s and currently about 42 percent of these structures are structurally deficient, in need of strengthening and rehabilitation [1, 2, 3]. Particularly in Hawaii, about one-third of all the bridges in the state are obsolete or structurally deficient. It has been estimated that the investments needed to enhance the performance of deficient infrastructures exceed $900 billion worldwide [2, 3, 4]. These statistics underline the importance of developing reliable and cost effective methods for massive rehabilitation as well as securing investments for the coming years. The State of Hawaii is located in one of the seismic active regions. This exacerbates the problem of gradual deterioration of the civil infrastructure over time by introducing new damage to the structure or increasing existing damage. In order for the State of Hawaii Department of Transportation (HDOT) to effectively manage the state-owned bridges, it is essential to understand the true state of health and rate of degradation of each significant bridge of the transportation system. This critical information provides a rational basis for the optimum allocation of limited financial resources towards the maintenance, rehabilitation and strengthening of the transportation system as a whole. Currently in Hawaii, the state-owned highway bridges are managed by the Bridge Section of the Hawaii Department of Transportation using Pontis, an AASHTO bridge and highway management software package. Bridge maintenance is optimized taking account of all factors affecting bridge management. These factors include the condition of the structure, load carrying capacity, rate of deterioration, effect of traffic pattern, and the residual life of the structure, along

with other similar factors. In particular, the following information is necessary for bridge owners to develop optimal management strategies:

- the condition of each structural component of a bridge and the overall state of the complete bridge;
- the load carrying capacity of a bridge and its most structurally vulnerable components;
- the current extent and rate of deterioration of bridge components (to predict future conditions);
- predictions of the time when a bridge will become substandard in terms of the load carrying capacity;
- identification of maintenance requirements of a bridge;
- guidance on effective maintenance strategies and methods, and
- programs of maintenance work indicating the timing of specified maintenance methods needed in order to minimize the life cycle cost of a bridge.

Currently, evaluation of the health condition of highway bridges relies primarily on periodic visual inspection, which has been proved to have several issues [5]. First, visual examination is labor intensive and time consuming and therefore cannot be performed frequently. For example, to inspect the 758 state-owned bridges following a 6-month schedule would require about 5 bridges be inspected daily. This is certainly a prohibitively expensive task. Second, the reliability of visual inspections is questionable. Visual inspection is superficial and subjective in nature. Great disparity of the examination results is unavoidable even when the inspection is conducted by experienced and well-trained engineers. According to a recent investigation performed by FHWA [6], it was shown that the results of visual inspections, performed by different intensively trained and highly experienced inspectors, varied significantly. Third, visual inspections can be only performed at the component level, while the components that need inspection must be readily accessible and safe to access. However, in order to optimize resource allocation, it is necessary to determine the overall structural safety and serviceability, which can only be evaluated based on system-level bridge assessment. System level assessment, however, cannot be achieved by mechanically summing up the component conditions obtained from visual inspections. Fourth, visual inspections do not provide any information on the deterioration rate or the evolution of the live load of the bridge inspected. It is then very difficult

to estimate the life-cycle maintenance cost and as a result optimized maintenance strategies cannot be developed. Finally, hidden damage and damage at early stages cannot be easily identified with visual inspections. Preventive maintenance strategies thus cannot be implemented.

The constantly changing and improving design guidelines also call for re-evaluation of the condition of existing bridges designed with out-of-date design codes. Many existing bridges were designed based on the allowable stress method. Such deterministic design methodology, however, does not take into account the uncertainties in a real world environment, such as randomness in material properties, boundary conditions, etc. Such uncertainties can only be analyzed using probabilistic theory. Reliability analysis is thus necessary for accurate evaluation of the condition and performance of the bridges designed this manner [7].

1.2 Objectives

The goal of this project was to help the State of Hawaii establish a database for structural health management of its highway bridges. Particularly, this project aims at fulfilling the following objectives:

- to collect data and evaluate bridges using novel sensing technologies;
- to identify and quantify the types and ranges of typical parameters required for monitoring;
- to develop and validate appropriate techniques for structural health monitoring and evaluation of concrete bridges in Hawaii;
- to develop an IT-based framework for data analysis and condition evaluation, and
- to evaluate the structural reliability of highway bridges.

The project are carried out in two phases. In Phase I, efforts are focused on the development and deployment of instrumentation systems. IT-based framework is also established in this phase for data collection and analysis. In Phase II, continuous, long-term data will be analyzed so that a long-term structural performance can be evaluated, and finally, the reliability of selected bridges can be assessed.

1.3 Overview of chapters

This report is organized as follows.

Chapter 2 provides a brief literature review of bridge monitoring technologies. It discusses the differences and similarities between structural health monitoring and non-destructive evaluation. The state-of-the-art technologies and applications in the practice of bridge monitoring are also summarized.

Chapter 3 presents the bridge selection process and philosophy. Several bridges were considered as candidates for this project. Results obtained from inspection of the candidate bridges are summarized. Waiau Interchange was selected for instrumentation and its plan is also presented.

Chapter 4 describes the design of the monitoring system. The systems contains sensors, a data acquisition subsystem, a power subsystem, and a data transmission subsystem. The sensors include linear variable displacement transducers (LVDT), strain gauges, and temperature sensors. The data acquisition, power, and data transmission subsystems were customized to meet the needs of the project.

Chapter 5 describes the installation process. The deployment of the system was accomplished in two phases. In Phase 1, a power supply system was designed and installed. The sensors and supporting subsystems were then installed in Phase 2.

Chapter 6 presents a portion of the data collected. The activities of the cracks being monitored are successfully captured by the system.

Chapter 7 offers a summary and conclusion of this project. The bridge is being continuously monitored, with data being wirelessly transmitted to a server located at University of Hawaii, Mānoa.

Chapter 2

BRIDGE MONITORING

2.1 Structural Health Monitoring

Structural health monitoring (SHM) is a relatively new practice in civil engineering. The objectives of a SHM system may generally include [8]: (1) to validate design assumptions and parameters; (2) to detect anomalies; (3) to provide realtime information about structural safety and performance; (4) to provide information for prioritizing activities and resources. A SHM system typically consists of three major components, which are (1) sensing units that provide necessary measurement data; (2) data acquisition and transmission components; and (3) signal processing components that automatically analyze the obtained data and quantitatively determine the condition of the structure.

Structural health monitoring is highly related to the traditional field of nondestructive evaluation (NDE) [9], both of which can be classified under the framework of monitoring and assessment methods for structural evaluation [10]. In general, SHM focuses more on monitoring globally the in-service structural behavior, while NDE is more considered as associated with damage identification, which can be achieved at different levels, such as

1. Onset of damage
2. Localization of damage
3. Classification and severity of damage
4. Residual service life of the structure

It is noted that the definition of structural health monitoring has been changing and its distinction from non-destructive evaluation has not been clear-cut. In a more recent study, SHM is defined as the process of implementing a damage identification strategy [11].

2.2 State-of-the-art Technologies

Historically, methods of structural health monitoring have been classified into two categories, i.e. the global methods and local methods. The global vibration-based techniques are methods that determine the health condition of structures by the changes in their dynamic properties or responses. These techniques should be well suited to automation and should have a minimum reliance on the engineering judgment of the users and on an analytic model of the structure. These ideal techniques should also be able to take into account operational constraints and to identify different types of damage including both linear and nonlinear conditions. A great deal of early research work on damage detection has been focused on detecting the change of structural modal properties, such as natural frequency, mode shape, and others. Summaries of these research efforts can be found in Chong [12], Kirmidjian et al. [13], and Doebling et al. [14]. Recently, novel techniques in modeling, sensing and signal processing have been used by many researchers to develop more effective and efficient methods. For example, empirical mode decomposition, wavelet analysis have been used to develop global damage detection methods [15, 16, 17, 18, 19]. Lus et al. [20], Dyke et al. [21], among others, have used modern system identification techniques to develop methods for damage detection and identification. Real time health monitoring has also been studied by the author and his colleagues [22].

The local detection techniques are either visual or localized experimental methods such as the use of X-rays [23], strain gauges [24], optical fibers [25, 26], ultrasonic vibrations [27, 28], eddy currents [29], acoustic emissions [30], infrared measurements [31, 32], and lamb waves [33]. Kessler and Spearing [34] summarized and compared the strengths and the limitations of these mechanisms as well as their potential in structural health monitoring applications. These local techniques generally require prior knowledge about the vicinity of damage and the portion of the structure being examined by these local techniques should be readily accessible.

It is obvious that the local and the global techniques, having their own advantages and limitations, would compliment each other and contribute to a more complete health monitoring system for civil engineering structures. While the global vibration-based techniques have the potential to detect an occurrence and to locate an approximate location of possible structural damage, it is the local detection tech-

niques that can provide more direct and accurate assessment about the severity and extent of the damage.

Long-term structural health monitoring systems have been implemented on many in-service bridges all over the world. For example, in Europe, the Westend bridge was among the earlier bridges instrumented for automatic monitoring [35]. This bridge is a 243 m long continuous pre-stress concrete bridge and consists of a three-cell box girder. Instruments were installed in 1994 to monitor the growth of multiple cracks within the girder. In 1996, the Versoix bridge in Swiss was instrumented to monitor possible differential shrinkage due to additional concrete added asymmetrically [36]. Over 100 fiber optic sensors were deployed to monitor the bridge deflection. In 2000, the Skovdiget bridge in Copenhagen, Denmark was instrumented to monitor unexpected settlement [37]. A summary of the SHM applications in Europe can be found in Casciati et al. [38]. In the US, bridges of different types have been instrumented for a variety of purposes [39]. Particularly, there are currently about 40 long-span bridges, with spans of 100 m or larger, have been instrumented worldwide for structural health monitoring purposes. Examples include the Great Belt bridge in Denmark [40], the Confederation bridge in Canada [41], the Tsing Ma bridge in Hong Kong [42], the Commodore Barry bridge in the US [43], the Akashi Kaikyo Bridge in Japan [44], and the Seohae Bridge in Korea [45].

Chapter 3

BRIDGE SELECTION

3.1 Bridges considered

Based on the need of HDOT, eight box-girder bridges and a steel bascule bridge were identified from the bridge inventory record to be suitable for this project. The bridges are listed in Table 3.1. Due to limited time and resources, the list was then narrowed down to five bridges that were later inspected to select the final bridge for this project. The bridges selected for inspection included:

- Puowaina Interchange (On Ramp)
- Puowaina Interchange (Off Ramp)
- Waiau Interchange
- Airport Interchange (Paiea On-Ramp)
- Harbor Bridge #2 (Steel Bascule)

Inspection of these bridges was not carried out in place of the two-year regular bridge inspection, but rather, it was for the purpose of determining a candidate bridge for the research project. The following factors were weighted more during inspection.

- Bridge condition (cracking)
- Traffic (excessive vibration)
- Safety for field work
- Easy access

Name	Location	Type	Comment
Puowaina I.C.	Honolulu	Box Girder	On ramp
Puowaina I.C.	Honolulu	Box Girder	Off ramp
Halawa I. C.	Honolulu	Box Girder	
Waiau I.C.	Honolulu	Box Girder	
Pearl Harbor I.C.	Honolulu	Box Girder	
Airport I.C.	Honolulu	Box Girder	
Kapiolani I.C.	Honolulu	Box Girder	Functionally obsolete
Hanamanu Viaduct	Kauai	Box Girder	
Harbor Bridge #2	Honolulu	Steel bascule	

Table 3.1: Bridges considered as candidates of the project

3.2 Findings

The selected bridges were visited multiple times within a week. The volume of traffic during the day, especially during rush hours for all the bridges were quite large. Among them, Harbor Bridge #2, through which many heavily loaded trucks pass every day and Waiau Interchange seemed to have the most traffic loads. Particularly, excessive vibration due to traffic was observed from Waiau Interchange. Cracking was observed in almost all of the concrete bridges. The number of cracks of Waiau Interchange again far exceeds that of the other bridges. Relatively long shear and flextural cracks were observed in Waiau Interchange. However, as the inspection was carried out in a rather qualitative manner, i.e. visual inspection with no measurements made, the level of bridge vibration or the detailed information about the cracks were not quantitatively determined during inspection.

Based on the observed bridge condition, traffic volume, and the inspection reports provided by the HDOT bridge maintenance section, Waiau Interchange and Harbor Bridge #2 were considered as more suitable for this project. However, Harbor Bridge #2 is over water and thus making it more difficult for instrumentation. This higher installation cost led to the selection of Waiau Interchange for this project.

3.3 Waiau Interchange

The Waiau Interchange Bridge, built in 1970s, is a continuous concrete box girder bridges located on Island of Oahu in Hawaii (see Figure 3.1). An overpass of a local road (Moanalua Rd) with two spans, the Waiau Interchange bridge is part of the H1 freeway. After more than 30 years of service, many cracks have developed. Both

shear cracks on the web and flexure cracks in the middle of the span are present and extensive (Figure 3.2). The major concern of the bridge is its current health status due to severe cracking. Monitoring of the crack extension and measure of its current resistance capacity are most valuable for the decision making on the maintenance of the bridge. This project is to develop and install a Bridge Monitoring System focusing on the progress of crack opening, strain values due to traffic loads at strategically selected locations, as well as the temperature values at various locations. The ultimate goal is to determine the resistance capacity of the bridge and to determine whether the current cracking poses a safety concern.

3.4 Instrumentation plan

Waiau Interchange was instrumented to monitor crack opening and propagation of several existing cracks as well as bridge vibrations due to traffic loads. Cracks are monitored using potentiometers and/or LVDTs. Fiber optical systems for this purpose were considered due to the improved accuracy of the measurement. However, the plan of using fiber optical systems was discarded due to limitation of research funds. The measured data is wirelessly transmitted to a central server and will be available for download through Internet connection.

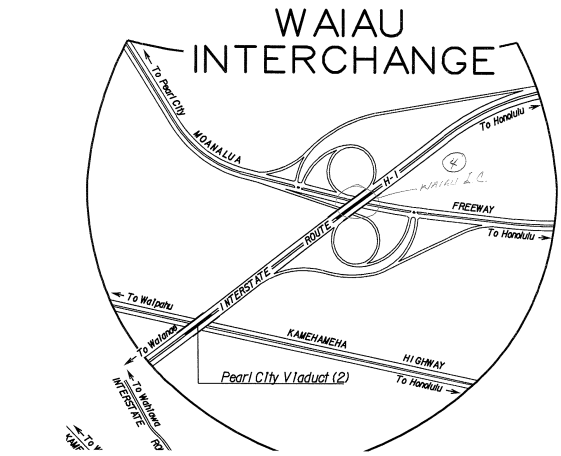

(a) Plot plan

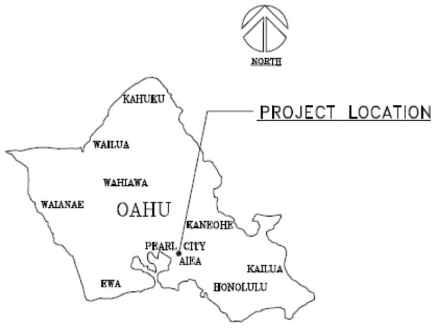

(b) Vicinity map

(c) Local area

Figure 3.1: Geographical location of Waiau Interchange

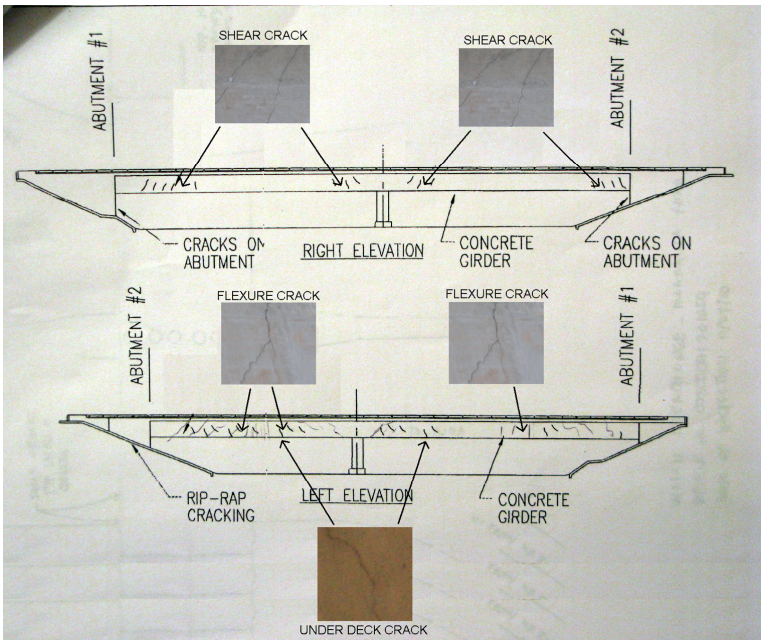

Figure 3.2: Cracks observed on the bridge

Chapter 4

SYSTEM DESIGN

4.1 System architecture

The primary concern of the Waiau interchange is cracking and the high volume of traffic load. Instrumentation is focused on cracking monitoring. Three types of sensors are used in this project, i.e. linear variable displacement transducers (LVDT), strain gauges, and temperature sensors. The primary locations to be monitored are shown in Figure 4.1.

The system consists of sensors, data acquisition system, power supply, data transmission module, server, and client. The system architecture is shown in Figure 4.2. The substation consists of signal conditioners for the sensors, a single board computer (SBC) for multifunctional data acquisition and processing, and a wireless data transmission module. The substation is developed so that the raw data obtained from different types of sensors can be processed simultaneously. Using the embedded signal conditioners, the substation transfers pre-processed data wirelessly to a remote server via secured wireless internet connection. The server is equipped with an SQL database that is used to store the data, generate reports, manage data communication and other management tasks. Users obtain access to the database via a software designed specifically for client usage.

In this project, ten cracks from the two sides of the bridge are selected to be monitored using LVDTs as indicated in Figure 4.1. Four strain rosettes are installed on the inbound side to monitored the principle strain of the two spans. Tensile strain gauges are installed at the bottom of the box girder of the outbound side for the two spans, respectively. Ambient temperature, as well as the temperature inside the concrete, is also monitored with four temperature sensors. The data acquisition system, power supply, and the data transmission module are installed on the inbound

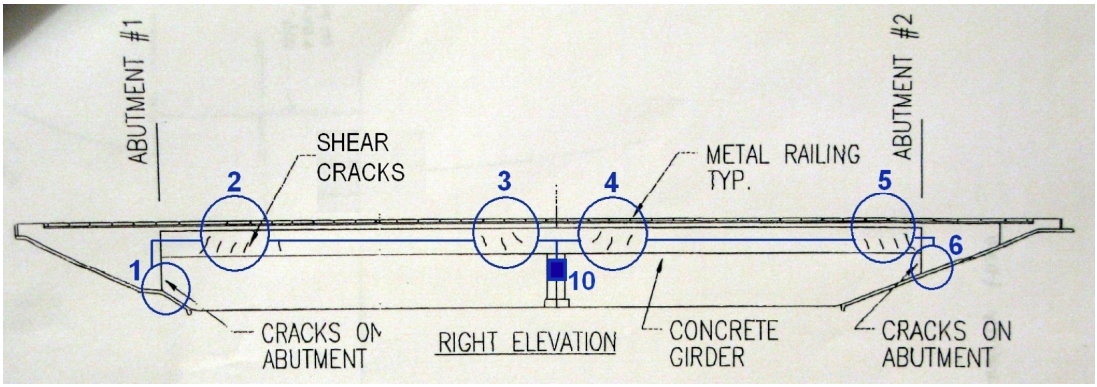

(a) Inbound side

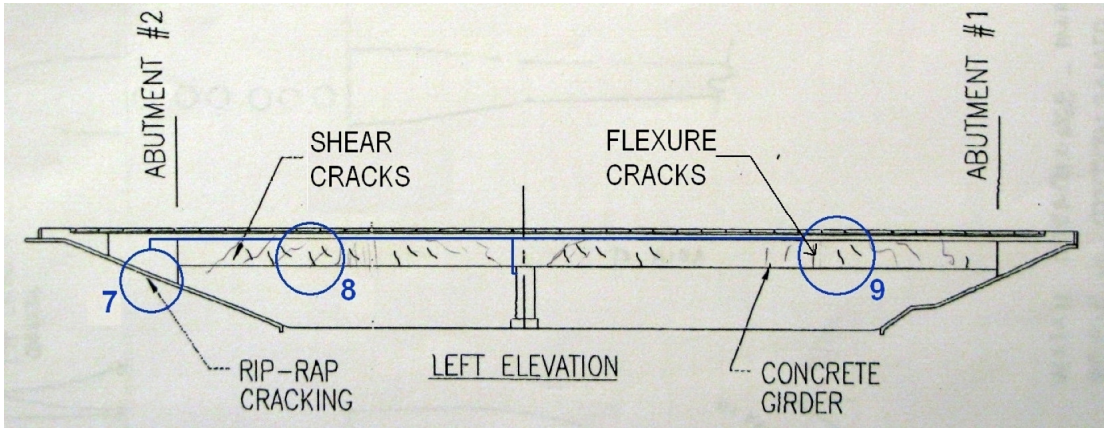

(b) Outbound side

Figure 4.1: Crack location

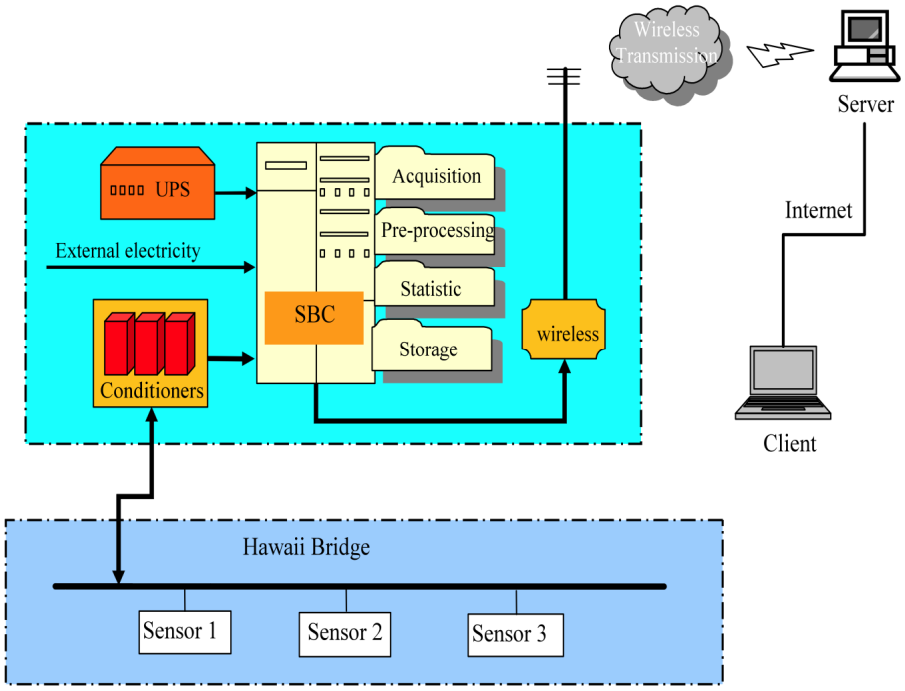

Figure 4.2: System architecture

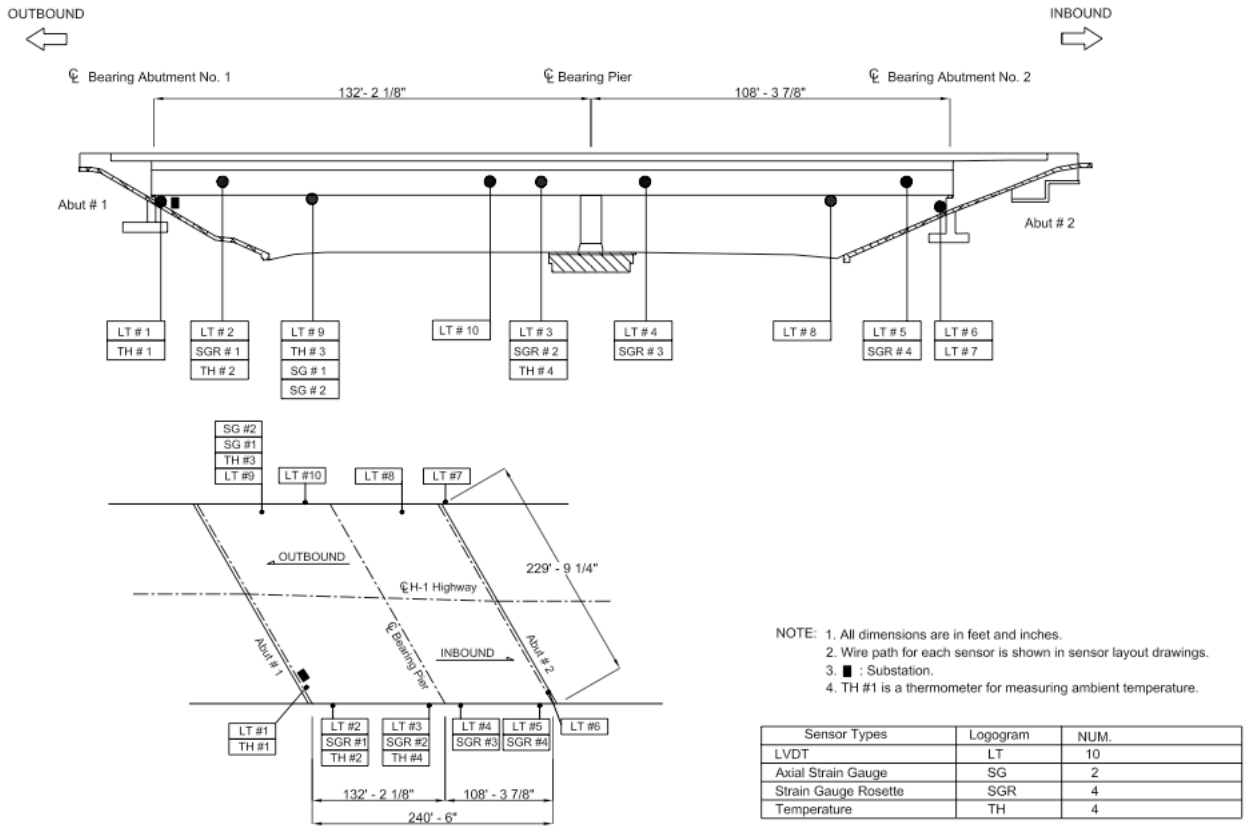

Figure 4.3: Sensor layout

side of abutment #1.

4.2 Sensors and substation

Ten LVDT sensors are installed to monitor crack opening displacements (COD). Each LVDT sensor is composed of a transducer and an amplifier as the signal conditioner. Two axial strain gauges are used for measuring longitudinal strains for the two spans, which can be used to infer bridge curvature for later detailed analysis. Four strain gauge rosettes are used for measuring principal strains/stresses. Four temperature sensors are used to measure the temperatures of girder and ambience. The location of the sensors is shown in Figure 4.3. The layout of the substation is shown in Figure 4.4.

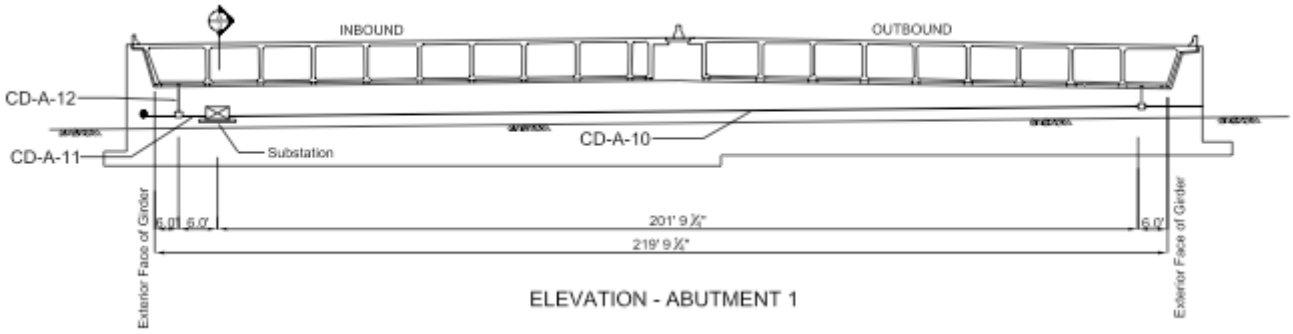

Figure 4.4: Substation layout

The functional diagram of the substation is shown in Figure 4.5 Such a design was determined to be ideal for the moderate level of analog signal monitoring required in this project. In addition, the on-board processor significantly reduces the amount of programming required to aggregate bandwidth. All of the raw signals collected from the sensors are transferred to the single-board computer to be analyzed and transmitted. The substation provides the following functionalities:

- Interface with analog signals, digital signals, and counter/timer signals from sensors;
- Calibrate sensors and pre-process data;
- Perform statistic evaluation of the data, such as average, maximum, minimum, frequency, and deviation;
- Provide temporary real time data storage in the case of interrupted communication with server and resume data transmission upon connection reestablished;
- Provide early warning when abnormality detected;
- Self-test and power management;
- Designed to be water proof and static electrical isolation;

The software in substation is characterized by the following:

- The embedded software in the substation includes three parts. Part one deals with communication between sensors and server, which is through an embedded

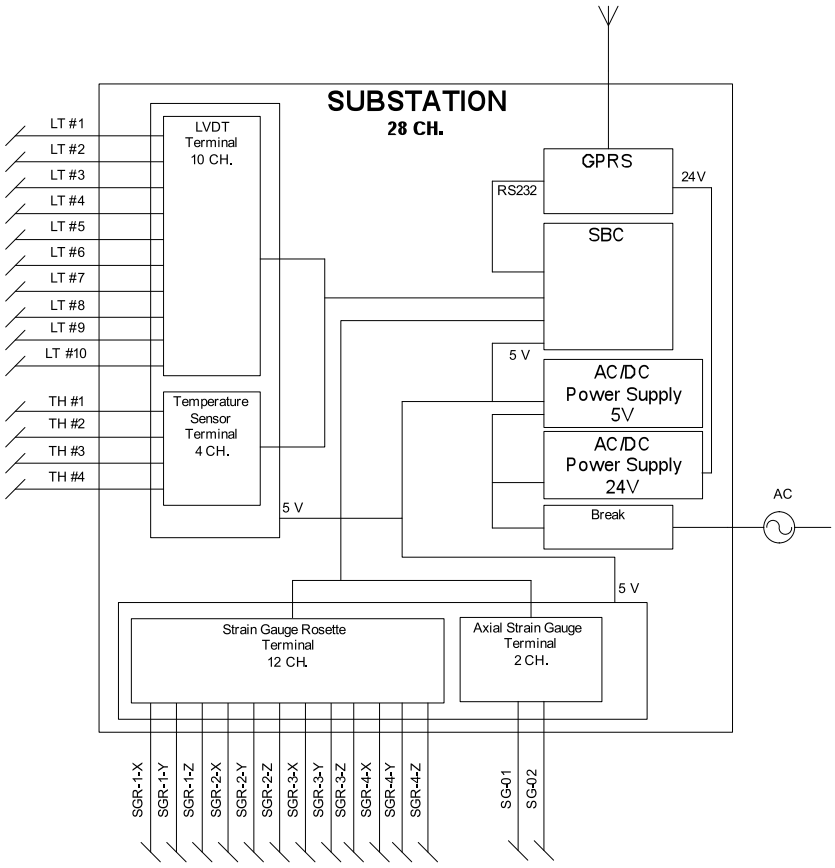

(a) Functional diagram of substation

(b) Substation

Figure 4.5: Substation configuration

wireless module. Part two performs data processing. Part three controls the configuration of the station such as sensor type, data acquisition frequency, and storage length, etc.;

- Signals from sensors are calibrated and filtered to be meaningful real-time data;
- Real-time data are stored in station for one month or other specified period depending on the capacity of storage.

Through a GPRS system, such as 3G network cell phone technology, both real-time data and saved data are wirelessly transmitted to a server at University of Hawaii. The processed data from on site station will be stored in the server. The storage capacity will allow processed data to be stored for up to 5 years without requiring a new hard disk. Client software can also run on server. The software in the server has the following features.

- Includes server program and client versions;
- The server version manages the database on server. It receives processed data from substation and saves them in the database;
- The client version provides a user interface. It has the functionality of data analysis, e.g. correlation analysis, spectrum analysis. Crack development due to temperature and traffic effect can be distinguished by correlation analysis.

The overall requirements for the data acquisition are listed below.

- Low-power VIA Eden processor (800MHz Pentium-III class processor)
- On-board data acquisition circuit with auto-calibration
- Signal conditioner for strain gauges and LVDTs
- -40°C to +85°C operating temperature
- 512MB SDRAM soldered on board
- Rugged design ideal for outdoor applications
- 32 wide-range analog inputs, +/-10V down to 0-1.25V
- 16-bit A/D resolution
- 2048 A/D sample FIFO with programmable threshold

- 250KHz max sample rate
- Programmable input ranges

4.2.1 LVDT system

Each LVDT sensor set is composed of a transducer and a conditioner. The transducer is of model GT2500 and the conditioner is of model S7TW, as illustrated in Figure 4.6. Both were product of RDP Electronics Ltd., UK.

As is well known, LVDT sensor is probably the most robust and reliable position sensor type available. The strength of its principle is that there is no electrical contact across the transducer position sensing element, which for the user of the sensor, means clean data, infinite resolution and a very long life. The GT series gauging transducer employs precision linear bearings to optimize the LVDTs measurement precision and repeatability. It features high cycle life, stainless steel, infinite resolution, very high accuracy, precision linear bearings, and miniature.

The GT2500 is a kind of spring return LVDTs which are appropriate where it is not possible to connect the transducer armature to the moving component being measured. It has bearings to guide the armature inside the measurement sensor and a spring which pushes the armature to the fully out position.

The main specifications of GT2500 are as follows:

- Range ± 2.5mm ($\pm 0.1''$)
- Linearity error (% F.S.) $< \pm 0.25/ \pm 0.1''$
- Total weight 0.4oz
- Spring force at X 4.1oz
- Spring rate 24.2oz/inch
- Inward over-travel $0.03''$
- Outward over-travel $0.01''$
- Sensitivity (nominal) 375mV/V
- Size L=$2.26''$, X=$0.80''$, B=$0.71''$ (No clamp zone)

(a) Transducer GT2500 (left) and amplifier S7TW (right)

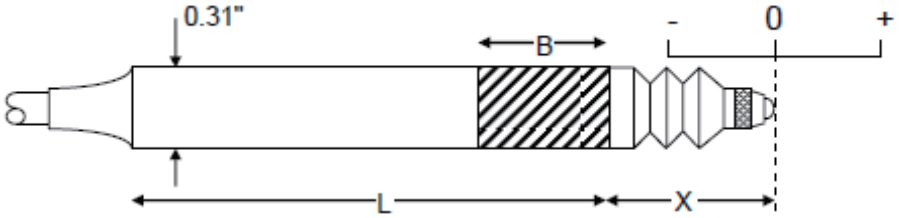

(b) Transducer outline

Figure 4.6: LVDT sensor set

Channel Name	Serial No.	Linearity (%)	Sensitivity S_{LVDT} (mV/V/mm)
LT-01	130036	0.23	152.77
LT-02	130037	0.24	151.63
LT-03	130038	0.24	156.42
LT-04	130039	0.23	153.67
LT-05	130040	0.19	159.62
LT-06	130041	0.24	160.09
LT-07	130042	0.21	153.25
LT-08	130043	0.14	157.96
LT-09	130044	0.24	160.37
LT-10	130045	0.25	160.22

Table 4.1: Summary of 10 LVDT channels calibration result

The sensitivity of LVDT sensor was calibrated as follows

$$S_{LVDT} = \frac{(V_{LVDT} - V_0)/V_{EXC}}{d} \quad (mV/V/mm) \tag{4.1}$$

where

$$\begin{aligned} d \quad & -- \text{ displacement (mm);} \\ V_{LVDT} \quad & = (mA \times 24.9\Omega) \times \text{Gain} \text{ — raw data (mV), Gain=2.0;} \\ V_0 \quad & -- \text{ initial voltage at zero setting (mV);} \\ V_{EXC} \quad & -- \text{ Exciter voltage (V).} \end{aligned}$$

The original calibration record by RDP LLC., UK, for the ten LVDT channels LT-01 – LT-10 are given in Appendix I. Table 4.1 summarizes the calibration result.

There are two kinds of connections from LVDT sensors to substation. One is the connection between a LVDT transducer and its amplifier or conditioner; the other is between the conditioner and substation. Each LVDT transducer has six wires for connecting to its conditioner, and an extension cable with two core wires, which is used for connecting the conditioner to substation. The detailed connection and color codes are demonstrated in Figure 4.7 and Table 4.2, respectively. The layout of the LVDT subsystem is shown in Figure 4.8.

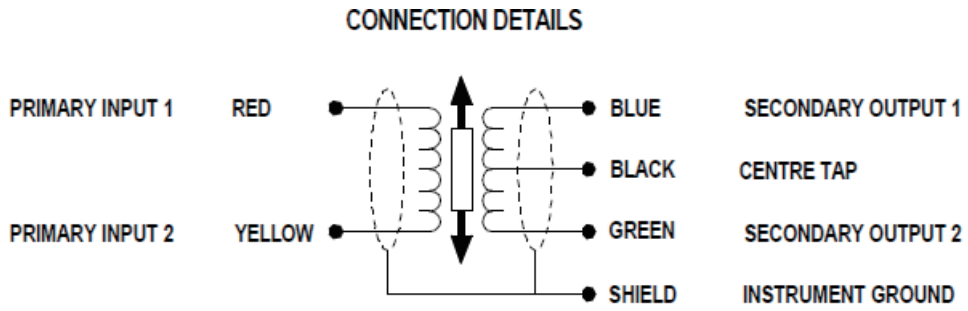

(a) LVDT transducer diagram

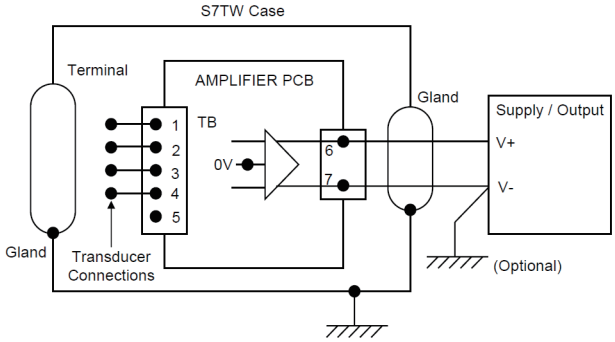

(b) Conditioner diagram

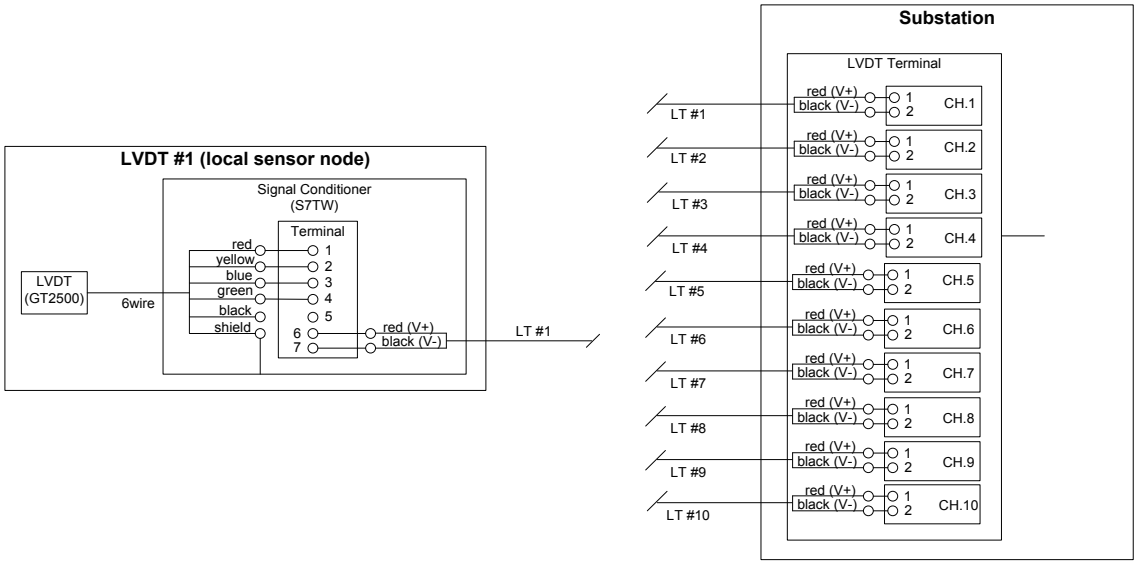

(c) Terminal connection of LVDTs, conditioners and substation (Among the 10 channels, only the detail for the 1^{st} LT-01 is shown)

Figure 4.7: Connection details of LVDT sensors, conditioners and substation

LVDT Sensor (GT2500)	Conditioner (S7TW)	Extension Wire	Substation
Red	1, Exciter		
Yellow	2, Exciter		
Blue	3, Signal		
Green	4, Signal		
Black	N/A		
	6	Red (V+)	1
	7	Black (V-)	2

Table 4.2: Color code for LVDT terminals

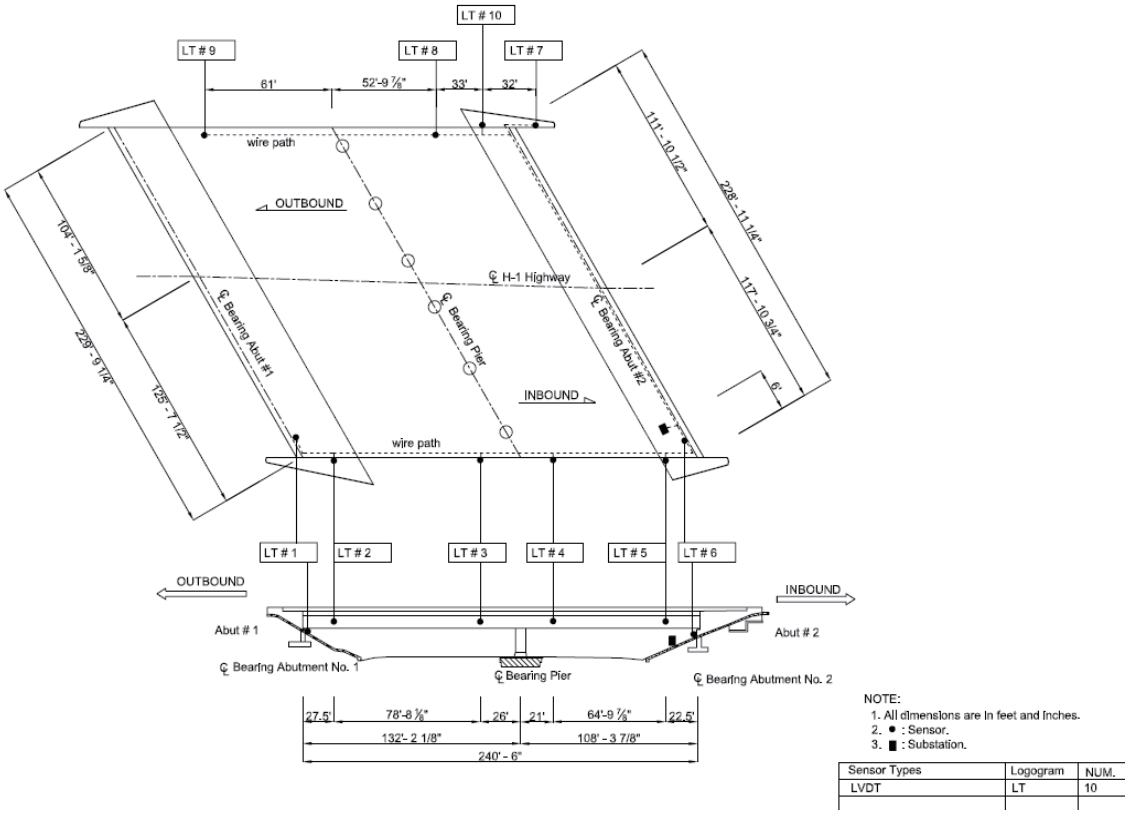

Figure 4.8: LVDT subsystem layout

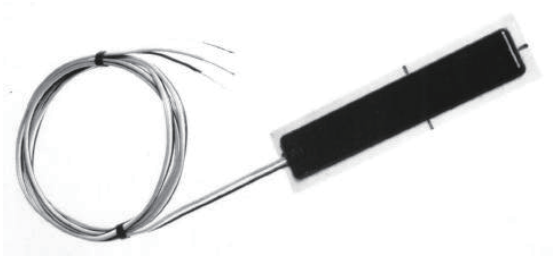

Figure 4.9: Strain gauge (HBP-35-250-06-3VR)

4.2.2 Strain measurements

For the axial strain measurement, Polymide Carrier Strain Gauge HBP-35-250-06-3VR (Hitec Products, Inc., see Figure 4.9) was chosen, which features

- Strain Range: ..... $\pm 2000\mu$
- Gauge Resistance: ..... 350Ω standard, 120Ω optional
- Temperature Range: ..... -50 °F to 180°F
- Waterproof

Whereas, for the strain gauge rosette encapsulated strain gauge DMS/Serie Y 1-RV91-6/120 (Dehnungsmessstreifen & Zubehör, Germany, see Figure 4.9) was chosen, which features

- Encapsulated strain gauges
- High mechanical protection
- Temperature Range: ..... -70 °C to 200°C
- Strain Range: ..... $\pm 20,000\mu$
- Nominal Resistance: 120Ω

To facilitate processing the strain measurements, some expressions are given below. The differential strain between the gauge locations is related to the curvature Δ_k as follows

$$\Delta_k = \frac{\Delta\epsilon_{top} - \Delta\epsilon_{bot.}}{L} \tag{4.2}$$

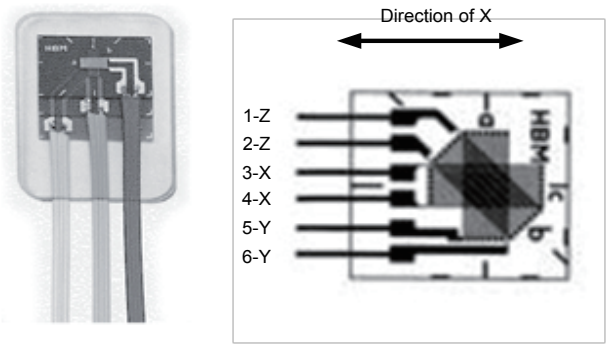

Figure 4.10: A 1-RV91-6/120 strain gauge rosette

where L is the vertical distance between the locations of top and bottom strain gauges. The curvature Δ_k is directly related to the bending moment due to load ΔM, material properties and geometry via

$$\Delta M = \Delta_k \left(E_c I_c \right) \tag{4.3}$$

where the Young's modulus of concrete $E_c = 38$ GPa, the moment of inertia (obtained from typical as-built drawings) $I_c = 15.65$ m^4. Equation 4.3 provides several possibilities for bridge monitoring, including estimation of dynamic vehicle loading (load monitoring) or monitoring for gradual changes in the local flexural rigidity (structure monitoring). Estimation of dynamic vehicle load is important in assessing the potential of fatigue damage processes and in determining whether design ratings are being locally exceeded. The procedure is not straightforward, particularly in the case of multiple vehicles arriving at the bridge in rapid succession, due to dynamic effects. The latter monitoring possibility - structure monitoring - is to use Equation 4.3 to directly monitor the integrity of the sectional moment of inertia.

Signals from the axial strain gauge and strain gauge rosette are conditioned by Dataforth modules SCM5B38-33 (in half bridge connection) and SCM5B38-31 (in full bridge connection), respectively. The manufacturer data sheets of the strain gauges and input modules are given in Appendix II.

As principal strain sensors, strain gauge rosettes are installed on the side of the box girder in which the shear reinforcement has been determined to be under the greatest stress. The measurements allow indirect determination of the stress level in shear reinforcement and are consequently best suited for monitoring for signs of impending yield conditions. The principal strains, orientation angle and principal

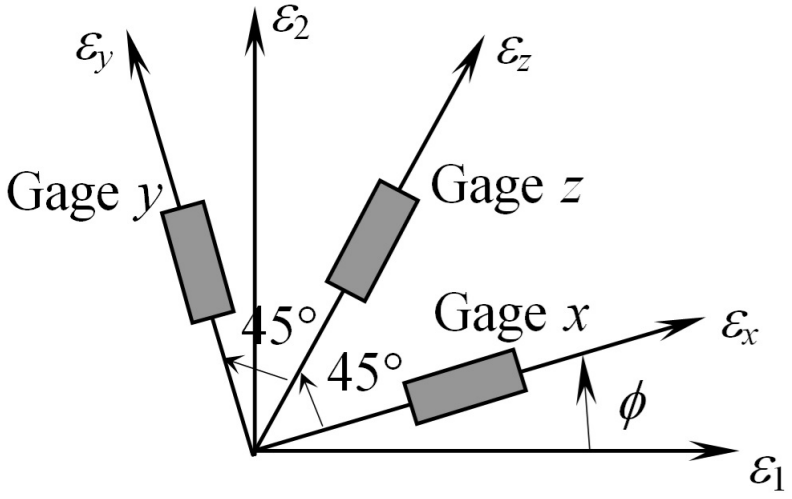

Figure 4.11: Orientation of the rectangular strain gage rosette

normal stresses are calculated as follows:

$$\epsilon_{1,2} = \frac{\epsilon_x + \epsilon_y}{2} \pm \frac{1}{\sqrt{2}}\sqrt{(\epsilon_x - \epsilon_z)^2 + (\epsilon_y - \epsilon_z)^2} \tag{4.4}$$

$$\phi = \frac{1}{2}\arctan\left(\frac{\epsilon_x - 2\epsilon_z + \epsilon_y}{\epsilon_x - \epsilon_y}\right) \tag{4.5}$$

$$\sigma_{1,2} = \frac{E_c}{1-\nu}\frac{\epsilon_x - \epsilon_y}{2} \pm \frac{E_c}{\sqrt{2}\,(1+\nu)}\sqrt{(\epsilon_x - \epsilon_z)^2 + (\epsilon_y - \epsilon_z)^2} \tag{4.6}$$

where

ν Poisson ratio;

$\epsilon_x, \epsilon_y, \epsilon_z$ Strains in the angular directions of 0°, 45°, and 90°, respectively, as shown in Figure 4.11.

There are two kinds of connections from strain gauge sensors to substation. One is the connection between a strain gauge and its conditioner; the other is between a conditioner and the substation. For strain gauge rosettes, each rosette has six wires for connecting to its conditioner, and three extension cables with three core wires are used for connecting the conditioner to the substation. The detailed connection and layout of the strain gauge rosette subsystem are demonstrated in Figure 4.12

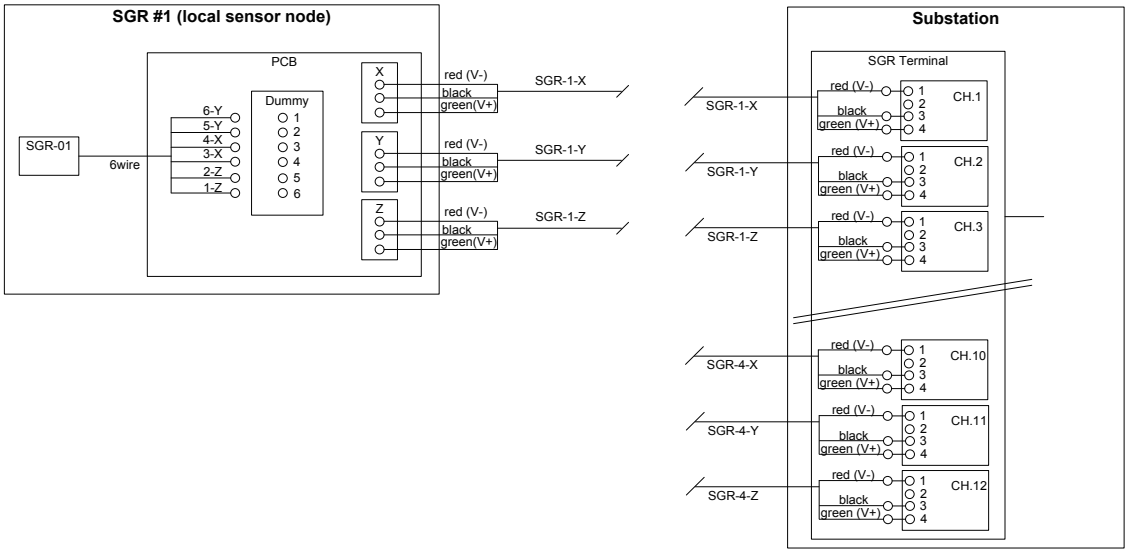

Figure 4.12: Strain gauge rosettes connection

and 4.13. As for axial strain gauges, each gauge has four wires for connecting to its conditioner, and four extension cables are used for connecting the conditioner to the substation. The detailed connection and layout of the axial strain gauge subsystem are demonstrated in Figure 4.14 and 4.15.

The strain of a strain gauge was calibrated as follows

$$\epsilon = \frac{4V_{SG}}{(V_{ex} - 2V_{SG}) \times GF} \quad (\mu\text{m/mm}) \tag{4.7}$$

where

V_{SG} $--$ raw data from strain gauge (mV);
V_{ex} $--$ excitation voltage (3.333 V);
GF $--$ gauge factor (= 2.0 for strain gauge rosette, = 2.1 for axial strain gauge)

The original calibration record by Dataforth Corporation, USA, for all the strain gauge channels are given in Appendix III. Table 4.3 summarizes the calibration result.

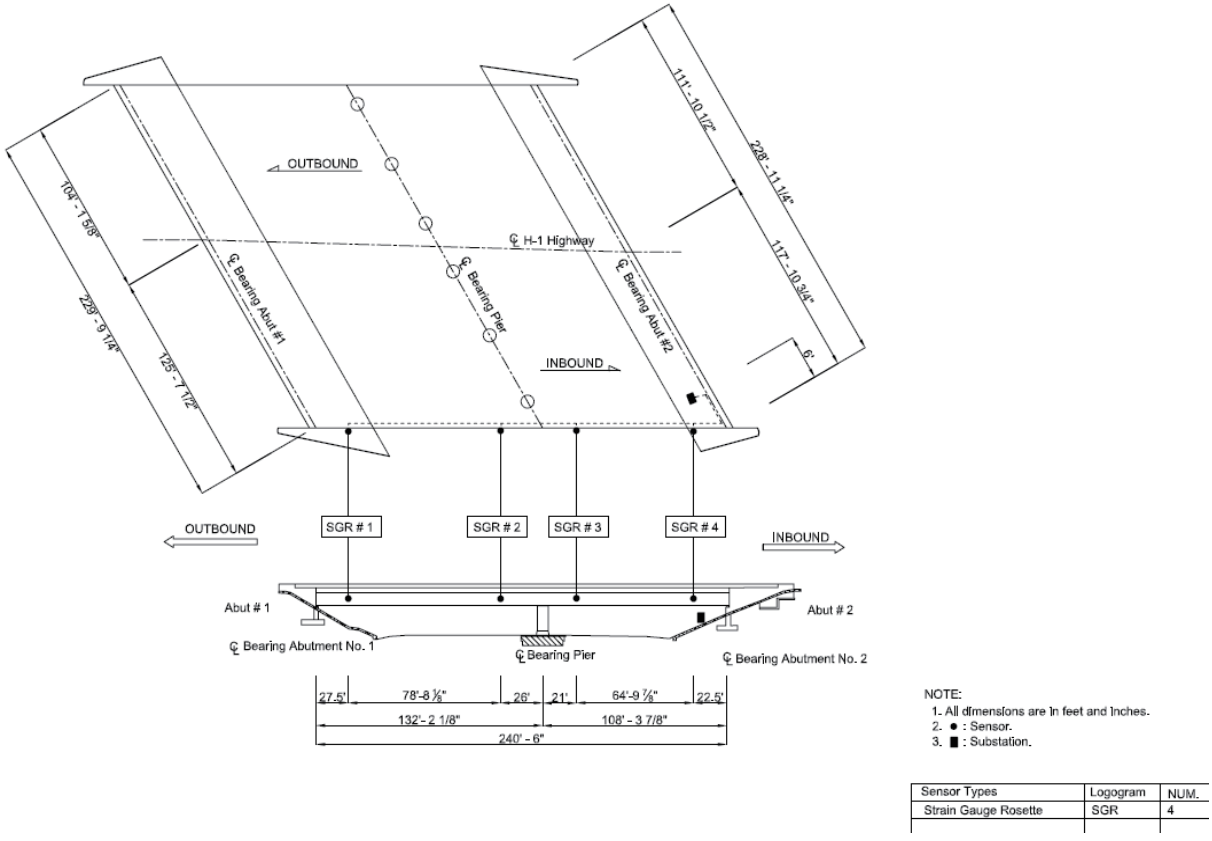

Figure 4.13: Strain gauge rosette subsystem layout

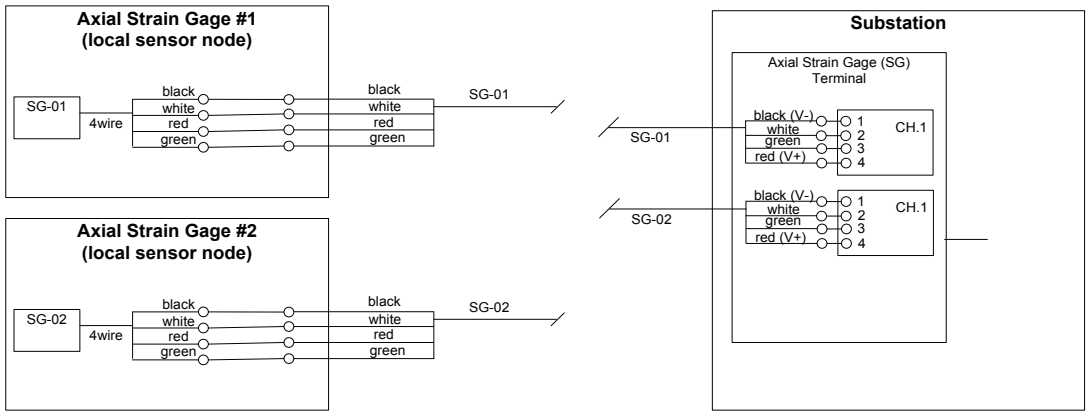

Figure 4.14: Axial strain gauges connection

Channel Name	Serial No.	Description	
SGR-1-X	SN.45717-30		
SGR-1-Y	SN.45717-31		
SGR-1-Z	SN.45717-32		
SGR-2-X	SN.49040-1		
SGR-2-Y	SN.49040-2	Strain gauge rosette	
SGR-2-Z	SN.49040-4	1-RV91-6/120	
SGR-3-X	SN.49040-5	(with SCM5B38-33)	
SGR-3-Y	SN.49040-6		
SGR-3-Z	SN.49040-7		
SGR-4-X	SN.49040-8		
SGR-4-Y	SN.49040-9		
SGR-4-Z	SN.49040-10		
SG-01	SN.57592-4	top	Axial strain gauge
SG-02	SN.57592-6	bottom	HBP-35-250-06-3 VR
			(with SCM5B38-31)

Table 4.3: Summary of calibration records for strain gauges

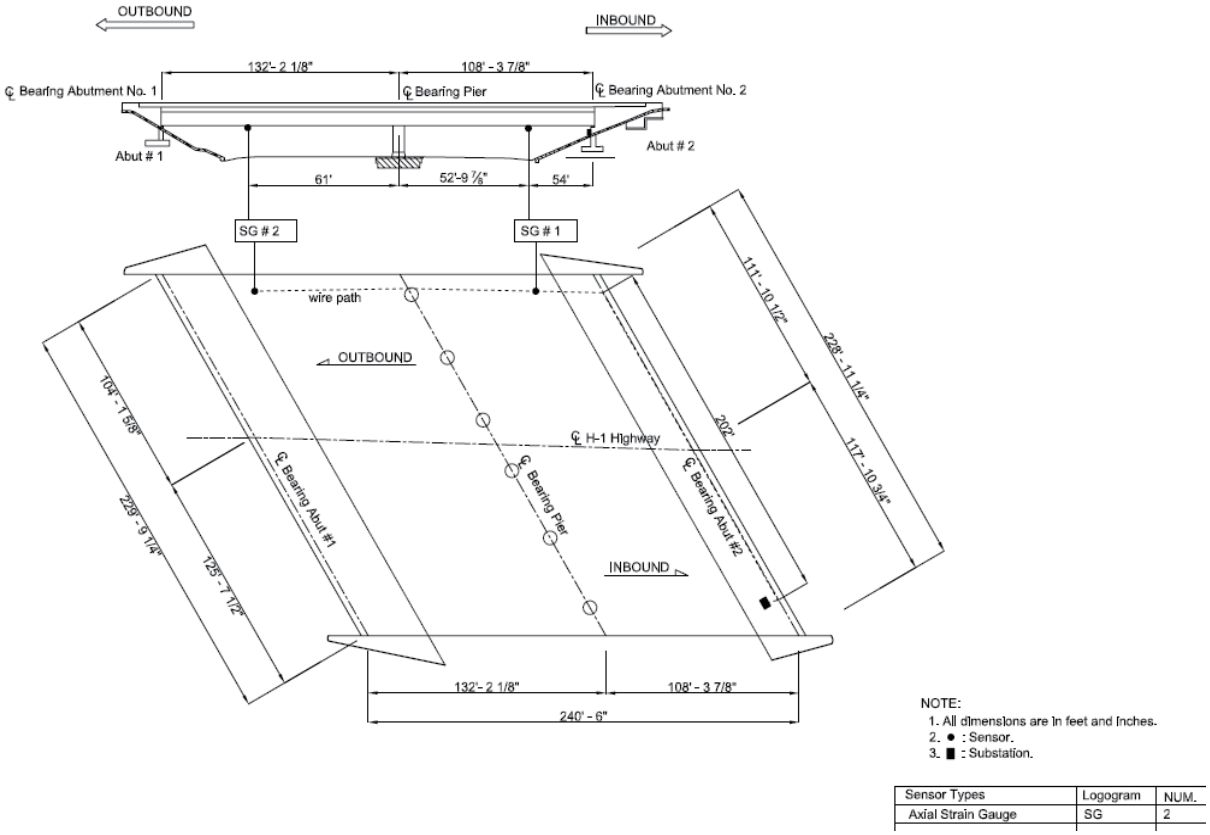

Figure 4.15: Axial strain gauge layout

Channel	TH-01	TH-02	TH-03	TH-04
Location	Ambient Temperature	Concrete on south web	Concrete on north web	Concrete on south web

Table 4.4: Temperature sensor assignments

4.2.3 Temperature measurements

The monitoring system provides four channels of thermistor conditioning for the measurement of in-situ, external air and internal concrete temperatures. Four channels of NTC 3K Vishay thermistor (Figure 4.16) are selected for maximum versatility. Temperature sensor (HBWTG-5V-AD22100-XTR) (see Fig. A-5) has the following features:

- 200°C temperature span
- Accuracy better than ±2% of full scale
- linearity better than ±1% of full scale
- Temperature coefficient of 22.5 mV/°C
- Output proportional to temperature × V+
- Single-supply operation
- Reverse voltage protection
- Minimal self-heating
- High level, low impedance output

The channel assignments for these thermistors are summarized in Table 4.4. Temperature equation of the thermistor is

$$T = \frac{1}{A + B\left(\ln R\right) + C\left(\ln R\right)^3} - 273.2 \tag{4.8}$$

where T = temperature in °C, $\ln R$ = natural log of thermistor resistance, $A = 1.4051 \times 10^{-3}$, $B = 2.369 \times 10^{-4}$, $C = 1.019 \times 10^{-7}$, and

$$R = \frac{R_0 \times V_T}{V_0 - V_T} \tag{4.9}$$

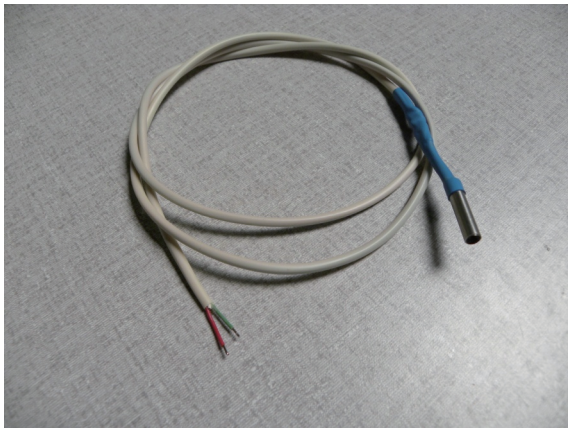

(a) Outline

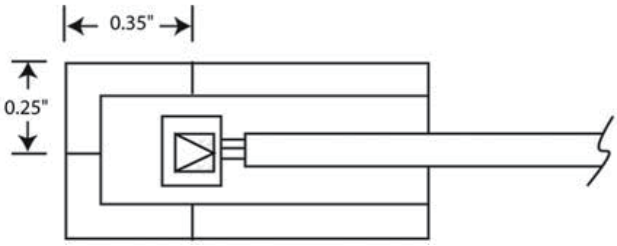

(b) Internal structure

Figure 4.16: Thermistor HBWTG-5V-AD22100-XTR

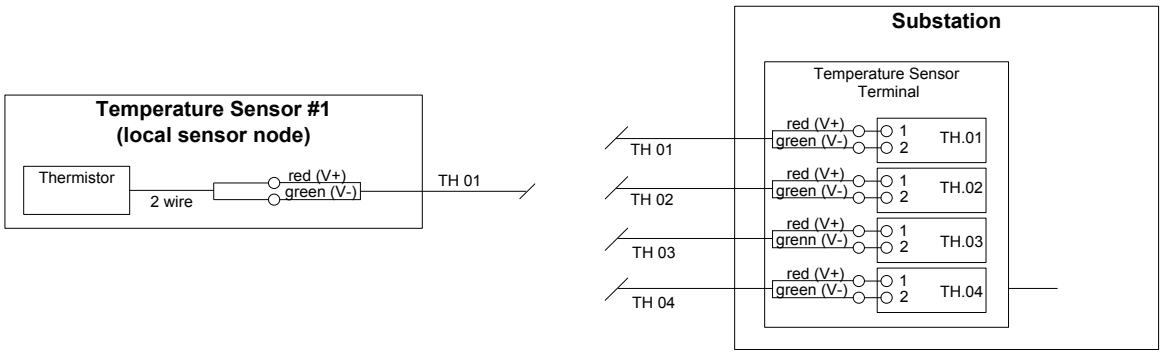

Temperature sensor color coding

Sensor	Extension wire	Substation
Red	Red	1
Green	Green	2
		3

Figure 4.17: Wire connection and color coding of temperature sensors subsystem

with $R_0 =$ initial resistance of thermistor (3000Ω), $V_T =$ raw data (V), $V_0 =$ excitation (10V). The R-T conversion table of NTC thermistors is given in Figure 4.18.

There are two kinds of connections from temperature sensors to substation. One is between each sensor and its extension cables; the other is between the extension cables and the substation. Each temperature sensor has 2 wires to be connected to conditioner and substation. The detailed wire connection and color coding is shown in Figure 4.17.

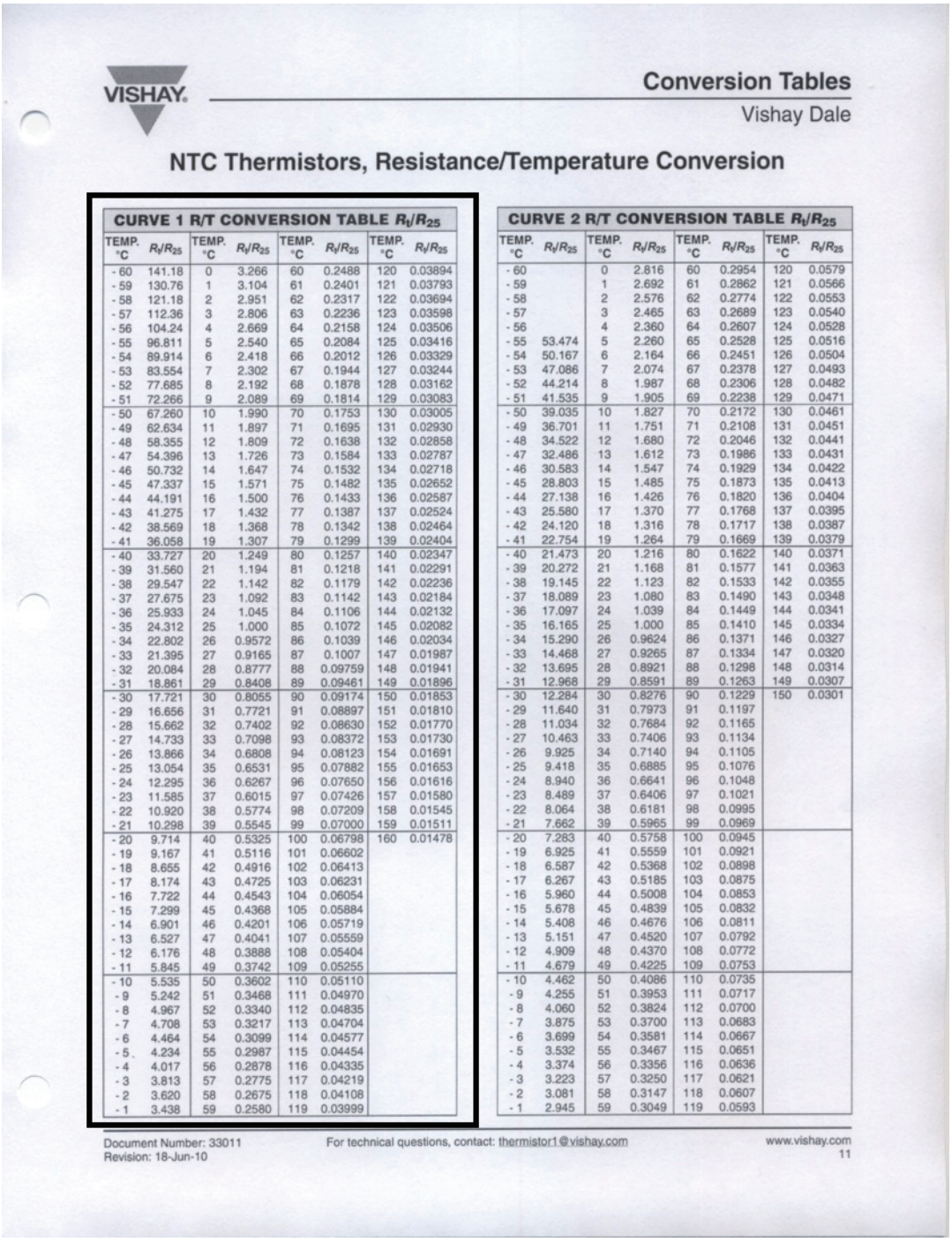

VISHAY

Conversion Tables

Vishay Dale

NTC Thermistors, Resistance/Temperature Conversion

CURVE 1 R/T CONVERSION TABLE R_t/R_{25}

TEMP. °C	R_t/R_{25}	TEMP. °C	R_t/R_{25}	TEMP. °C	R_t/R_{25}	TEMP. °C	R_t/R_{25}
- 60	141.18	0	3.266	60	0.2488	120	0.03894
- 59	130.76	1	3.104	61	0.2401	121	0.03793
- 58	121.18	2	2.951	62	0.2317	122	0.03694
- 57	112.36	3	2.806	63	0.2236	123	0.03598
- 56	104.24	4	2.669	64	0.2158	124	0.03506
- 55	96.811	5	2.540	65	0.2084	125	0.03416
- 54	89.914	6	2.418	66	0.2012	126	0.03329
- 53	83.554	7	2.302	67	0.1944	127	0.03244
- 52	77.685	8	2.192	68	0.1878	128	0.03162
- 51	72.266	9	2.089	69	0.1814	129	0.03083
- 50	67.260	10	1.990	70	0.1753	130	0.03005
- 49	62.634	11	1.897	71	0.1695	131	0.02930
- 48	58.355	12	1.809	72	0.1638	132	0.02858
- 47	54.396	13	1.726	73	0.1584	133	0.02787
- 46	50.732	14	1.647	74	0.1532	134	0.02718
- 45	47.337	15	1.571	75	0.1482	135	0.02652
- 44	44.191	16	1.500	76	0.1433	136	0.02587
- 43	41.275	17	1.432	77	0.1387	137	0.02524
- 42	38.569	18	1.368	78	0.1342	138	0.02464
- 41	36.058	19	1.307	79	0.1299	139	0.02404
- 40	33.727	20	1.249	80	0.1257	140	0.02347
- 39	31.560	21	1.194	81	0.1218	141	0.02291
- 38	29.547	22	1.142	82	0.1179	142	0.02236
- 37	27.675	23	1.092	83	0.1142	143	0.02184
- 36	25.933	24	1.045	84	0.1106	144	0.02132
- 35	24.312	25	1.000	85	0.1072	145	0.02082
- 34	22.802	26	0.9572	86	0.1039	146	0.02034
- 33	21.395	27	0.9165	87	0.1007	147	0.01987
- 32	20.084	28	0.8777	88	0.09759	148	0.01941
- 31	18.861	29	0.8408	89	0.09461	149	0.01896
- 30	17.721	30	0.8055	90	0.09174	150	0.01853
- 29	16.656	31	0.7721	91	0.08897	151	0.01810
- 28	15.662	32	0.7402	92	0.08630	152	0.01770
- 27	14.733	33	0.7098	93	0.08372	153	0.01730
- 26	13.866	34	0.6808	94	0.08123	154	0.01691
- 25	13.054	35	0.6531	95	0.07882	155	0.01653
- 24	12.295	36	0.6267	96	0.07650	156	0.01616
- 23	11.585	37	0.6015	97	0.07426	157	0.01580
- 22	10.920	38	0.5774	98	0.07209	158	0.01545
- 21	10.298	39	0.5545	99	0.07000	159	0.01511
- 20	9.714	40	0.5325	100	0.06798	160	0.01478
- 19	9.167	41	0.5116	101	0.06602		
- 18	8.655	42	0.4916	102	0.06413		
- 17	8.174	43	0.4725	103	0.06231		
- 16	7.722	44	0.4543	104	0.06054		
- 15	7.299	45	0.4368	105	0.05884		
- 14	6.901	46	0.4201	106	0.05719		
- 13	6.527	47	0.4041	107	0.05559		
- 12	6.176	48	0.3888	108	0.05404		
- 11	5.845	49	0.3742	109	0.05255		
- 10	5.535	50	0.3602	110	0.05110		
- 9	5.242	51	0.3468	111	0.04970		
- 8	4.967	52	0.3340	112	0.04835		
- 7	4.708	53	0.3217	113	0.04704		
- 6	4.464	54	0.3099	114	0.04577		
- 5	4.234	55	0.2987	115	0.04454		
- 4	4.017	56	0.2878	116	0.04335		
- 3	3.813	57	0.2775	117	0.04219		
- 2	3.620	58	0.2675	118	0.04108		
- 1	3.438	59	0.2580	119	0.03999		

CURVE 2 R/T CONVERSION TABLE R_t/R_{25}

TEMP. °C	R_t/R_{25}	TEMP. °C	R_t/R_{25}	TEMP. °C	R_t/R_{25}	TEMP. °C	R_t/R_{25}
- 60		0	2.816	60	0.2954	120	0.0579
- 59		1	2.692	61	0.2862	121	0.0566
- 58		2	2.576	62	0.2774	122	0.0553
- 57		3	2.465	63	0.2689	123	0.0540
- 56		4	2.360	64	0.2607	124	0.0528
- 55	53.474	5	2.260	65	0.2528	125	0.0516
- 54	50.167	6	2.164	66	0.2451	126	0.0504
- 53	47.086	7	2.074	67	0.2378	127	0.0493
- 52	44.214	8	1.987	68	0.2306	128	0.0482
- 51	41.535	9	1.905	69	0.2238	129	0.0471
- 50	39.035	10	1.827	70	0.2172	130	0.0461
- 49	36.701	11	1.751	71	0.2108	131	0.0451
- 48	34.522	12	1.680	72	0.2046	132	0.0441
- 47	32.486	13	1.612	73	0.1986	133	0.0431
- 46	30.583	14	1.547	74	0.1929	134	0.0422
- 45	28.803	15	1.485	75	0.1873	135	0.0413
- 44	27.138	16	1.426	76	0.1820	136	0.0404
- 43	25.580	17	1.370	77	0.1768	137	0.0395
- 42	24.120	18	1.316	78	0.1717	138	0.0387
- 41	22.754	19	1.264	79	0.1669	139	0.0379
- 40	21.473	20	1.216	80	0.1622	140	0.0371
- 39	20.272	21	1.168	81	0.1577	141	0.0363
- 38	19.145	22	1.123	82	0.1533	142	0.0355
- 37	18.089	23	1.080	83	0.1490	143	0.0348
- 36	17.097	24	1.039	84	0.1449	144	0.0341
- 35	16.165	25	1.000	85	0.1410	145	0.0334
- 34	15.290	26	0.9624	86	0.1371	146	0.0327
- 33	14.468	27	0.9265	87	0.1334	147	0.0320
- 32	13.695	28	0.8921	88	0.1298	148	0.0314
- 31	12.968	29	0.8591	89	0.1263	149	0.0307
- 30	12.284	30	0.8276	90	0.1229	150	0.0301
- 29	11.640	31	0.7973	91	0.1197		
- 28	11.034	32	0.7684	92	0.1165		
- 27	10.463	33	0.7406	93	0.1134		
- 26	9.925	34	0.7140	94	0.1105		
- 25	9.418	35	0.6885	95	0.1076		
- 24	8.940	36	0.6641	96	0.1048		
- 23	8.489	37	0.6406	97	0.1021		
- 22	8.064	38	0.6181	98	0.0995		
- 21	7.662	39	0.5965	99	0.0969		
- 20	7.283	40	0.5758	100	0.0945		
- 19	6.925	41	0.5559	101	0.0921		
- 18	6.587	42	0.5368	102	0.0898		
- 17	6.267	43	0.5185	103	0.0875		
- 16	5.960	44	0.5008	104	0.0853		
- 15	5.678	45	0.4839	105	0.0832		
- 14	5.408	46	0.4676	106	0.0811		
- 13	5.151	47	0.4520	107	0.0792		
- 12	4.909	48	0.4370	108	0.0772		
- 11	4.679	49	0.4225	109	0.0753		
- 10	4.462	50	0.4086	110	0.0735		
- 9	4.255	51	0.3953	111	0.0717		
- 8	4.060	52	0.3824	112	0.0700		
- 7	3.875	53	0.3700	113	0.0683		
- 6	3.699	54	0.3581	114	0.0667		
- 5	3.532	55	0.3467	115	0.0651		
- 4	3.374	56	0.3356	116	0.0636		
- 3	3.223	57	0.3250	117	0.0621		
- 2	3.081	58	0.3147	118	0.0607		
- 1	2.945	59	0.3049	119	0.0593		

Figure 4.18: NTC thermistors R-T conversion tables

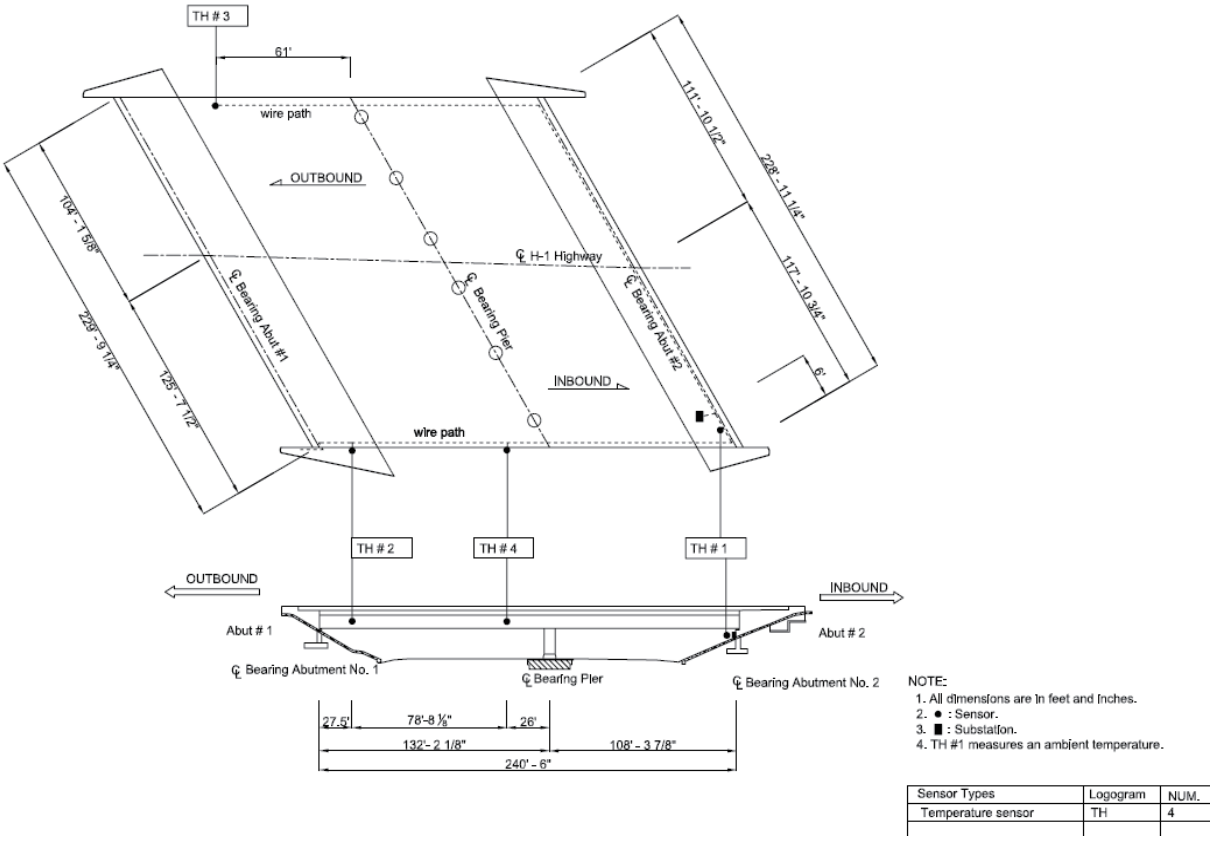

Figure 4.19: Temperature sensor subsystem layout

Chapter 5

INSTALLATION

5.1 Power and traffic control

5.1.1 Introduction

There was no existing standard a.c. power supply in the vicinity of the bridge which could be utilized for the monitoring system. Therefore, a new special electrical power is necessary to this project. The a.c. power source is designed to be extended from a light pole (for the traffic illumination) to the location of the substation.

The BMS installation was done during the two periods in January 2013. The first period was for installing the conduit network and sensors, and the second period was for wiring the sensor system and subsystem. To minimize the effect on the local traffic, the BMS installation process is conducted in the night time from 9PM to 4AM.

5.1.2 Power for BMS equipment

The site plan and electrical panel design of the power are shown in Figures 5.1 and 5.2. The capacity of the a.c. power is chosen to be 2 Kw. Considering that the attainable local a.c. 110V power supply is only for the traffic illumination network and does not operate in the day time, a set of rechargeable battery along with a charging device should be used.

The electrical specifications of the a.c. power are as follows:

1. All work shall be done in strict accordance with the national electric code and other regulatory agency having jurisdiction in this area;

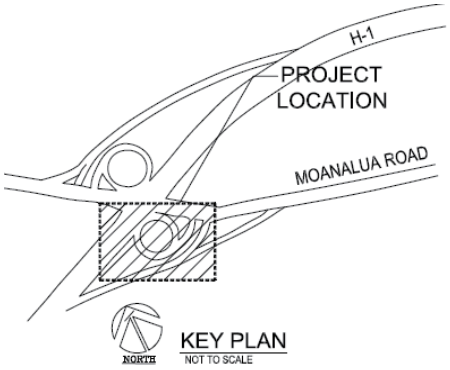

(a) Key plan

(b) Equipment elevation

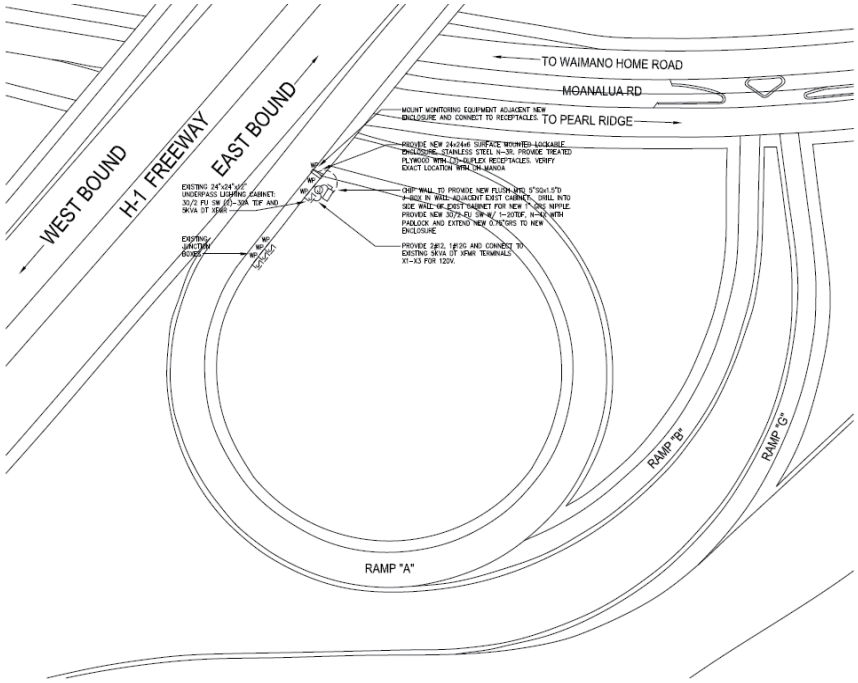

(c) Site plan

Figure 5.1: Electrical power supply site plan

(a) Overview

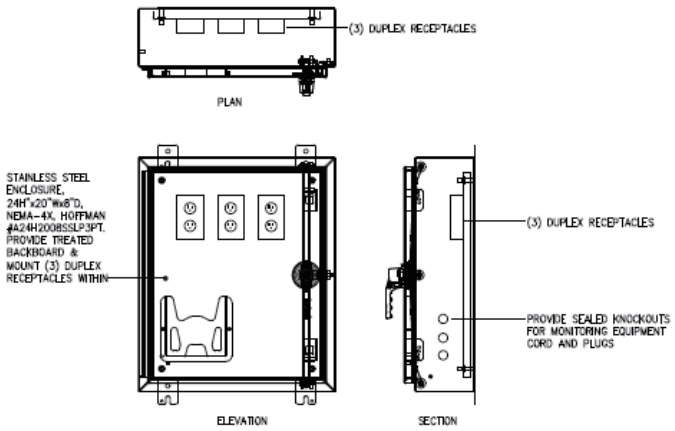

(b) Drawings

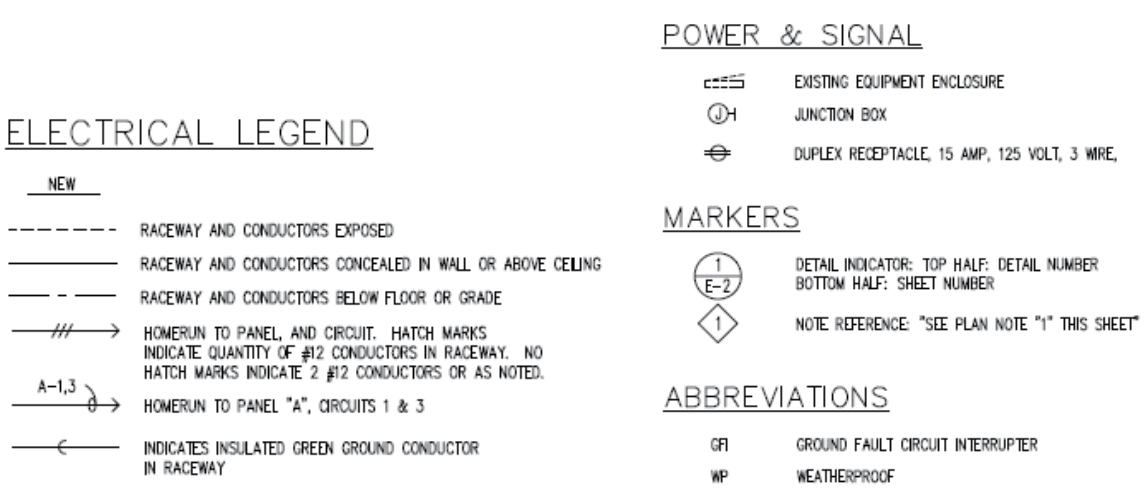

(c) Legend

Figure 5.2: Electrical panel equipment

2. Contractor shall verify existing condition as required for power coordination of new construction involving all trades;

3. All conductors shall be copper, insulation THW, THHM, or THWN, conduit fill, shall not exceed N.E.C. requirements;

4. Conduit concealed in wall and above ceiling shall be EMT, except flexible metal conduit shall be used for light fixture connections, and as indicated on plans, liquid tight flexible metal conduit shall be used for equipment connections. Type "MC" cable shall be allowed where fished and/or as indicated on plans;

5. Contractor shall supply all miscellaneous parts and materials for the complete lighting and electrical systems, provide properly functioning systems;

6. Light fixtures shall be provided with lamps and all accessories required. Substitutions must be approved by engineer. All ballasts shall be energy saving HPF CBM approved and match switches or lighting control system;

7. Locations shown for electrical equipment outlets are approximate. Contractor shall coordinate exact location to watch equipment supplied. Provide cord and plug to match receptacle with N.E.C.;

8. Contractor shall verify loads with all equipment selected and make all changes required to installation is in conformance with N.E.C.;

9. All work shall be performed under the safety regulations of OSHA standard and other agencies as well as safety and quality assurance programs set forth by project documents;

10. All construction practice shall conform to the latest edition of American Electrician's Handbook by Croft;

11. Existing electrical equipment, devices locations shown are approximate and were obtained from existing drawings and a limited amount of field work, Verify existing conditions priori to bidding and make necessary adjustments in the field;

12. Contractor to provide complete submittal approval for all electrical apparatus priori to construction. All receptacles shall be specification grade with gray color and stainless steel cover plates;

13. Obtain and pay for electrical permit, arrange for periodic inspection by regulatory authorities and deliver certificate of final inspection to owner;

14. Electrical contractor shall guarantee inspection for not less than one (1) year. All defective parts, materials and installation shall be replaced at no additional cost to the owner;

15. As a part of contract closeout documents to owner, the electrical contractor shall prove "as-built" drawings to the owner. "As-built" drawings shall be "neatly" done on a new reproduced set of plans. All circuiting and routing of conduits shall be indicated using a "red ink" pen.

5.1.3 Traffic control for installation

The traffic control scheme is divided into the following six phases.

Phase 1 For Moanalua Road lane closure (Figure 5.3)

Phase 2 For Moanalua Road right lane closure (Figures 5.4 and 5.5)

Phase 3 For Moanalua Road left lane closure (Figures 5.6 and 5.7)

Phase 4 For Moanalua Road left lane closure (Figure 5.8)

Phase 5 For Moanalua Road right lane closure (Figure 5.9)

Phase 6 For Moanalua Road Waimalu on ramp closure (Figure 5.10)

5.2 BMS installation

5.2.1 Wire/conduit

For a long-term monitoring system, the conduit for the connecting wires between sensors and substation is required. The overall layout of wire path/conduit system is illustrated in Figure 5.11. The layouts of different portions of wire conduit are depicted in Figures 5.12 to 5.15. The connection of conduit is shown in Figure 5.16. Figure 5.17 shows the photograph for the practice of conduit network.

Besides, to protect workers as well as drivers passing under the bridge, a supporting (scaffold or bridge inspection truck) during the installation of conduit and sensors is also required.

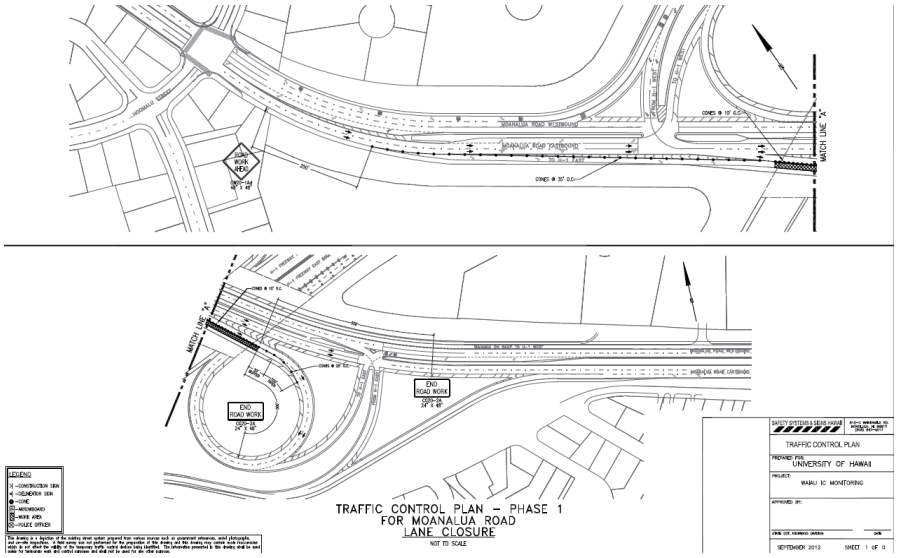

Figure 5.3: Traffic Control: Phase 1

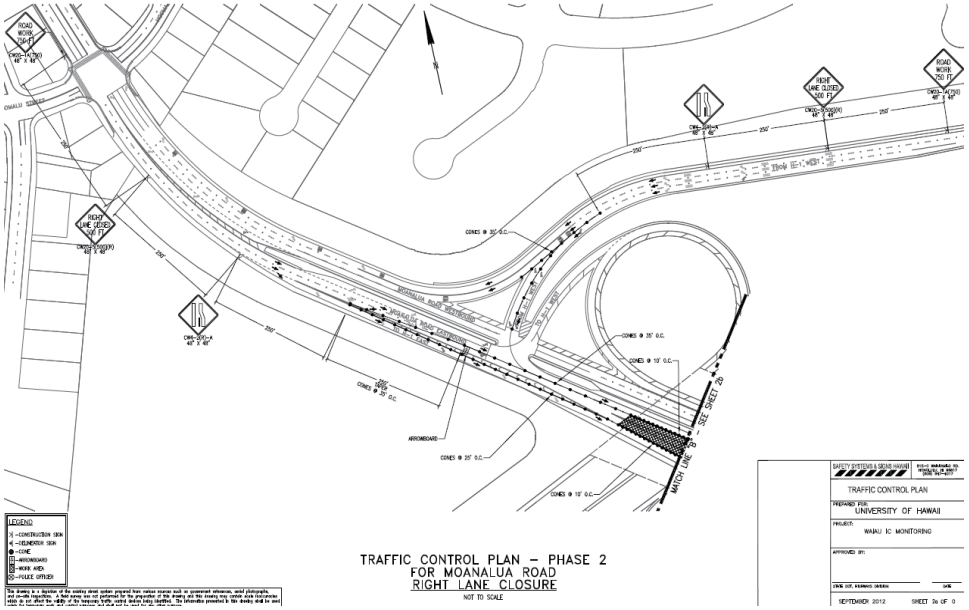

Figure 5.4: Traffic Control: Phase 2a

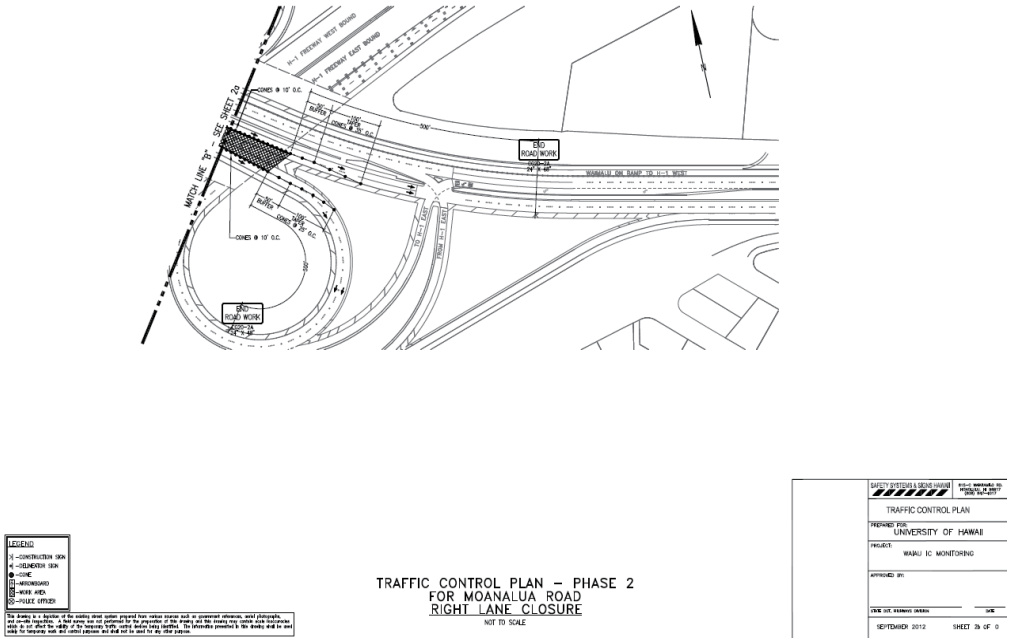

Figure 5.5: Traffic Control: Phase 2b

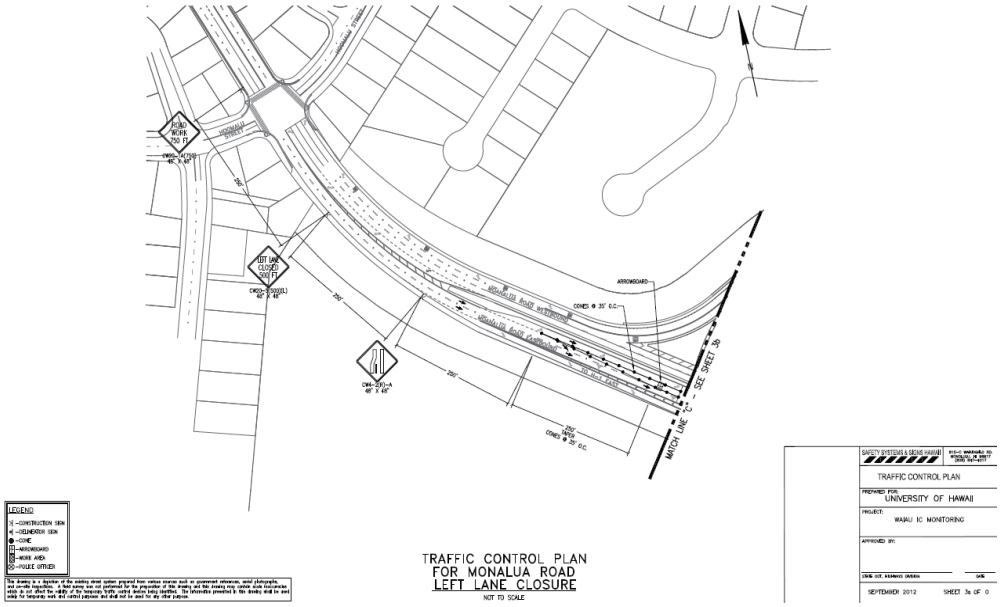

Figure 5.6: Traffic Control: Phase 3a

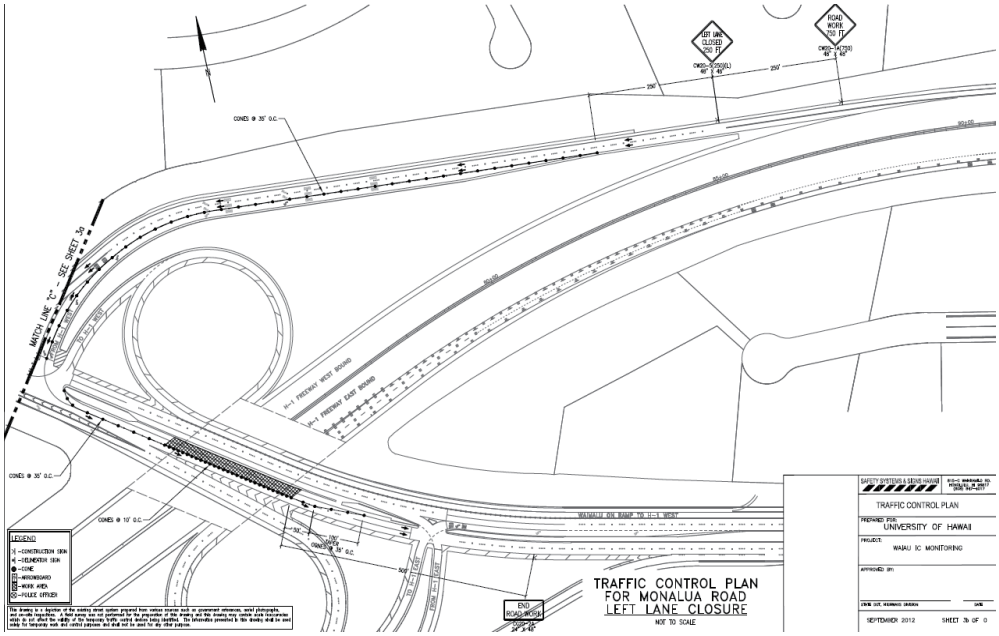

Figure 5.7: Traffic Control: Phase 3b

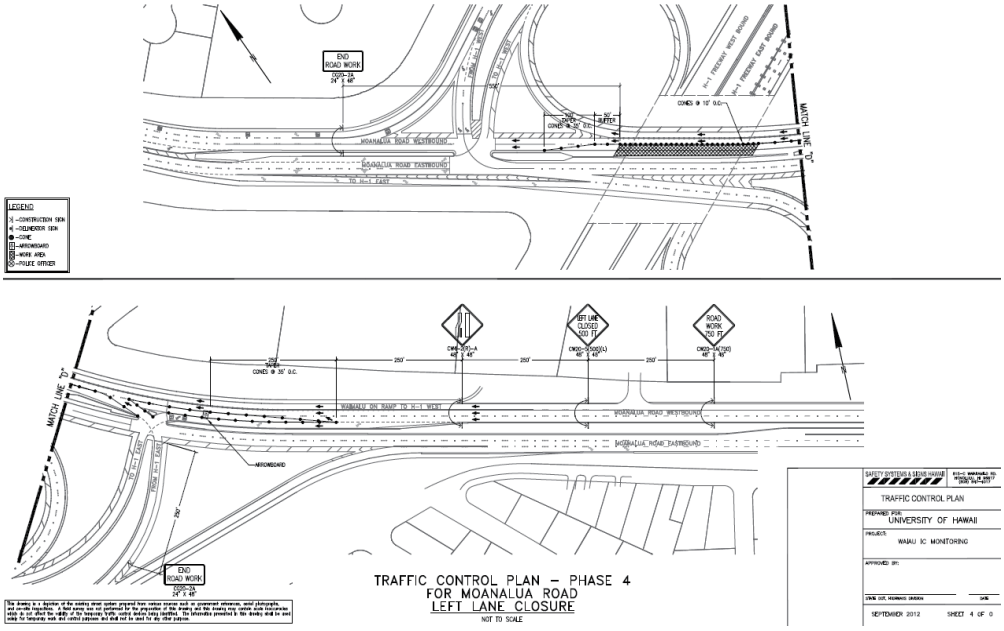

Figure 5.8: Traffic Control: Phase 4

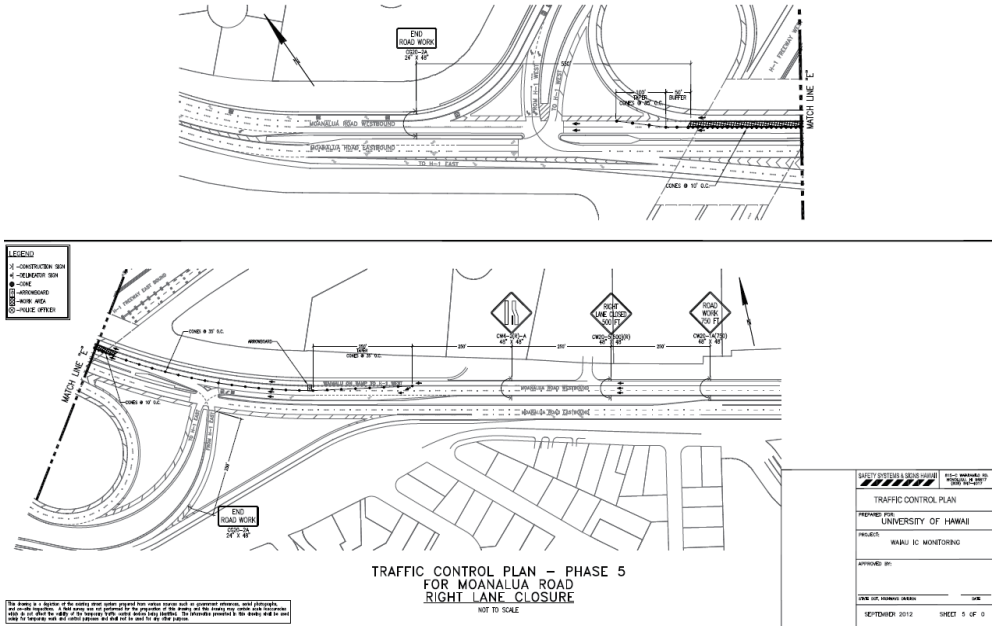

Figure 5.9: Traffic Control: Phase 5

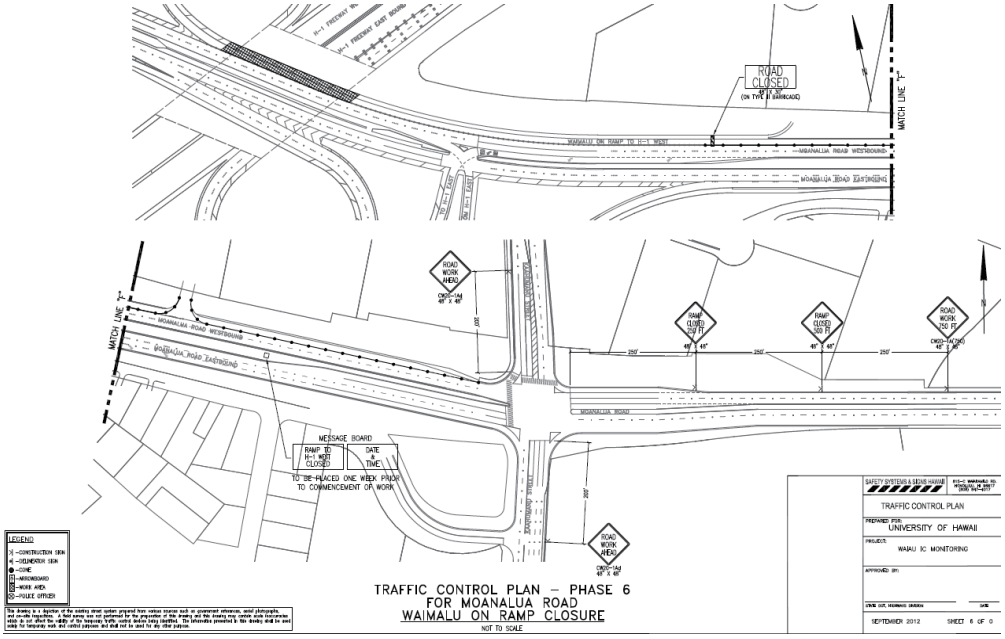

Figure 5.10: Traffic Control: Phase 6

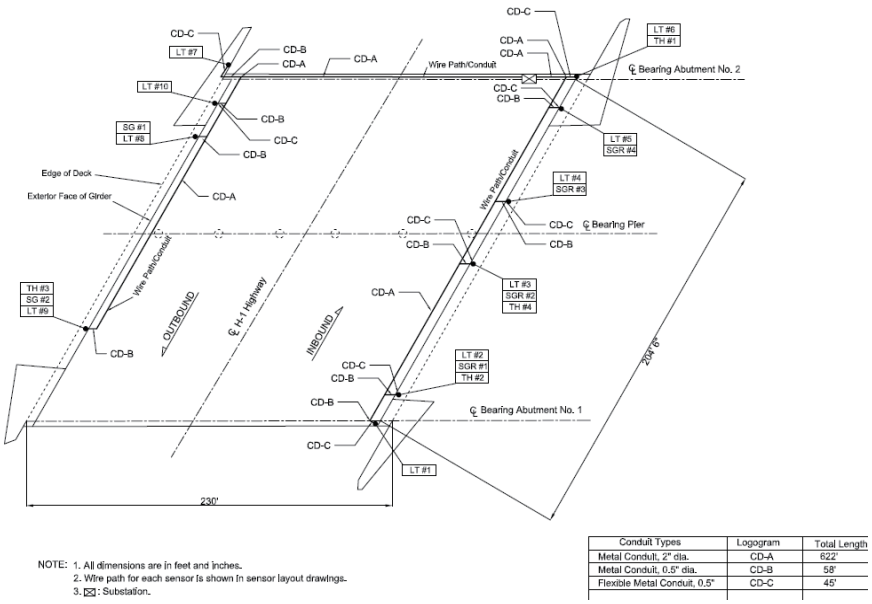

NOTE: 1. All dimensions are in feet and inches.
2. Wire path for each sensor is shown in sensor layout drawings.
3. ⊠: Substation.

Conduit Types	Logogram	Total Length
Metal Conduit, 2" dia.	CD-A	622'
Metal Conduit, 0.5" dia.	CD-B	58'
Flexible Metal Conduit, 0.5"	CD-C	45'

Figure 5.11: Wire conduit layout (Overview)

5.2.2 Sensor system and substation

The LDVT sensor is working in the way of "Bipolar Application". After installation onto the bridge, zero setting was made for each LDVT sensor according to the following procedures:

1. Connect the transducer and power supply as shown in Figure 5.18;
2. Move the armature to an extreme position A so that the reading of voltmeter becomes minimum (about $V_- = 0.7 - 0.8$ V);
3. Move the armature to another extreme position B so that the reading of voltmeter becomes maximum (about $V_+ = 1.5 - 1.6$ V);
4. Adjust the armature to a medium position so that the reading of voltmeter is equal to $(V_- + V_+)/2$;
5. Set the current position as the transducer center stroke position.

One of the installed LVDTs along with a strain rosette are shown in Figure 5.20

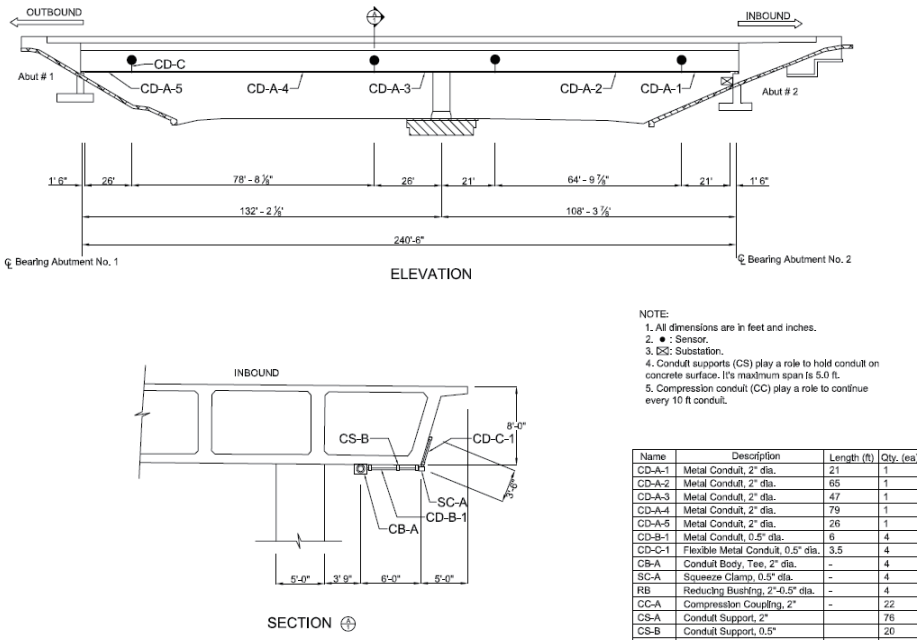

Name	Description	Length (ft)	Qty. (ea
CD-A-1	Metal Conduit, 2" dia.	21	1
CD-A-2	Metal Conduit, 2" dia.	65	1
CD-A-3	Metal Conduit, 2" dia.	47	1
CD-A-4	Metal Conduit, 2" dia.	79	1
CD-A-5	Metal Conduit, 2" dia.	26	1
CD-B-1	Metal Conduit, 0.5" dia.	6	4
CD-C-1	Flexible Metal Conduit, 0.5" dia.	3.5	4
CB-A	Conduit Body, Tee, 2" dia.	-	4
SC-A	Squeeze Clamp, 0.5" dia.	-	4
RB	Reducing Bushing, 2"-0.5" dia.	-	4
CC-A	Compression Coupling, 2"	-	22
CS-A	Conduit Support, 2"		76
CS-B	Conduit Support, 0.5"		20

Figure 5.12: Wire conduit layout (1)

5.2.3 Wireless modem configuration

Data transmission is achieved using a 3G wireless Internet connection. An onCell G3110-HSDPA modem was used for this purpose. The G3110 modem can be connected either to a host computer or router via Ethernet port. When a host computer attempts to connect G3110, both devices should be in the same local area network. The first step is to connect the modem with a host computer. The procedure is described below:

1. Insert the SIM card;
2. Supply 12V for PWR1;
3. Use a cable to connect a computer to G3110;
4. The default IP address of G3110 is 192.168.127.254, the IP address for the computer should be same as G3110 except the last portion. We arbitrarily used 192.168.127. 5 as the IP address of the computer. Click start—Control Panel—view network status and tasks—local area Connection, the dialogue window shows up. Click properties—IPV4, and set IP address as 192.168.127.5;

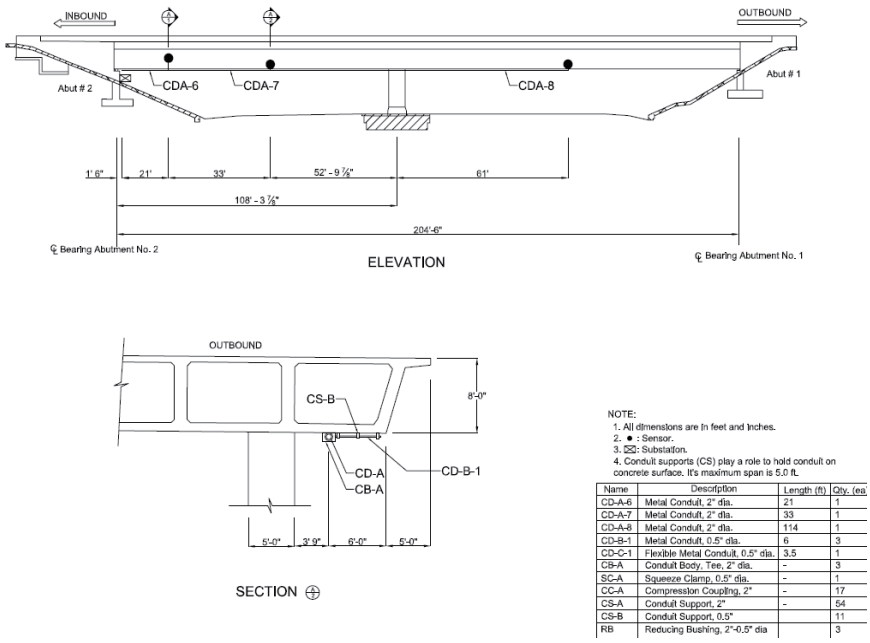

Name	Description	Length (ft)	Qty. (ea
CD-A-6	Metal Conduit, 2" dia.	21	1
CD-A-7	Metal Conduit, 2" dia.	33	1
CD-A-8	Metal Conduit, 2" dia.	114	1
CD-B-1	Metal Conduit, 0.5" dia.	6	3
CD-C-1	Flexible Metal Conduit, 0.5" dia.	3.5	1
CB-A	Conduit Body, Tee, 2" dia.	-	3
SC-A	Squeeze Clamp, 0.5" dia.	-	1
CC-A	Compression Coupling, 2"	-	17
CS-A	Conduit Support, 2"	-	54
CS-B	Conduit Support, 0.5"		11
RB	Reducing Bushing, 2"-0.5" dia		3

Figure 5.13: Wire conduit layout (2)

5. Open a webpage and input the IP address of G3110, the web console is shown to configure the OnCell G3110.

The second step is to use the web console to configure the modem with the following procedure:

1. Set destination address as the static IP address of the computer to which G3110 will transmit data. The static IP address of the server is 128.171.78.61. The path of destination address is Main menu>Serial Port Settings>Port 1> Operation Modes. TCP port number is 63950, and Cmd port number is 63966. The mode is reverse RealCOM;

2. Set up the parameters of the serial port. Set Baud Rate to be 115200, Data Bits to be 8 bits, and select RS-232;

3. Click network settings>GSM GPRS Settings and select GPRS/EDGE/UMTS/HSDPA. The APN is isp.cingular;

The final step is to configure OnCell Windows Drive Manager with the following procedure:

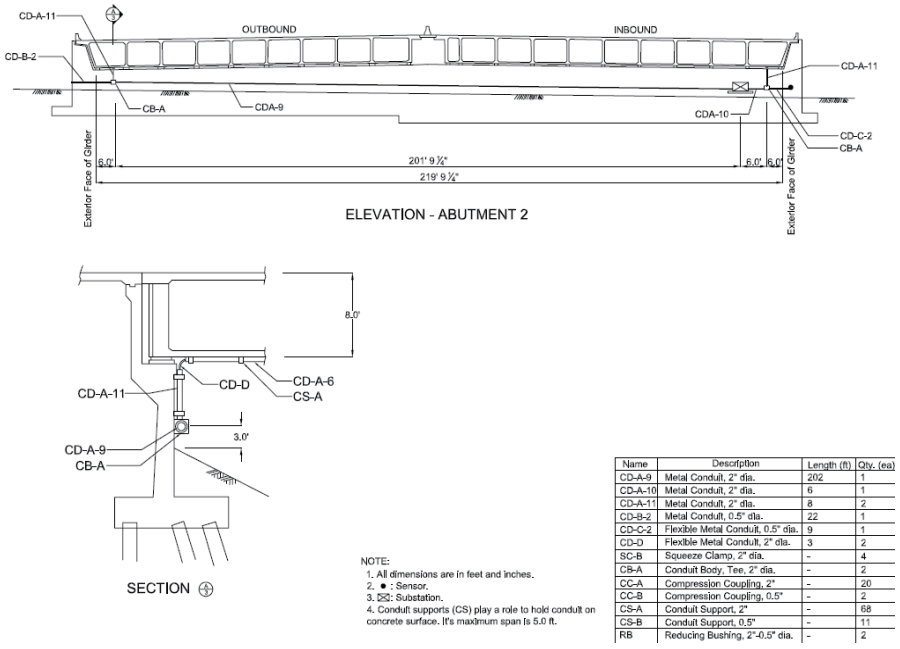

Name	Descrpftion	Length (ft)	Qty. (ea)
CD-A-9	Metal Conduit, 2" dia.	202	1
CD-A-10	Metal Conduit, 2" dia.	6	1
CD-A-11	Metal Conduit, 2" dia.	8	2
CD-B-2	Metal Conduit, 0.5" dia.	22	1
CD-C-2	Flexible Metal Conduit, 0.5" dia.	9	1
CD-D	Flexible Metal Conduit, 2" dia.	3	2
SC-B	Squeeze Clamp, 2" dia.	-	4
CB-A	Conduit Body, Tee, 2" dia.	-	2
CC-A	Compression Coupling, 2"	-	20
CC-B	Compression Coupling, 0.5"	-	2
CS-A	Conduit Support, 2"	-	68
CS-B	Conduit Support, 0.5"	-	11
RB	Reducing Bushing, 2"-0.5" dia.	-	2

Figure 5.14: Wire conduit layout (3)

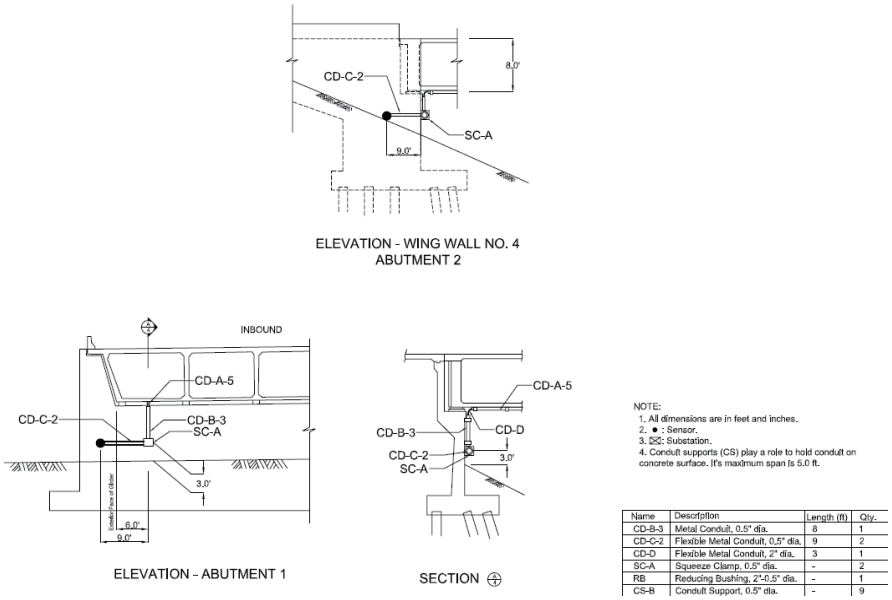

Name	Descrpftion	Length (ft)	Qty.
CD-B-3	Metal Conduit, 0.5" dia.	8	1
CD-C-2	Flexible Metal Conduit, 0.5" dia.	9	2
CD-D	Flexible Metal Conduit, 2" dia.	3	1
SC-A	Squeeze Clamp, 0.5" dia.	-	2
RB	Reducing Bushing, 2"-0.5" dia.	-	1
CS-B	Conduit Support, 0.5" dia.	-	9

Figure 5.15: Wire conduit layout (4)

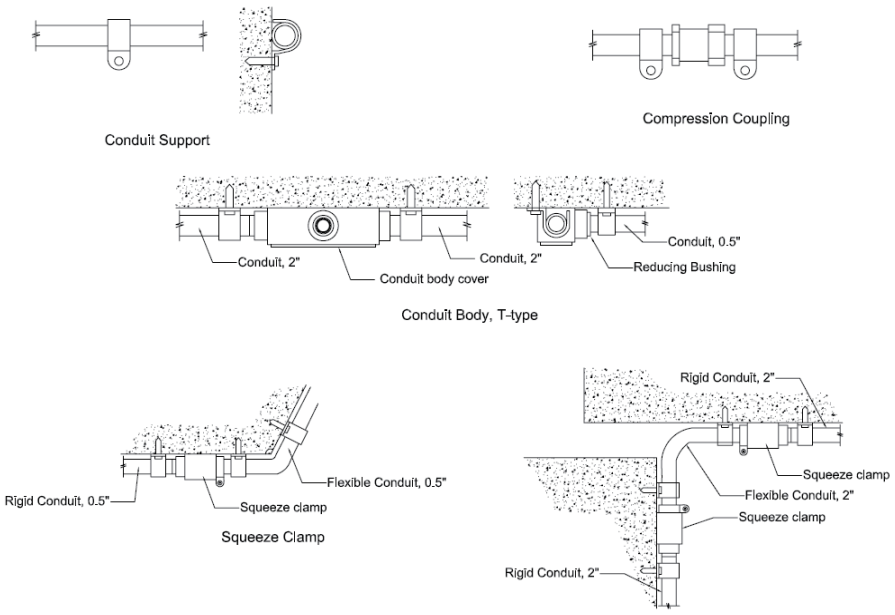

Figure 5.16: Conduit connection

1. Open Add OnCell window and set LAN MAC address to be 00:90:E8:20:3A:32;
2. Select Hi-Performance for Tx mode and enable FIFO.

Configure the server using the same parameters, i.e. the same COM port, Baud rate of 115200, data bits of 8 with stop bit of 1. Then, click Start button to start data transmission. For a successful connection, the lights of PWR1, READY, UMTS, and HSDPA are green and the light for signal is on.

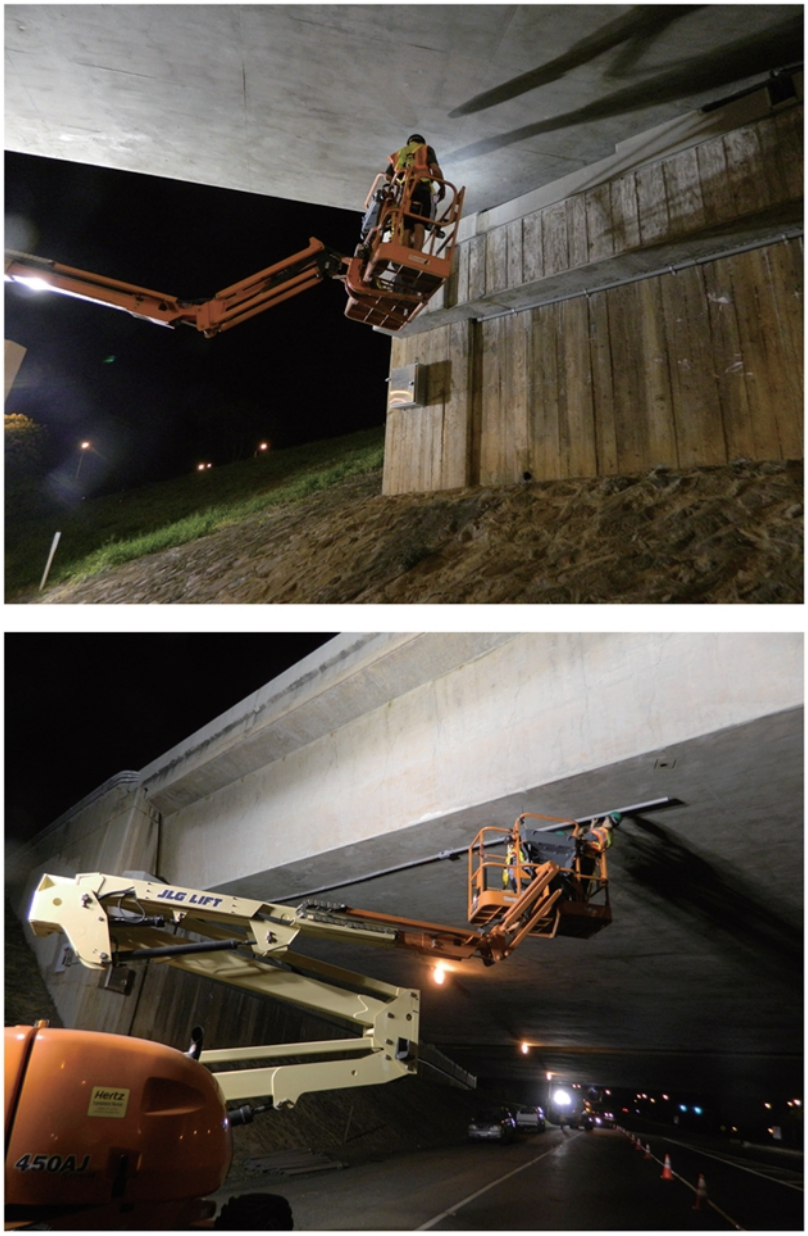

Figure 5.17: Conduit installation

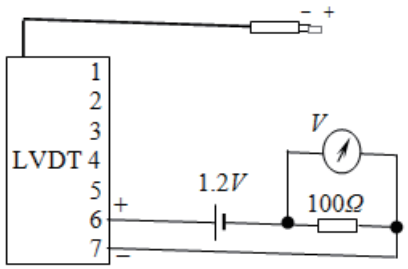

Figure 5.18: LVDT zero setting circuit

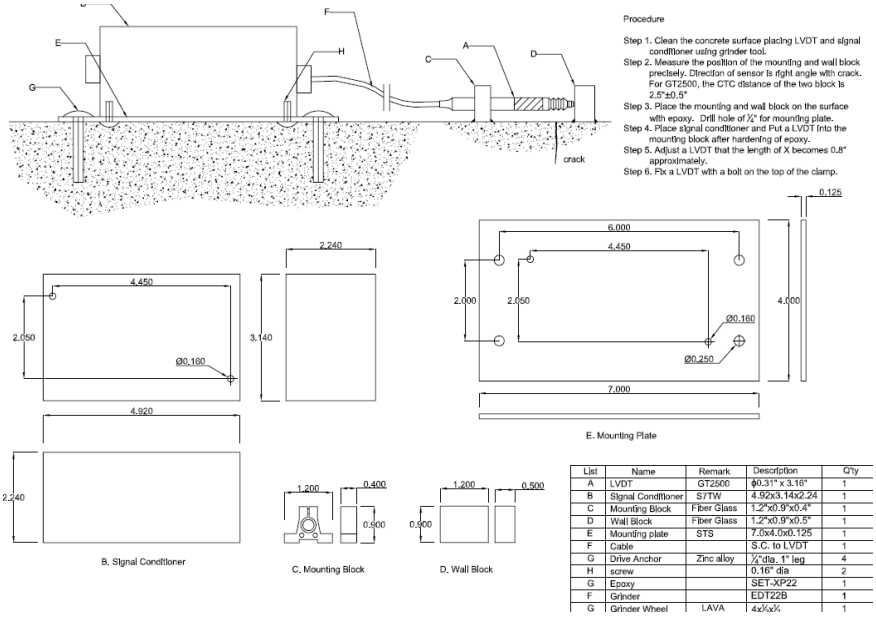

List	Name	Remark	Description	Q'ty
A	LVDT	GT2500	ϕ0.31" x 3.16"	1
B	Signal Condtitoner	ST7W	4.92x3.14x2.24	1
C	Mounting Block	Fiber Glass	1.2"x0.9"x0.4"	1
D	Wall Block	Fiber Glass	1.2"x0.9"x0.5"	1
E	Mounting plate	STS	7.0x4.0x0.125	1
F	Cable		S.C. to LVDT	1
G	Drive Anchor	Zinc alloy	¼"dia. 1" leg	4
H	screw		0.16" dia	2
G	Epoxy		SET-XP22	1
F	Grinder		EDT22B	1
G	Grinder Wheel	LAVA	4x¾x¾	1

Figure 5.19: LVDT installation

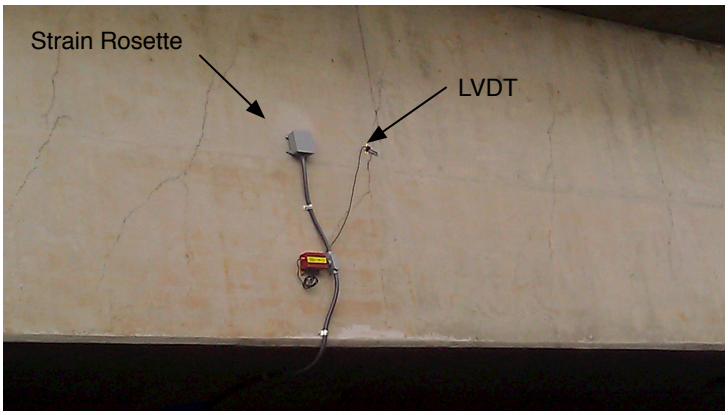

Figure 5.20: LVDT and strain rosette

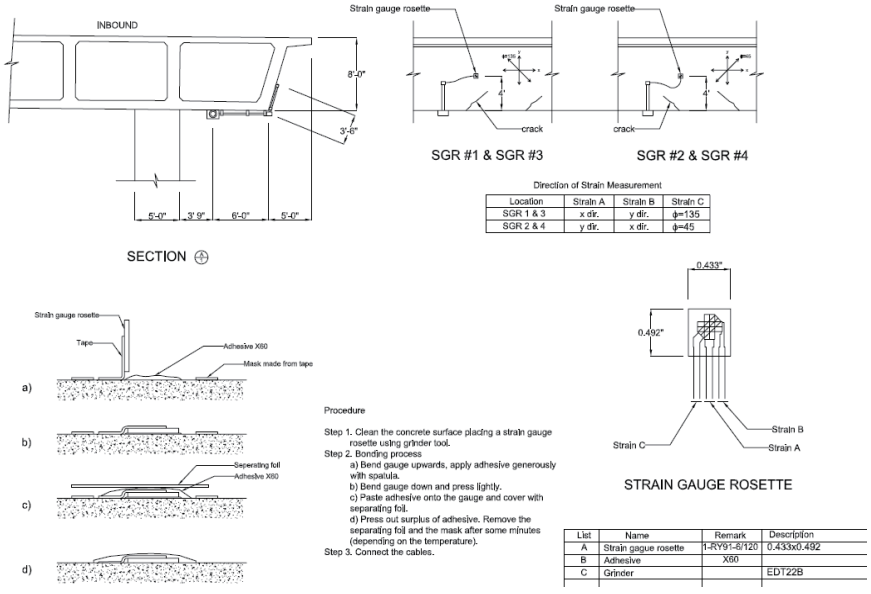

Figure 5.21: Axial strain gauge installation

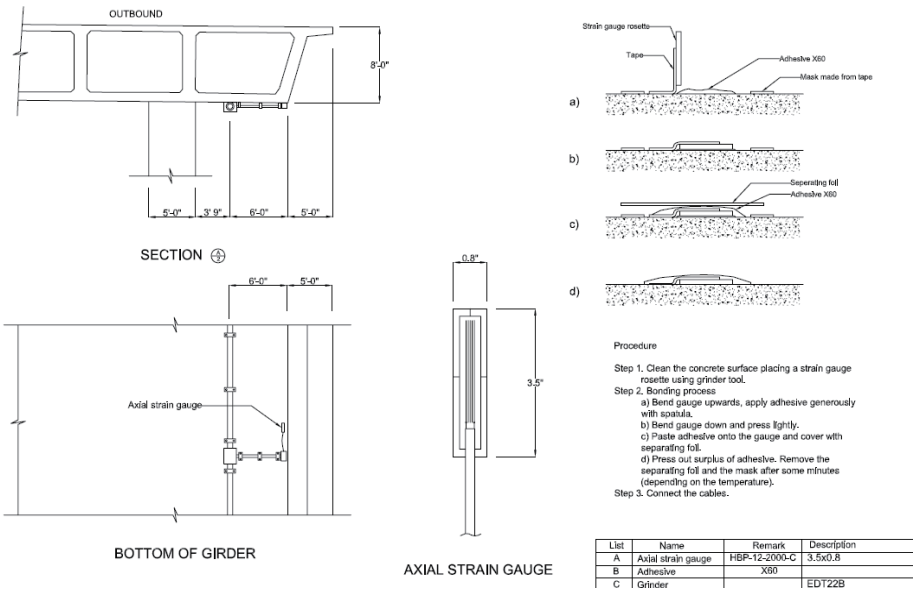

Figure 5.22: Temperature sensor installation

Chapter 6

RESULTS

In situ data is streamed continuously from the substation to the server located at The University of Hawaii. In this chapter, some of the data is presented to demonstrate the functionality and effectiveness of the monitoring system.

Figures 6.1-6.3 respectively show the raw records of displacements from LVDT 3-5 and LVDT 8-10, strains from Sgr2, Sgr3 and Sgr4, and temperatures from Temp 1-4, from 02/17/2013 (Sunday) 10:00PM through 02/19/2013 (Tuesday) 8:00PM. It is apparent that during high volume traffic hours (6-8AM, 5-7PM), the crack openings and the strains are the largest. Throughout the rest of the day, the strains remain close their original value. Figures 6.1 and 6.2 indicate this trend of enlargement of the crack openings throughout the day. Figure 6.3 presents that the ambient temperature changes from 21°C to 27°C each day, with the lowest degree occuring in the early morning (around 4:00AM) and the highest degree registered in the afternoon (about 3:00PM).

The principal strains and orientation angle for three strain gauge rosettes are summarized in Figure 6.4. Figure 6.4(a) depicts how the principal normal strains of the three strain gauge rosettes slowly increase with the time. The largest principal normal strains ϵ_1 and ϵ_2 are detected by Sgr3 and Sgr2 during rush hour, respectively. In addition, the results presented in Figure 6.4(b) show that the orientation angles of Sgr2 and Sgr4 are in the same direction, but different from that of Sgr3. These results are consistent with the orientation of the actual cracks.

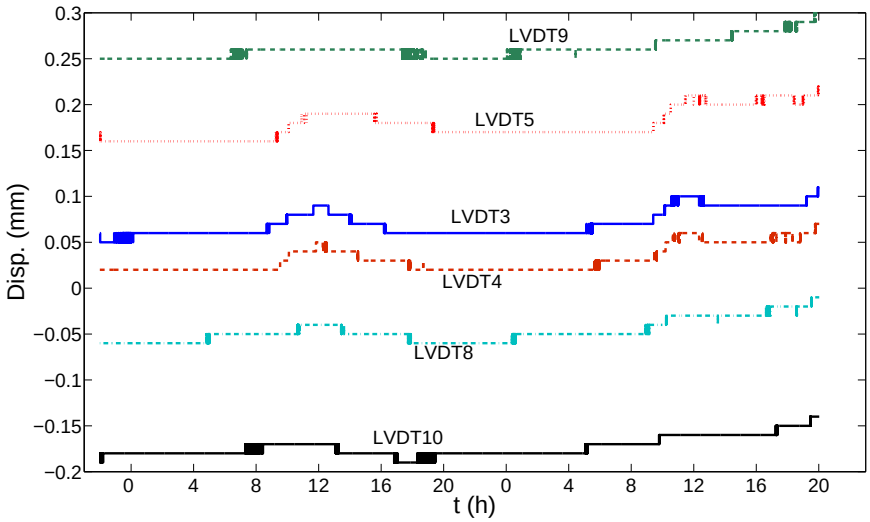

Figure 6.1: Original record of displacements from LVDT3 5 and LDVT8 10

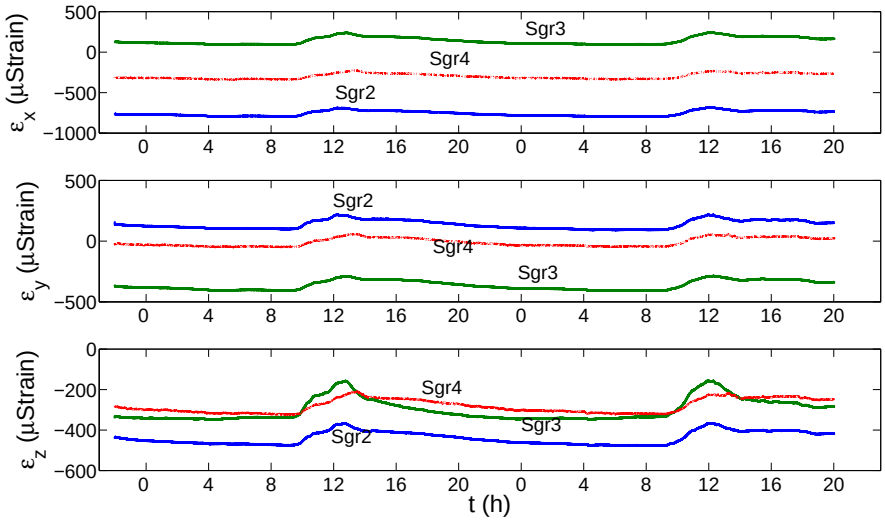

Figure 6.2: Original record of strain gauge rosettes Sgr2, Sgr3 and Sgr4

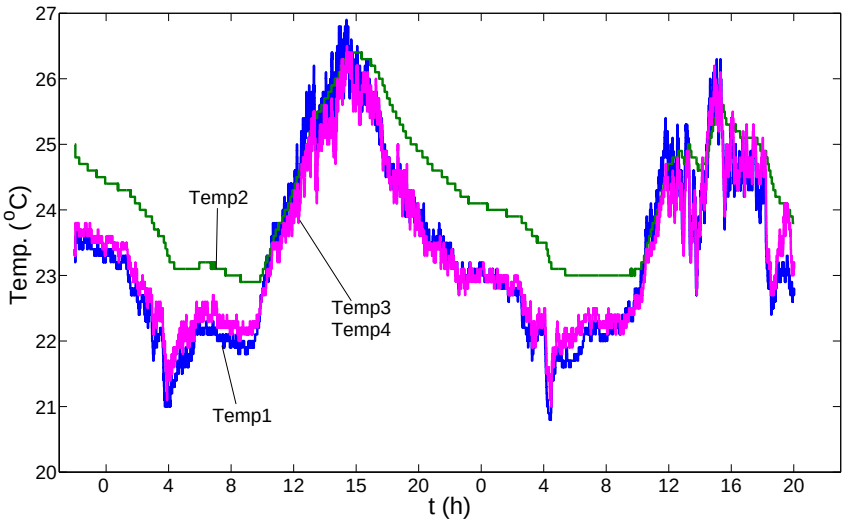

Figure 6.3: Original record of temperatures Temp1, Temp2, Temp3 and Temp4

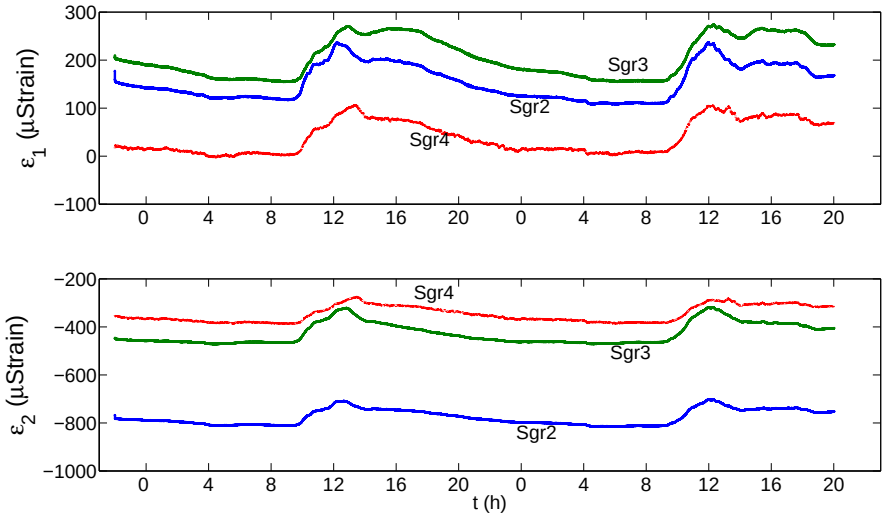

(a) Principal strains

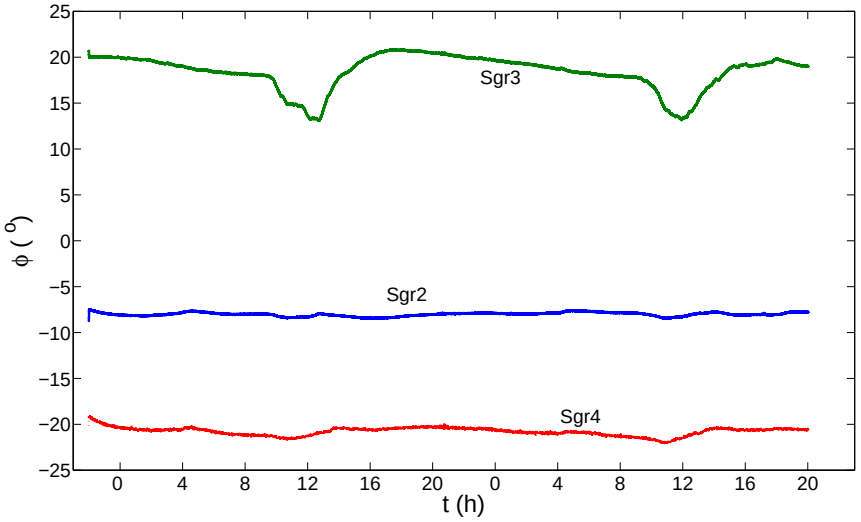

(b) Orientation angle

Figure 6.4: Principal strains converted from strain gauge rosettes Sgr2, Sgr3 and Sgr4

Chapter 7

CONCLUSIONS

This project has resulted in the deployment of an autonomous, realtime, structural health monitoring system. The system has been designed to focus on existing cracks on the box girder of Waiau Interchange, a highway bridge in the Hawaii highway system. Detailed description of the system architecture and the configuration has been included in the report. Data has been continuously streamed via wireless Internet connection from the bridge to the server located at The University of Hawaii. The software developed provides an automatic means of data processing and visualization, thus enabling the autonomy and long-term operation of the system. A subset of the data collected has been analyzed and presented in the report. The results from such preliminary analysis have demonstrated the effectiveness of the system. It has been shown that all of the cracks monitored are active, showing a trend in growth. A more detailed analysis of future data collected over a longer period of time will be conducted in the second phase of the research project. This will allow the crack growth to be validated and quantified to facilitate further safety and reliability evaluation of the entire bridge as well as a system level assessment of the bridge. It is also noted that the crack behavior may be directly related to heavy truck loads, however, such relationship needs further investigation and validation in phase II of the project so that approaches may be developed to detect and quantify overload truck loads and the critical loads that contribute to the growth of the cracks. Additional instruments for capturing bridge dynamics at a finer level and field testing with known truck loads may be needed for such a purposes.

This project has demonstrated the potential benefits of collecting objective data through autonomous structural health monitoring systems as a complimentary approach to the traditional visual inspection. It is recommended that such structural health monitoring systems be deployed on more bridges at critical locations of the

highway system. This will provide the State of Hawaii with an overall evaluation of the reliability of the transportation system. Such an evaluation will lay a solid foundation for the improvement of the resilience and sustainability of the Hawaii transportation infrastructural system.

Bibliography

[1] J. M. Stalling, J. W. Tedesco, M. El-Mihilmy, and M. McCauley, "Field performance of frp bridge repairs," *Journal of Bridge Engineering, ASCE*, vol. 5, no. 2, pp. 107–113, 2000.

[2] E. Aktan, S. Chase, D. Inman, and D. Pines, "Monitoring and managing the health of infrastructure systems," in *the 2001 SPIE Conference on Health Monitoring of Higway Transportation Infrastructure*, (San Diego), March 2001.

[3] N. Catbas, K. Ciloglu, A. Celebioglu, J. Popovics, and E. Aktan, "Fleet health monitoring of large populations: Aged concrete t-beam bridges in pennsylvania," in *6th Annual International Symposium on NDE for Health Monitoring and Diagnostics, SPIE*, (Newport Beach, CA), 2001.

[4] ISIS, "Strengthening reinforced concrete structures with externally bonded fiber reinforced polymers," tech. rep., University of Manitoba, Winnipeg, Manitoba, Canada.

[5] FHWA, "Reliablity of visual inspection for highway bridges, volumn i," tech. rep., 2001.

[6] FHWA, "Reliability of visual inspection for highway bridges, volumn ii," tech. rep., Turner-Fairbank Highway Research Center, 2001.

[7] AASHTO, *LRFD Bridge Design Specifications, 3rd Ed.*

[8] J. Ko and Y. Ni, "Technology developments in structural health monitoring of large-scale bridges," *Engineering Structures*, vol. 27, pp. 1715–1725, 2005.

[9] P. Chang, A. Flatau, and S. Liu, "Review paper: Health monitoring of civil infrastructure," *Structural Health Monitoring*, vol. 2, no. 3, pp. 256–267, 2003.

[10] K. Worden and J. Dulieu-Barton, "An overview of intelligent fault detection in systems and structures," *Structural Health Monitoring*, vol. 3, no. 2, pp. 85–98, 2004.

[11] C. Farrar and K. Worden, "An introduction to structural health monitoring," *Phil. Trans. R. Soc. A*, vol. 365, pp. 303–315, 2007.

[12] K. Chong, "Health monitoring of civil infrastructures," *Structural Health Monitoring, Current Status and Perspectives*, pp. 339–350, 1997.

[13] A. S. Kiremidjian, E. G. Straser, T. Meng, K. Law, and H. Soon, "Structural damage monitoring for civil structures," *Structural Health Monitoring, Current Status and Perspectives*, pp. 371–382, 1997.

[14] S. Doebling, C. Farrar, and M. Prime, "A summary review of vibration-based damage identification methods," *Shock and Vibration Digest*, vol. 30, no. 2, pp. 91–105, 1998.

[15] J. N. Yang, Y. Lei, S. Pan, and N. Huang, "System identification of linear structures based on hilbert-huang spectral analysis, part 1: normal modes," *Earthquake Engrg. and struct. Dyn.*, vol. 32, pp. 1443 – 1467, 2003.

[16] J. N. Yang, Y. Lei, S. Pan, and N. Huang, "System identification of linear structures based on hilbert-huang spectral analysis. part 2: complex modes," *Earthquake Engrg. and struct. Dyn.*, vol. 32, pp. 1533 – 1554, 2003.

[17] J. N. Yang, Y. Lei, S. Lin, and N. Huang, "Hilbert-huang based approach for structural damage detection," *Journal of Engineering Mechanics, ASCE*, vol. 130, no. 1, pp. 85 – 95, 2004.

[18] Z. Sun and C. C. Chang, "Structural damage assessment based on wavelet packet transform," *Journal of Structural Engineering, ASCE*, vol. 128, no. 10, pp. 1354 – 1361, 2003.

[19] A. Hera and Z. Hou, "Application of wavelet approach for asce structural health monitoring benchmark studies," *Journal of Engineering Mechanics, ASCE*, vol. 130, no. 1, pp. 96–104, 2004.

[20] H. Lus, R. Betti, J. Yu, and M. D. Angelis, "Investigation of a system identification methodology in the context of the asce benchmark problem," *Journal of Engineering Mechanics, ASCE*, vol. 130, no. 1, pp. 71–84, 2004.

[21] J. M. Caicedo, S. J. Dyke, and E. A. Johnson, "Natural excitation technique and eigensystem realization algorithm for phase i of the iasc-asce benchmark problem: Simulated data," *Journal of Engineering Mechanics, ASCE*, vol. 130, no. 1, pp. 49 – 60, 2004.

[22] T. W. Ma, H. T. Y. Yang, and C. C. Chang, "Direct damage diagnosis of structural component using global vibration response," in *Proceedings of SPIE* (T. Kundu, ed.), vol. 5394, pp. 192 – 200, 2004.

[23] S. Lu, E. Landis, and D. Keane, "X-ray microtomographic studies of pore structure and permeability in portland cement concrete," *Material and Structures*, vol. 39, pp. 609–618, 2006.

[24] T. Hou and J. Lynch, "Monitoring strain in engineered cementitious composites using wireless sensors," in *Proceedings of the International Conference on Fracture (ICF XI)*, (Turin, Itlay), 2005.

[25] A. Mufti, G. Tadros, and P. Jones, "Field assessment of fibre-optic bragg grating strain sensors in the confederation bridge," *Canadian Journal of Civil Engineering*, vol. 24, no. 6, pp. 963–966, 1997.

[26] T. Chan, H. Tam, Y. Ni, S. Liu, B. Guan, and W. Chung, "Using optical fibre sensors for structural health monitoring of tsing ma bridge," in *Advanced Smart Materials and Structures Technology*, pp. 539–546, 2004.

[27] M. Beard, M. Lowe, and P. Cawley, "Ultrasonic guided waves for the inspection of grouted tendons and bolts," *ASCE Journal of Materials in Civil Engineering*, vol. 15, pp. 212–218, 2003.

[28] X. Chen, J. Kim, K. Kurtis, S. Wu, and L. Jacobs, "Characterization of progressive microcracking in portland cement mortar using nonlinear ultrasonics," *NDT& E International*, vol. 41, pp. 112–118, 2008.

[29] H. A. Sodano, "Development of an automated eddy current structural health monitoring technique with and extended sensing region for corrosion detection," *Structural Health Monitoring*, vol. 6, no. 2, pp. 111–119, 2007.

[30] K. Warnemeunde and H. Wu, "Actively modulated acoustic non-destructive evaluation of concrete," *Cement and Concrete Research*, vol. 34, pp. 563–570, 2004.

[31] X. Han, V. Loggins, Z. Zeng, L. Favro, and R. Thomas, "Mechanical model for the generation of acoustic chaos in sonic ir imaging," *Applied Physics Letters*, vol. 85, no. 8, pp. 1332–1334, 2004.

[32] X. Han, Z. Zeng, W. Li, M. Islam, J. Lu, V. Loggins, E. Yitamben, L. Favro, G. Newaz, and R. Thomas, "Acoustic chaos for enhanced detectability of cracks by sonic infrared imaging," *Journal of Applied Physics*, vol. 95, no. 7, pp. 3792–3797, 2004.

[33] C. Pruell, J. Kim, J. Ou, and L. Jacobs, "Evaluation of plasticity driven material damage using lamb waves," *Applied Physics Letters*, vol. 91, p. 231911, 2007.

[34] S. Kessler and S. Spearing, "Design of a piezoelectric-based structural health monitoring system for damage detection in composite materials," in *Proceedings of the SPIE's 9th International Symposium on Smart Structures and Materials*, 2002.

[35] M. Link, R. Rohrmann, and S. Pietrzko, "Experience with the automated procedure for adjusting the finite element model of a complex highway bridge to experimental model data," in *Proc. of the 14th IMAC*, (Dearborn), 1996.

[36] S. Vurpillot, N. Casanova, D. Inaudi, and P. Kronenberg, "Bridge spatial deformation monitoring with 100 fiber optic deformation sensors," in *SPIE 5th Annual Meeting on Smart Structures and materials*, vol. 3043, pp. 51–57, 1997.

[37] P. e. a. Goltermann, "Smart structures integrated monitoring systems for durability assessment of concrete structures, project report," tech. rep., Ramboll, 2002.

[38] F. Casciati, "An overview of structural health monitoring expertise within the european union," in *Structural Health Monitoring and Intelligent Infrastructure* (Z. Wu and M. Abe, eds.), pp. 31–37, 2003.

[39] D. J. Pines and A. Aktan, "Status of structural health monitoring of long-span bridges in the united states," *Progress in Structural Engineering and Materials*, vol. 4, no. 4, pp. 372–380, 2002.

[40] E. Andersen and L. Pedersen, "Structural monitoring of the great belt east bridge," in *Strait Crossings* (J. Krokebogr, ed.), pp. 184–195, 1994.

[41] M. Cheung, G. Tadros, T. Brown, W. Dilger, and D. Lau, "Field monitoring and research on performance of the confederation bridge," *Canadian Journal of Civil Engineering*, vol. 24, no. 6, pp. 951–962, 1997.

[42] C. Lau, W. Mak, K. Wong, W. Chan, and K. Man, "Structural health monitoring of threee cable-supported bridges in hong kong," in *Structural Health Monitoring* (F. Chang, ed.), pp. 45–60, 1999.

[43] R. Barrish, K. Grimmelsman, and A. Aktan, "Instrumented monitoring of the commodore barry bridge," in *Nondestructive Evaluation of Highways, Utilities, and Pipelines IV* (A. Aktan and S. Gosselin, eds.), pp. 112–126, 2000.

[44] S. Sumitro, Y. Matsui, M. Kono, T. Okamoto, and K. Fujii, "Long span bridge health monitoring in japan," in *Health Monitoring and Management of Civil Infrastructure Systems* (A. Aktan, ed.), pp. 517–524, 2001.

[45] C. S. Kim, S. and J. Lee, "Autonomous on-line health monitoring system for a cable-stayed bridge," in *Proc. of the 1st European Workshop on Structural Health Monitoring* (D. Balageas, ed.), 2002.

APPENDIX

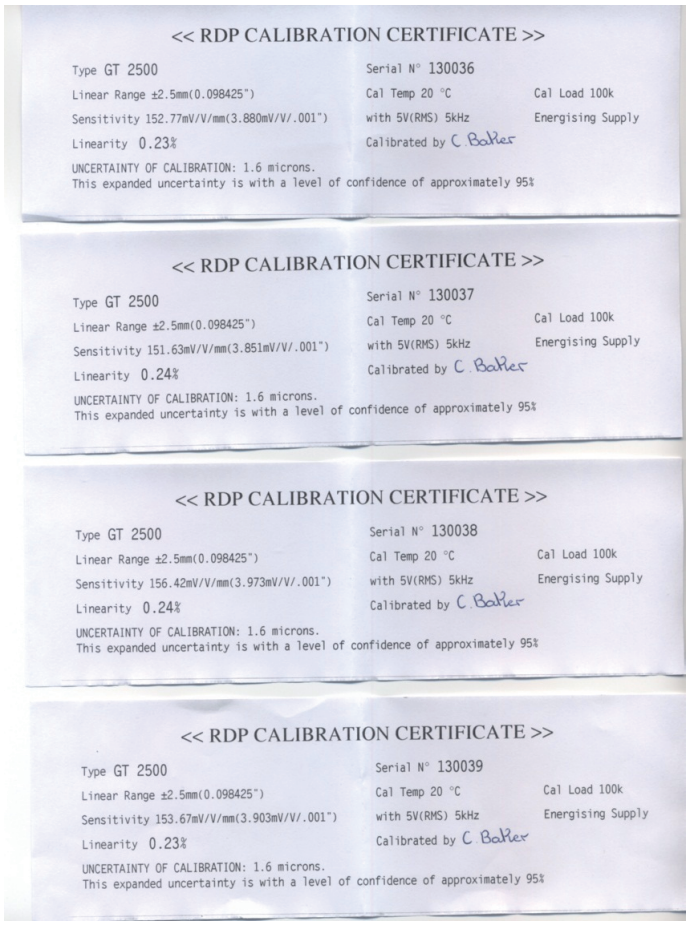

<< RDP CALIBRATION CERTIFICATE >>

Type GT 2500 — Serial N° 130036
Linear Range ±2.5mm(0.098425") — Cal Temp 20 °C — Cal Load 100k
Sensitivity 152.77mV/V/mm(3.880mV/V/.001") — with 5V(RMS) 5kHz — Energising Supply
Linearity 0.23% — Calibrated by C Baker
UNCERTAINTY OF CALIBRATION: 1.6 microns.
This expanded uncertainty is with a level of confidence of approximately 95%

<< RDP CALIBRATION CERTIFICATE >>

Type GT 2500 — Serial N° 130037
Linear Range ±2.5mm(0.098425") — Cal Temp 20 °C — Cal Load 100k
Sensitivity 151.63mV/V/mm(3.851mV/V/.001") — with 5V(RMS) 5kHz — Energising Supply
Linearity 0.24% — Calibrated by C Baker
UNCERTAINTY OF CALIBRATION: 1.6 microns.
This expanded uncertainty is with a level of confidence of approximately 95%

<< RDP CALIBRATION CERTIFICATE >>

Type GT 2500 — Serial N° 130038
Linear Range ±2.5mm(0.098425") — Cal Temp 20 °C — Cal Load 100k
Sensitivity 156.42mV/V/mm(3.973mV/V/.001") — with 5V(RMS) 5kHz — Energising Supply
Linearity 0.24% — Calibrated by C Baker
UNCERTAINTY OF CALIBRATION: 1.6 microns.
This expanded uncertainty is with a level of confidence of approximately 95%

<< RDP CALIBRATION CERTIFICATE >>

Type GT 2500 — Serial N° 130039
Linear Range ±2.5mm(0.098425") — Cal Temp 20 °C — Cal Load 100k
Sensitivity 153.67mV/V/mm(3.903mV/V/.001") — with 5V(RMS) 5kHz — Energising Supply
Linearity 0.23% — Calibrated by C Baker
UNCERTAINTY OF CALIBRATION: 1.6 microns.
This expanded uncertainty is with a level of confidence of approximately 95%

Figure 7.1: Calibration record for LVDT channels LT-01 L̃T-04

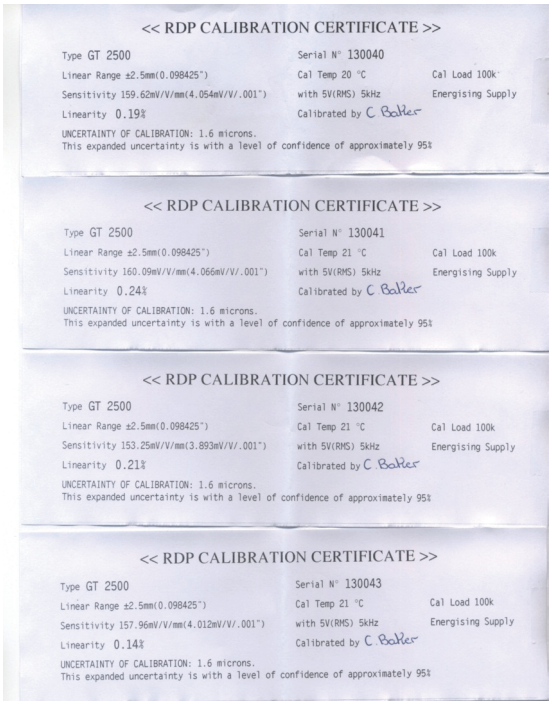

<< RDP CALIBRATION CERTIFICATE >>

Type GT 2500 | Serial N° 130040
Linear Range ±2.5mm(0.098425") | Cal Temp 20 °C | Cal Load 100k
Sensitivity 159.62mV/V/mm(4.054mV/V/.001") | with 5V(RMS) 5kHz | Energising Supply
Linearity 0.19% | Calibrated by C Baker
UNCERTAINTY OF CALIBRATION: 1.6 microns.
This expanded uncertainty is with a level of confidence of approximately 95%

<< RDP CALIBRATION CERTIFICATE >>

Type GT 2500 | Serial N° 130041
Linear Range ±2.5mm(0.098425") | Cal Temp 21 °C | Cal Load 100k
Sensitivity 160.09mV/V/mm(4.066mV/V/.001") | with 5V(RMS) 5kHz | Energising Supply
Linearity 0.24% | Calibrated by C Baker
UNCERTAINTY OF CALIBRATION: 1.6 microns.
This expanded uncertainty is with a level of confidence of approximately 95%

<< RDP CALIBRATION CERTIFICATE >>

Type GT 2500 | Serial N° 130042
Linear Range ±2.5mm(0.098425") | Cal Temp 21 °C | Cal Load 100k
Sensitivity 153.25mV/V/mm(3.893mV/V/.001") | with 5V(RMS) 5kHz | Energising Supply
Linearity 0.21% | Calibrated by C Baker
UNCERTAINTY OF CALIBRATION: 1.6 microns.
This expanded uncertainty is with a level of confidence of approximately 95%

<< RDP CALIBRATION CERTIFICATE >>

Type GT 2500 | Serial N° 130043
Linear Range ±2.5mm(0.098425") | Cal Temp 21 °C | Cal Load 100k
Sensitivity 157.96mV/V/mm(4.012mV/V/.001") | with 5V(RMS) 5kHz | Energising Supply
Linearity 0.14% | Calibrated by C Baker
UNCERTAINTY OF CALIBRATION: 1.6 microns.
This expanded uncertainty is with a level of confidence of approximately 95%

Figure 7.2: Calibration record for LVDT channels LT-05 $\tilde{\text{L}}$T-08

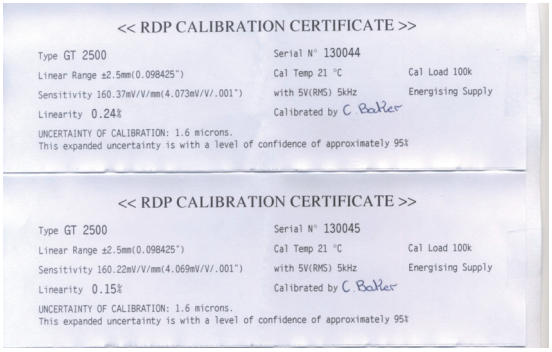

<< RDP CALIBRATION CERTIFICATE >>

Type GT 2500 | Serial N° 130044
Linear Range ±2.5mm(0.098425") | Cal Temp 21 °C | Cal Load 100k
Sensitivity 160.37mV/V/mm(4.073mV/V/.001") | with 5V(RMS) 5kHz | Energising Supply
Linearity 0.24% | Calibrated by C Baker
UNCERTAINTY OF CALIBRATION: 1.6 microns.
This expanded uncertainty is with a level of confidence of approximately 95%

<< RDP CALIBRATION CERTIFICATE >>

Type GT 2500 | Serial N° 130045
Linear Range ±2.5mm(0.098425") | Cal Temp 21 °C | Cal Load 100k
Sensitivity 160.22mV/V/mm(4.069mV/V/.001") | with 5V(RMS) 5kHz | Energising Supply
Linearity 0.15% | Calibrated by C Baker
UNCERTAINTY OF CALIBRATION: 1.6 microns.
This expanded uncertainty is with a level of confidence of approximately 95%

Figure 7.3: Calibration record for LVDT channels LT-09 $\tilde{\text{L}}$T-10

HBP SERIES POLYIMIDE CARRIER STRAIN GAGES

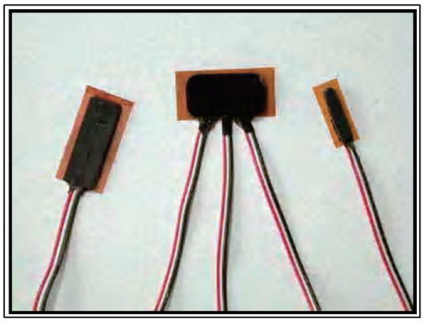

HPI polyimide carrier HBP series strain gages utilize bonded foil strain gages in a pre-wired and waterproofed package similar to our HBW weldable strain gage series. The polyimide shim permits extremely easy installation with any conventional room temperature curing strain gage adhesives including: M-Bond 200, M-Bond 300, AE-10, EASTMAN 910, or EPY-150. Configurations include axial, shear, rosette patterns. OEM pricing is available and custom versions are welcome.

The strain gage offers an alternative to weldable gages for many field applications (it can be installed on all materials). Its pricing will also make it attractive for many less rigorous applications because of the time savings it will offer the installer.

Gage Designation:	HBP-35-250-6-3VR, STANDARD
Active Grid:	1/4" or 1/8"
Strain Range:	± 2000 με nominal
Gage Resistance:	350 ohm standard, 120 ohm optional
Temperature Range:	-50°F to 180°F
Carrier:	1.00" (L) x 0.50" (W) x 0.005" (T) Polyimide May be trimmed to approximately 0.90" (L) x 0.40" (W)
Gage Factor:	2.1 nominal
Gage Adhesive:	Treated backing compatible with most room temperature curing strain gage adhesives
Availability:	Stock

HPI HITEC PRODUCTS, INC.
P.O. Box 790 • Ayer, MA 01432 USA
Tel: 978-772-6963 • Fax: 978-772-6966
www.hitecprod.com

Figure 7.4: HBP series polyimide carrier strain gauges

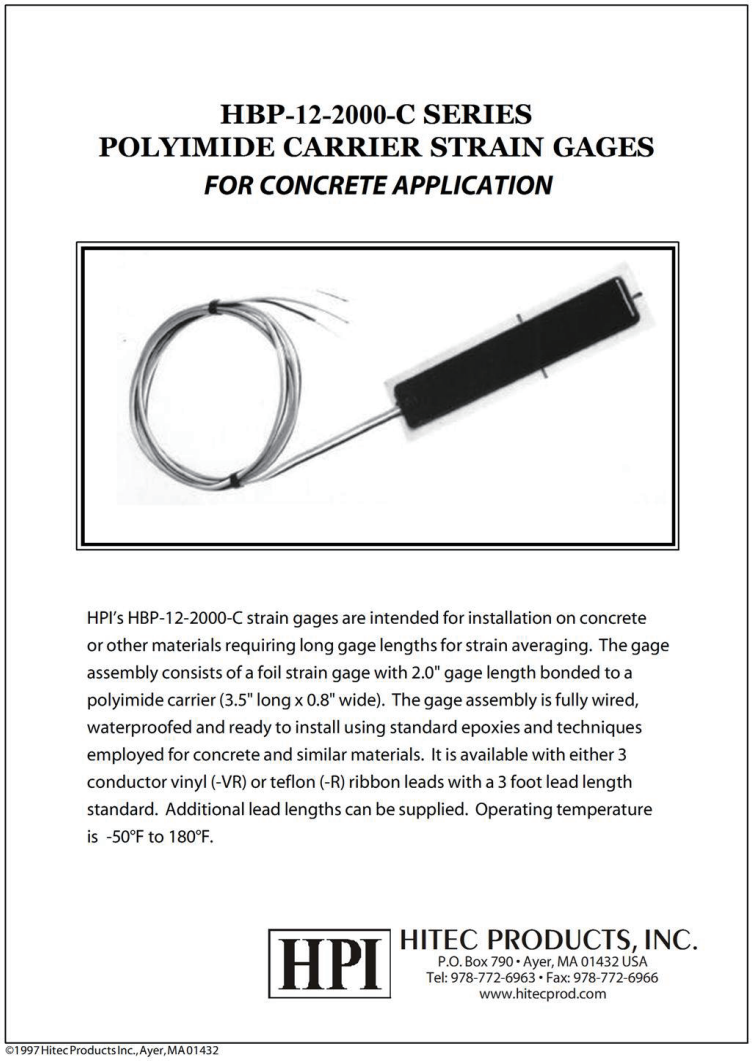

HBP-12-2000-C SERIES
POLYIMIDE CARRIER STRAIN GAGES
FOR CONCRETE APPLICATION

HPI's HBP-12-2000-C strain gages are intended for installation on concrete or other materials requiring long gage lengths for strain averaging. The gage assembly consists of a foil strain gage with 2.0" gage length bonded to a polyimide carrier (3.5" long x 0.8" wide). The gage assembly is fully wired, waterproofed and ready to install using standard epoxies and techniques employed for concrete and similar materials. It is available with either 3 conductor vinyl (-VR) or teflon (-R) ribbon leads with a 3 foot lead length standard. Additional lead lengths can be supplied. Operating temperature is -50°F to 180°F.

HPI HITEC PRODUCTS, INC.
P.O. Box 790 • Ayer, MA 01432 USA
Tel: 978-772-6963 • Fax: 978-772-6966
www.hitecprod.com

Figure 7.5: HBP-12-2000-C series polyimide carrier strain gauges

Specifications

strain gage construction		foil SG complete with embedded measuring grid
measuring grid		
material		Constantan foil
thickness	µm *(microinch)*	3.8 or 5 *(150 or 197)*, depending on strain gage type
carrier		
material		polyimide
thickness	µm *(microinch)*	45 ± 10 *(1.772 ± 394)*
cover		
material		polyimide
thickness	µm *(microinch)*	25 ± 5 *(984 ± 197)*
connections		nickel plated Cu leads, approx. 30 mm *(1.18 inch)* in length.
for strain gages without leads		integrated solder tabs, approx. 1.5 mm *(0.059 inch)* in length, approx. 1.6 ... 2.2mm *(0.063... 0.087 inch)* wide
nominal resistance[2]	Ω	120, 350, 700, or 1000, depending on SG type
resistance tolerance	%	± 0.3 without; ± 0.35 with leads
gage factor		approx. 2
nominal value of the gage factor		specified on each package
gage factor tolerance for 0.6mm *(0.024 inch)* and 1.5mm *(0.059 inch)* measuring grid length	%	± 1.5
for ≧3 mm *(0.118 inch)* measuring grid length	%	± 1
temperature coefficient of the gage factor	1/K *(1/°F)*	approx. (115 ± 10) · 10^{-6} *(64 ± 5.5) · 10^{-6}*
nominal value of the temperature coefficient of the gage factor		specified on each package
reference temperature	°C *(°F)*	23 *(73.4)*
operating temperature range		
for absolute, i.e. zero point related measurements	°C *(°F)*	-70... +200 *(-94... +392)*
for relative, i.e. not zero point related measurements	°C *(°F)*	-200... +200 *(-328... +392)*
transverse sensitivity		specified on each package
within reference temperature range using adhesive Z 70	%	- 0.1
on strain gage type LY 11-6/120		
temperature response		specified on each package
temperature response at customer's choice matched to the thermal expansion coefficient		
α for ferritic steel	1/K *(1/°F)*	10.8 · 10^{-6} *(6.0 · 10^{-6})*
α for aluminum	1/K *(1/°F)*	23 · 10^{-6} *(12.8 · 10^{-6})*
α for plastic material	1/K *(1/°F)*	65 · 10^{-6} *(36.1 · 10^{-6})*
α for austenitic steel	1/K *(1/°F)*	16 · 10^{-6} *(8.9 · 10^{-6})*
α for titanium/ gray steel	1/K *(1/°F)*	9 · 10^{-6} *(5.0 · 10^{-6})*
α for molybdenum	1/K *(1/°F)*	5.4 · 10^{-6} *(3.0 · 10^{-6})*
α for quartz	1/K *(1/°F)*	0.5 · 10^{-6} *(0.3 · 10^{-6})*
tolerance of the temperature response	1/K *(1/°F)*	±0.3 · 10^{-6} *(±0.17 · 10^{-6})*
temperature response with matching in the range of[3]	°C *(°F)*	-10... +120 *(14... 248)*
mechanical hysteresis[1]		
at reference temperature and strain ε = ± 1,000 µm/m *(microstrain)*		
on strain gage type LY 11-6/120		
at 1st load cycle and adhesive Z 70	µm/m *(microstrain)*	1
at 3rd load cycle and adhesive Z 70	µm/m *(microstrain)*	0.5
at 1st load cycle and adhesive X 60	µm/m *(microstrain)*	2.5
at 3rd load cycle and adhesive X 60	µm/m *(microstrain)*	1
at 1st load cycle and adhesive EP 250	µm/m *(microstrain)*	1
at 3rd load cycle and adhesive EP 250	µm/m *(microstrain)*	1
maximum elongation[1]		
at reference temperature using adhesive Z 70		
on strain gage type LY 11-6/120		
absolute strain value ε for positive direction	µm/m *(microstrain)*	50,000 (≙5 %)
absolute strain value ε for negative direction	µm/m *(microstrain)*	50,000 (≙5 %)
fatigue life[1]		
at reference temperature using adhesive X 60		
on strain gage type LY 11-6/120		
number of load cycles L_W at		
alternating strain ε_W = ± 1,000 µm/m and zero point drift ε_m Δ ≦300 µm/m *(microstrain)*		>> 10^7 (test was interrupted at 10^7)
ε_m Δ≦ 30 µm/m *(microstrain)*		> 10^7 (test was interrupted at 10^7)
minimum radius of curvature, longitudinal and transverse, at reference temperature		
for strain gages with leads	mm *(inch)*	0.3 *(0.012)*
for strain gages with integrated solder tabs		
within the measuring grid area	mm *(inch)*	0.3 *(0.012)*
within the area of the solder tabs	mm *(inch)*	2 *(0.079)*
bonding material that can be used		
cold curing adhesives		Z 70; X 60; X 280
hot curing adhesives		EP 250; EP 310S

[1] The data depend on the various parameters of the specific application and are therefore stated for representative examples only.
[2] With measuring grid lengths of 0.6 mm *(0.024 inch)*, the nominal resistance may deviate by ± 1%. For the types LY 51/ LY5x the deviation is ± 0.75%. For XY9x, RY9x and the KY types (per chain) it is ± 0.5%.
[3] Matching to plastic (code numer 8) is only possible in the temperature range of -10°C...+50°C *(14°F...+122°F)*.

Figure 7.6: Strain gauge rosettes DMSSerie Y

SCM5B38

Strain Gage Input Modules, Narrow Bandwidth

FEATURES

- INTERFACES TO 100Ω THRU 10kΩ, FULL-BRIDGE, HALF-BRIDGE, OR QUARTER-BRIDGE STRAIN GAGES
- HIGH LEVEL VOLTAGE OUTPUTS
- 1500Vrms TRANSFORMER ISOLATION
- ANSI/IEEE C37.90.1-1989 TRANSIENT PROTECTION
- INPUT PROTECTED TO 240VAC CONTINUOUS
- FULLY ISOLATED EXCITATION SUPPLY
- 160dB CMR
- 4Hz SIGNAL BANDWIDTH
- ±0.08% ACCURACY
- ±0.02% LINEARITY
- ±1µV/°C DRIFT
- MIX AND MATCH SCM5B TYPES ON BACKPANEL
- CSA CERTIFIED, FM APPROVED, CE COMPLIANT

DESCRIPTION

Each SCM5B38 Strain Gage input module provides a single channel of Strain Gage input which is filtered, isolated, amplified, and converted to a high level analog voltage output (Figure 1). This voltage output is logic switch controlled, which allows these modules to share a common analog bus without the requirement of external multiplexers.

The SCM5B modules are designed with a completely isolated computer side circuit which can be floated to ±50V from Power Common, pin 16. This complete isolation means that no connection is required between I/O Common and Power Common for proper operation of the output switch. If desired, the output switch can be turned on continuously by simply connecting pin 22, the Read-Enable pin to I/O Common, pin 19.

The SCM5B38 can interface to full-bridge or half-bridge transducers with a nominal resistance of 100Ω to 10kΩ. A matched pair of bridge-completion resistors (to ±1mV at +10V excitation) allows use of low cost half-bridge or quarter-bridge transducers (Figures 2, 3, 4).

Strain Gage excitation is provided from the module by a very stable 10V or 3.333V source. The excitation supply is fully isolated, allowing the amplifier inputs to operate over the full range of the excitation voltage. This feature offers significant flexibility in real world applications. Full scale sensitivities of 2mV/V, 3mV/V or 10mV/V are offered as standard. With 10V excitation, this results in ±20mV, ±30mV or ±100mV full scale input range producing ±5V full scale output.

After initial field side filtering the input signal is chopped by a proprietary chopper circuit. Isolation is provided by transformer coupling, again using a proprietary technique to suppress transmission of common mode spikes or surges. The module is powered from +5VDC, ±5%.

Special input circuits on the SCM5B38 module provide protection of the signal inputs and the isolated excitation supply up to 240VAC.

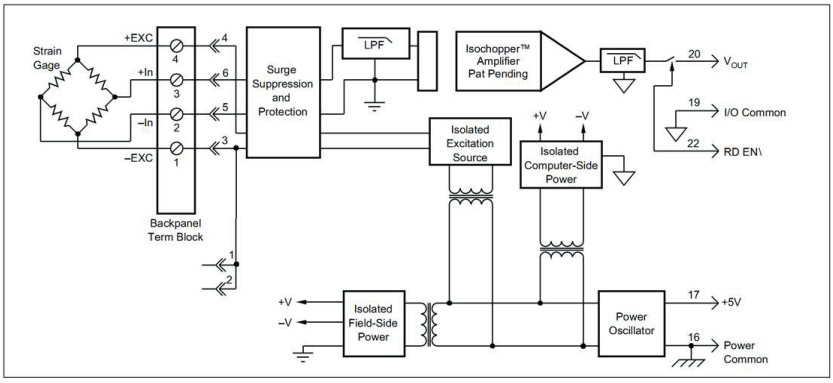

FIGURE 1. SCM5B38 Block Diagram.

Figure 7.7: SCM5B38 input modules

SPECIFICATIONS Typical at T_A = +25°C and +5V power.

Module	Full Bridge SCM5B38-31, -32, -35, -36, -37	Half Bridge SCM5B38-33, -34
Input Range	±10mV to ±100mV	*
Input Bias Current	±0.5nA	*
Input Resistance		
Normal	50MΩ	*
Power Off	40kΩ	*
Overload	40kΩ	*
Signal Input Protection		
Continuous	240Vrms max	*
Transient	ANSI/IEEE C37.90.1-1989	*
Excitation Output (-32, -34, -35, -37)	+10V ±3mV	*
Excitation Output (-31, -33, -36)	+3.333V ±2mV	*
Excitation Load Regulation	±5ppm/mA	*
Excitation Stability	±15ppm/°C	*
Half Bridge Voltage Level (-34)	NA	+5V ±1mV
Half Bridge Voltage Level (-33)	NA	+1.667V ±1mV
Isolated Excitation Protection		
Continuous	240Vrms max	*
Transient	ANSI/IEEE C37.90.1-1989	*
CMV, Input to Output		
Continuous	1500Vrms max	*
Transient	ANSI/IEEE C37.90.1-1989	*
CMR (50 or 60Hz)	160dB	*
NMR	95dB at 60Hz, 90dB at 50Hz	*
Accuracy[2]	±0.08% Span ±10µV RTI[3]	*
Nonlinearity	±0.02% Span	*
Stability		
Input Offset	±1µV/°C	*
Output Offset	±20µV/°C	*
Gain	±25ppm of Reading/°C	*
Noise		
Input, 0.1 to 10Hz	0.2µVrms	1µVrms
Output, 100kHz	200µVrms	*
Bandwidth, –3dB	4Hz	*
Response Time, 90% span	0.2s	*
Output Range	±5V	*
Output Resistance	50Ω	*
Output Protection	Continuous Short to Ground	*
Output Selection Time (to ±1mV of V_{OUT})	6µs at C_{load} = 0 to 2000pF	
Output Current Limit	±8mA	*
Output Enable Control		
Max Logic "0"	+0.8V	*
Min Logic "1"	+2.4V	*
Max Logic "1"	+36V	*
Input Current, "0,1"	0.5µA	*
Power Supply Voltage	+5VDC ±5%	*
Power Supply Current	170mA Full Exc. Load, 70mA No Exc. Load	*
Power Supply Sensitivity	±2µV/% RTI[3]	*
Mechanical Dimensions	2.28" x 2.26" x 0.60" (58mm x 57mm x 15mm)	*
Environmental		
Operating Temperature Range	–40°C to +85°C	*
Storage Temperature Range	–40°C to +85°C	*
Relative Humidity	0 to 95% Noncondensing	*
Emissions	EN50081-1, ISM Group 1, Class A (Radiated, Conducted)	*
Immunity	EN50082-1, ISM Group 1, Class A (ESD, RF, EFT)	*

FIGURE 2. Full Bridge Connection.

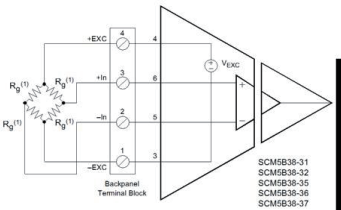

FIGURE 3. Half Bridge Connection.

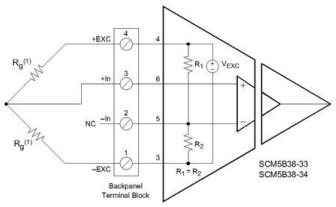

FIGURE 4. Quarter Bridge Connection.

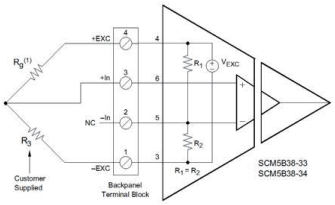

* Same as -31, -32, -35, -36, -37 modules.

NOTES: (1) Strain element. (2) Includes excitation error, nonlinearity, hysteresis and repeatability. (3) Referenced to input.

ORDERING INFORMATION

MODEL	INPUT BRIDGE TYPE	INPUT RANGE	EXCITATION	OUTPUT RANGE
SCM5B38-31	Full Bridge	100Ω to 10kΩ	3.333V at 3mV/V Sensitivity	–5V to +5V
SCM5B38-32	Full Bridge	300Ω to 10kΩ	10.0V at 3mV/V Sensitivity	–5V to +5V
SCM5B38-33	Half Bridge	100Ω to 10kΩ	3.333V at 3mV/V Sensitivity	–5V to +5V
SCM5B38-34	Half Bridge	300Ω to 10kΩ	10.0V at 3mV/V Sensitivity	–5V to +5V
SCM5B38-35	Full Bridge	300Ω to 10kΩ	10.0V at 2mV/V Sensitivity	–5V to +5V
SCM5B38-36	Full Bridge	100Ω to 10kΩ	3.333V at 10mV/V Sensitivity	–5V to +5V
SCM5B38-37	Full Bridge	300Ω to 10kΩ	10.0V at 10mV/V Sensitivity	–5V to +5V

Call 800-444-7644
For Information and Assistance

DATAFORTH® A Burr-Brown Company

Figure 7.8: SCM5B38 specifications

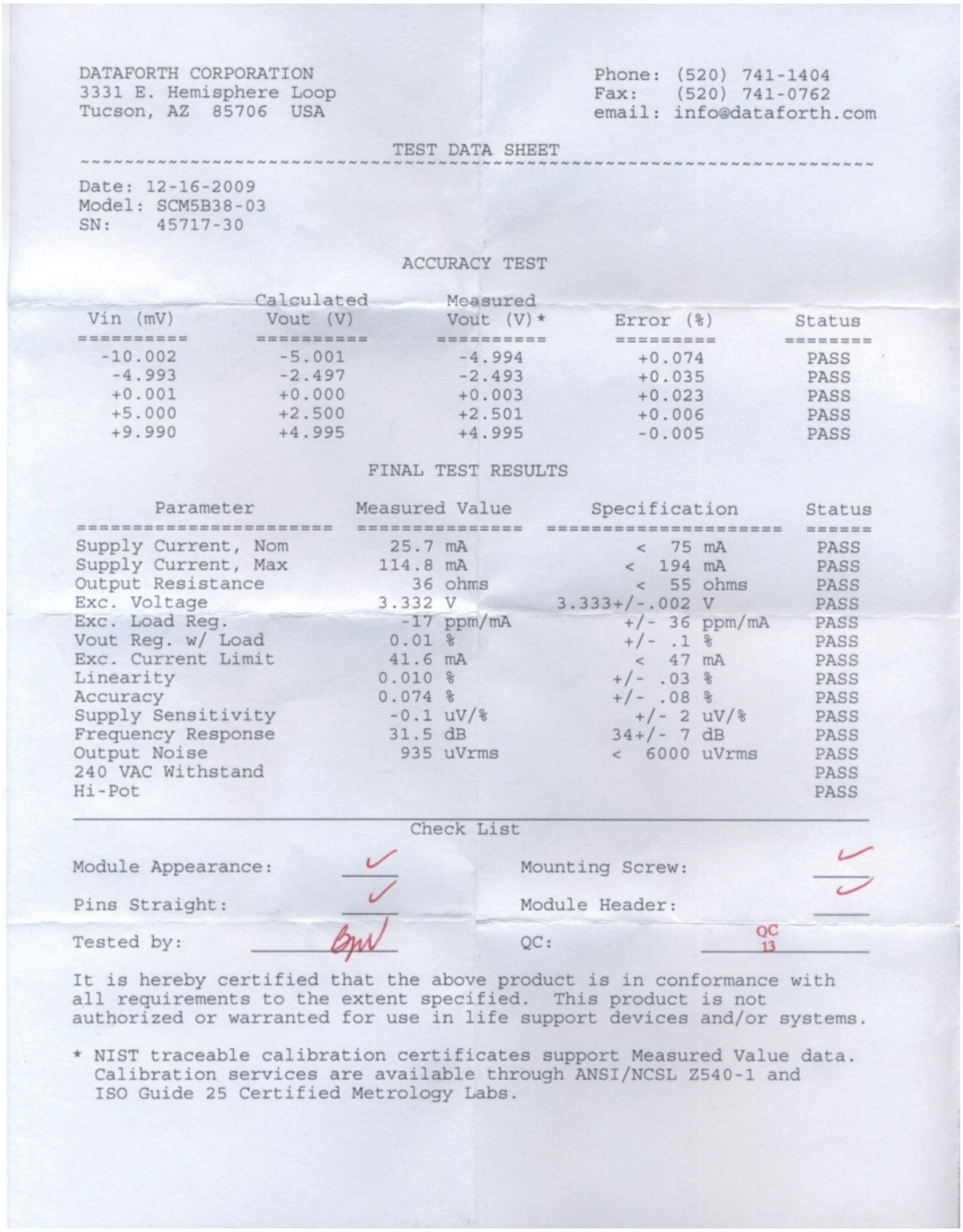

DATAFORTH CORPORATION
3331 E. Hemisphere Loop
Tucson, AZ 85706 USA

Phone: (520) 741-1404
Fax: (520) 741-0762
email: info@dataforth.com

TEST DATA SHEET

Date: 12-16-2009
Model: SCM5B38-03
SN: 45717-30

ACCURACY TEST

Vin (mV)	Calculated Vout (V)	Measured Vout (V)*	Error (%)	Status
-10.002	-5.001	-4.994	+0.074	PASS
-4.993	-2.497	-2.493	+0.035	PASS
+0.001	+0.000	+0.003	+0.023	PASS
+5.000	+2.500	+2.501	+0.006	PASS
+9.990	+4.995	+4.995	-0.005	PASS

FINAL TEST RESULTS

Parameter	Measured Value	Specification	Status
Supply Current, Nom	25.7 mA	< 75 mA	PASS
Supply Current, Max	114.8 mA	< 194 mA	PASS
Output Resistance	36 ohms	< 55 ohms	PASS
Exc. Voltage	3.332 V	3.333+/-.002 V	PASS
Exc. Load Reg.	-17 ppm/mA	+/- 36 ppm/mA	PASS
Vout Reg. w/ Load	0.01 %	+/- .1 %	PASS
Exc. Current Limit	41.6 mA	< 47 mA	PASS
Linearity	0.010 %	+/- .03 %	PASS
Accuracy	0.074 %	+/- .08 %	PASS
Supply Sensitivity	-0.1 uV/%	+/- 2 uV/%	PASS
Frequency Response	31.5 dB	34+/- 7 dB	PASS
Output Noise	935 uVrms	< 6000 uVrms	PASS
240 VAC Withstand			PASS
Hi-Pot			PASS

Check List

Module Appearance: ✓ Mounting Screw: ✓

Pins Straight: ✓ Module Header: ✓

Tested by: BW QC: QC 13

It is hereby certified that the above product is in conformance with all requirements to the extent specified. This product is not authorized or warranted for use in life support devices and/or systems.

* NIST traceable calibration certificates support Measured Value data. Calibration services are available through ANSI/NCSL Z540-1 and ISO Guide 25 Certified Metrology Labs.

Figure 7.9: Calibration record for channel Strain gauge rosette, SGR-1-X

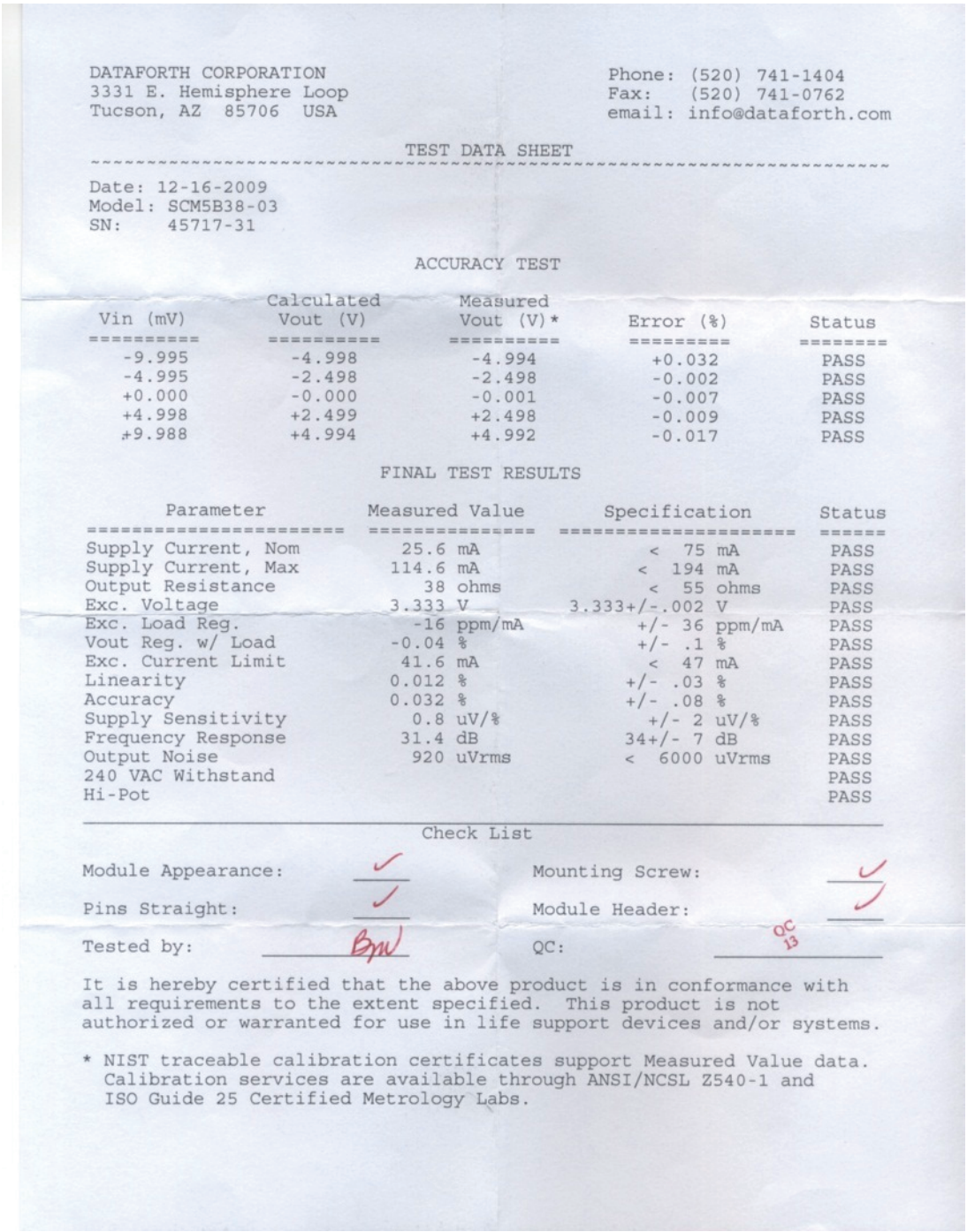

DATAFORTH CORPORATION
3331 E. Hemisphere Loop
Tucson, AZ 85706 USA

Phone: (520) 741-1404
Fax: (520) 741-0762
email: info@dataforth.com

TEST DATA SHEET

Date: 12-16-2009
Model: SCM5B38-03
SN: 45717-31

ACCURACY TEST

Vin (mV)	Calculated Vout (V)	Measured Vout (V)*	Error (%)	Status
-9.995	-4.998	-4.994	+0.032	PASS
-4.995	-2.498	-2.498	-0.002	PASS
+0.000	-0.000	-0.001	-0.007	PASS
+4.998	+2.499	+2.498	-0.009	PASS
+9.988	+4.994	+4.992	-0.017	PASS

FINAL TEST RESULTS

Parameter	Measured Value	Specification	Status
Supply Current, Nom	25.6 mA	< 75 mA	PASS
Supply Current, Max	114.6 mA	< 194 mA	PASS
Output Resistance	38 ohms	< 55 ohms	PASS
Exc. Voltage	3.333 V	3.333+/-.002 V	PASS
Exc. Load Reg.	-16 ppm/mA	+/- 36 ppm/mA	PASS
Vout Reg. w/ Load	-0.04 %	+/- .1 %	PASS
Exc. Current Limit	41.6 mA	< 47 mA	PASS
Linearity	0.012 %	+/- .03 %	PASS
Accuracy	0.032 %	+/- .08 %	PASS
Supply Sensitivity	0.8 uV/%	+/- 2 uV/%	PASS
Frequency Response	31.4 dB	34+/- 7 dB	PASS
Output Noise	920 uVrms	< 6000 uVrms	PASS
240 VAC Withstand			PASS
Hi-Pot			PASS

Check List

Module Appearance: ✓ Mounting Screw: ✓

Pins Straight: ✓ Module Header: ✓

Tested by: BJW QC: QC 13

It is hereby certified that the above product is in conformance with all requirements to the extent specified. This product is not authorized or warranted for use in life support devices and/or systems.

* NIST traceable calibration certificates support Measured Value data. Calibration services are available through ANSI/NCSL Z540-1 and ISO Guide 25 Certified Metrology Labs.

Figure 7.10: Calibration record for channel Strain gauge rosette, SGR-1-Y

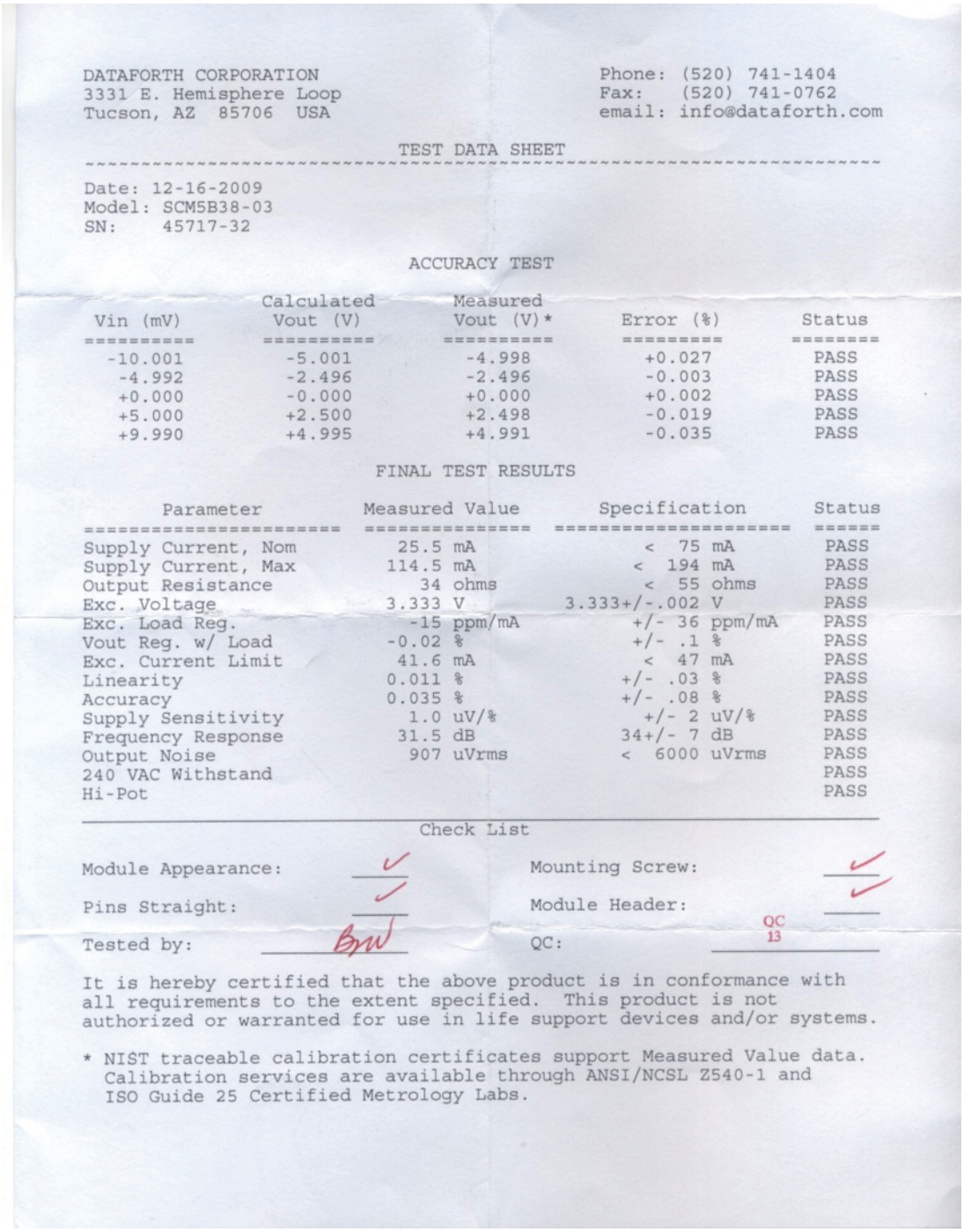

DATAFORTH CORPORATION
3331 E. Hemisphere Loop
Tucson, AZ 85706 USA

Phone: (520) 741-1404
Fax: (520) 741-0762
email: info@dataforth.com

TEST DATA SHEET

Date: 12-16-2009
Model: SCM5B38-03
SN: 45717-32

ACCURACY TEST

Vin (mV)	Calculated Vout (V)	Measured Vout (V)*	Error (%)	Status
-10.001	-5.001	-4.998	+0.027	PASS
-4.992	-2.496	-2.496	-0.003	PASS
+0.000	-0.000	+0.000	+0.002	PASS
+5.000	+2.500	+2.498	-0.019	PASS
+9.990	+4.995	+4.991	-0.035	PASS

FINAL TEST RESULTS

Parameter	Measured Value	Specification	Status
Supply Current, Nom	25.5 mA	< 75 mA	PASS
Supply Current, Max	114.5 mA	< 194 mA	PASS
Output Resistance	34 ohms	< 55 ohms	PASS
Exc. Voltage	3.333 V	3.333+/-.002 V	PASS
Exc. Load Reg.	-15 ppm/mA	+/- 36 ppm/mA	PASS
Vout Reg. w/ Load	-0.02 %	+/- .1 %	PASS
Exc. Current Limit	41.6 mA	< 47 mA	PASS
Linearity	0.011 %	+/- .03 %	PASS
Accuracy	0.035 %	+/- .08 %	PASS
Supply Sensitivity	1.0 uV/%	+/- 2 uV/%	PASS
Frequency Response	31.5 dB	34+/- 7 dB	PASS
Output Noise	907 uVrms	< 6000 uVrms	PASS
240 VAC Withstand			PASS
Hi-Pot			PASS

Check List

Module Appearance: ✓ Mounting Screw: ✓

Pins Straight: ✓ Module Header: ✓

Tested by: BW QC: QC 13

It is hereby certified that the above product is in conformance with all requirements to the extent specified. This product is not authorized or warranted for use in life support devices and/or systems.

* NIST traceable calibration certificates support Measured Value data. Calibration services are available through ANSI/NCSL Z540-1 and ISO Guide 25 Certified Metrology Labs.

Figure 7.11: Calibration record for channel Strain gauge rosette, SGR-1-Z

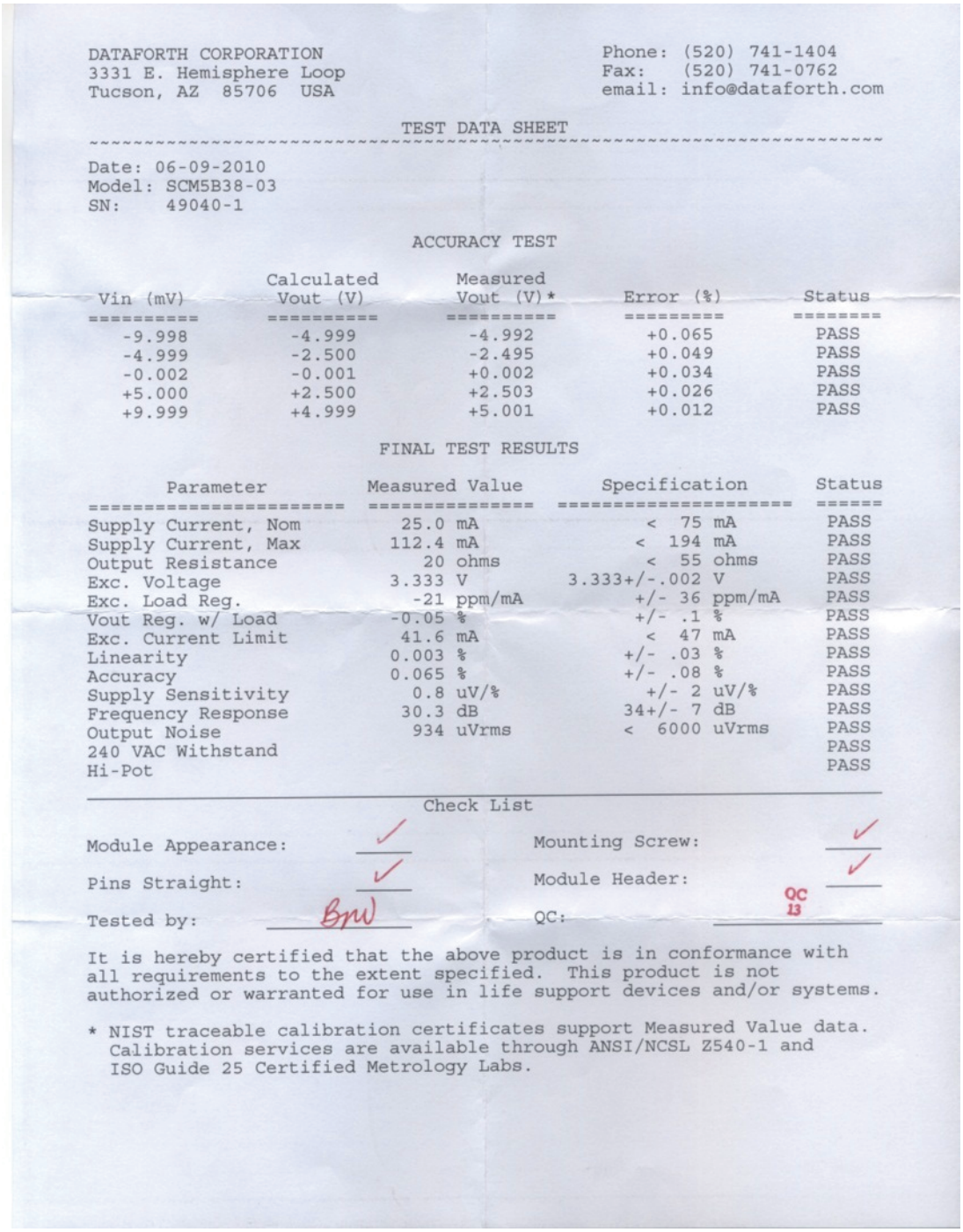

DATAFORTH CORPORATION
3331 E. Hemisphere Loop
Tucson, AZ 85706 USA

Phone: (520) 741-1404
Fax: (520) 741-0762
email: info@dataforth.com

TEST DATA SHEET

Date: 06-09-2010
Model: SCM5B38-03
SN: 49040-1

ACCURACY TEST

Vin (mV)	Calculated Vout (V)	Measured Vout (V)*	Error (%)	Status
-9.998	-4.999	-4.992	+0.065	PASS
-4.999	-2.500	-2.495	+0.049	PASS
-0.002	-0.001	+0.002	+0.034	PASS
+5.000	+2.500	+2.503	+0.026	PASS
+9.999	+4.999	+5.001	+0.012	PASS

FINAL TEST RESULTS

Parameter	Measured Value	Specification	Status
Supply Current, Nom	25.0 mA	< 75 mA	PASS
Supply Current, Max	112.4 mA	< 194 mA	PASS
Output Resistance	20 ohms	< 55 ohms	PASS
Exc. Voltage	3.333 V	3.333+/-.002 V	PASS
Exc. Load Reg.	-21 ppm/mA	+/- 36 ppm/mA	PASS
Vout Reg. w/ Load	-0.05 %	+/- .1 %	PASS
Exc. Current Limit	41.6 mA	< 47 mA	PASS
Linearity	0.003 %	+/- .03 %	PASS
Accuracy	0.065 %	+/- .08 %	PASS
Supply Sensitivity	0.8 uV/%	+/- 2 uV/%	PASS
Frequency Response	30.3 dB	34+/- 7 dB	PASS
Output Noise	934 uVrms	< 6000 uVrms	PASS
240 VAC Withstand			PASS
Hi-Pot			PASS

Check List

Module Appearance: ✓ Mounting Screw: ✓

Pins Straight: ✓ Module Header: ✓

Tested by: BW QC: QC 13

It is hereby certified that the above product is in conformance with all requirements to the extent specified. This product is not authorized or warranted for use in life support devices and/or systems.

* NIST traceable calibration certificates support Measured Value data. Calibration services are available through ANSI/NCSL Z540-1 and ISO Guide 25 Certified Metrology Labs.

Figure 7.12: Calibration record for channel Strain gauge rosette, SGR-2-X

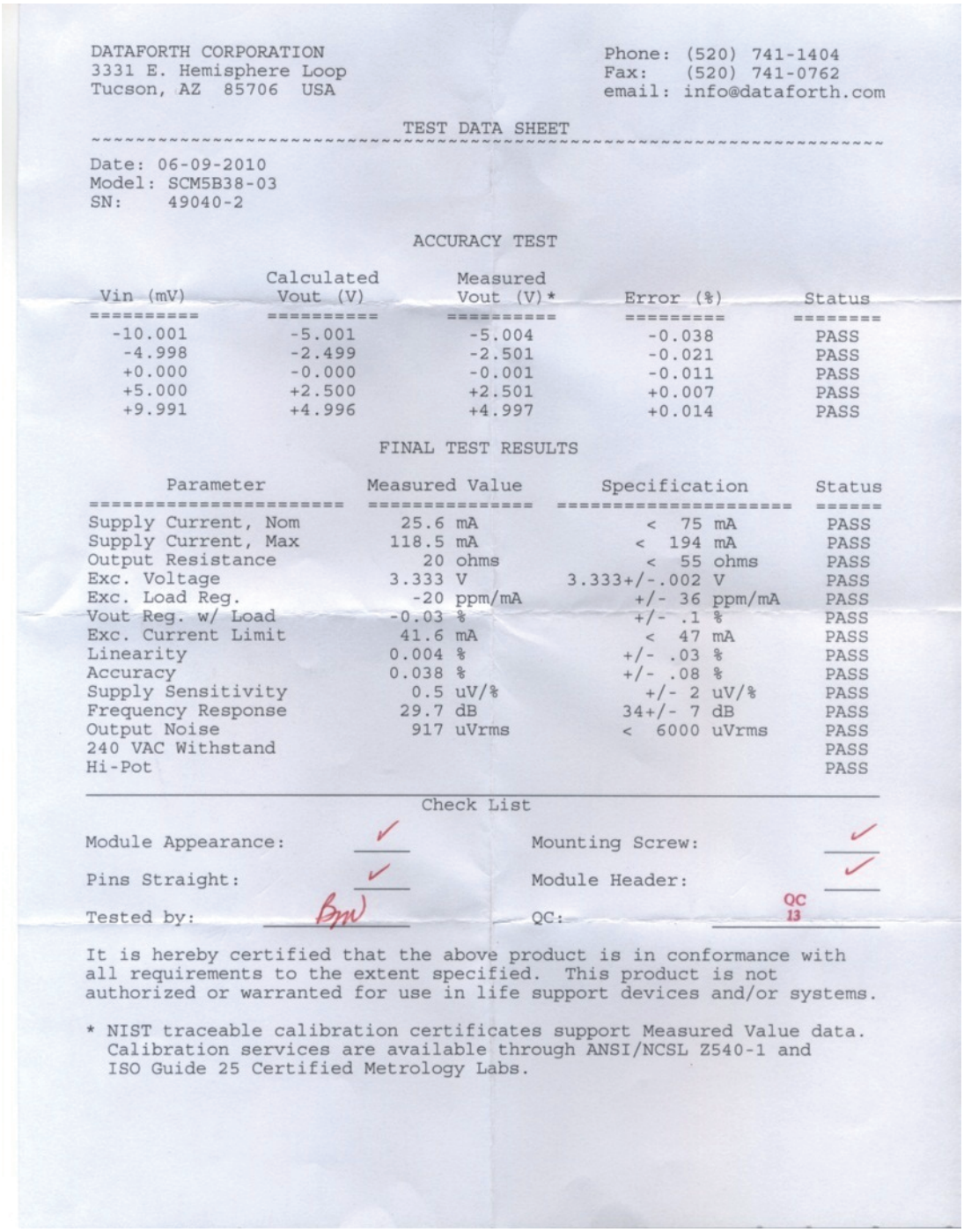

DATAFORTH CORPORATION
3331 E. Hemisphere Loop
Tucson, AZ 85706 USA

Phone: (520) 741-1404
Fax: (520) 741-0762
email: info@dataforth.com

TEST DATA SHEET

Date: 06-09-2010
Model: SCM5B38-03
SN: 49040-2

ACCURACY TEST

Vin (mV)	Calculated Vout (V)	Measured Vout (V)*	Error (%)	Status
-10.001	-5.001	-5.004	-0.038	PASS
-4.998	-2.499	-2.501	-0.021	PASS
+0.000	-0.000	-0.001	-0.011	PASS
+5.000	+2.500	+2.501	+0.007	PASS
+9.991	+4.996	+4.997	+0.014	PASS

FINAL TEST RESULTS

Parameter	Measured Value	Specification	Status
Supply Current, Nom	25.6 mA	< 75 mA	PASS
Supply Current, Max	118.5 mA	< 194 mA	PASS
Output Resistance	20 ohms	< 55 ohms	PASS
Exc. Voltage	3.333 V	3.333+/-.002 V	PASS
Exc. Load Reg.	-20 ppm/mA	+/- 36 ppm/mA	PASS
Vout Reg. w/ Load	-0.03 %	+/- .1 %	PASS
Exc. Current Limit	41.6 mA	< 47 mA	PASS
Linearity	0.004 %	+/- .03 %	PASS
Accuracy	0.038 %	+/- .08 %	PASS
Supply Sensitivity	0.5 uV/%	+/- 2 uV/%	PASS
Frequency Response	29.7 dB	34+/- 7 dB	PASS
Output Noise	917 uVrms	< 6000 uVrms	PASS
240 VAC Withstand			PASS
Hi-Pot			PASS

Check List

Module Appearance: ✓ Mounting Screw: ✓

Pins Straight: ✓ Module Header: ✓

Tested by: BW QC: QC 13

It is hereby certified that the above product is in conformance with all requirements to the extent specified. This product is not authorized or warranted for use in life support devices and/or systems.

* NIST traceable calibration certificates support Measured Value data. Calibration services are available through ANSI/NCSL Z540-1 and ISO Guide 25 Certified Metrology Labs.

Figure 7.13: Calibration record for channel Strain gauge rosette, SGR-2-Y

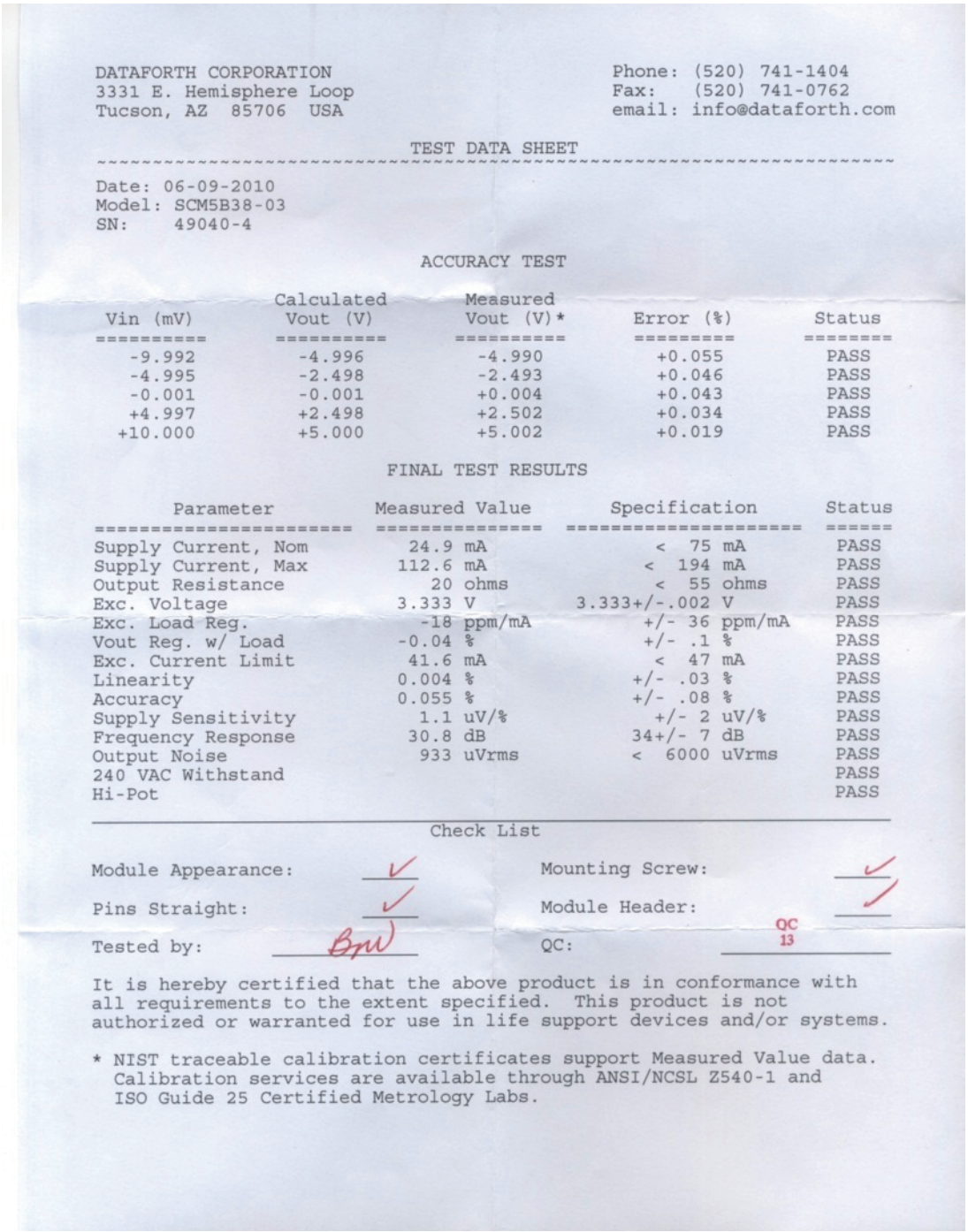

DATAFORTH CORPORATION
3331 E. Hemisphere Loop
Tucson, AZ 85706 USA

Phone: (520) 741-1404
Fax: (520) 741-0762
email: info@dataforth.com

TEST DATA SHEET

Date: 06-09-2010
Model: SCM5B38-03
SN: 49040-4

ACCURACY TEST

Vin (mV)	Calculated Vout (V)	Measured Vout (V)*	Error (%)	Status
-9.992	-4.996	-4.990	+0.055	PASS
-4.995	-2.498	-2.493	+0.046	PASS
-0.001	-0.001	+0.004	+0.043	PASS
+4.997	+2.498	+2.502	+0.034	PASS
+10.000	+5.000	+5.002	+0.019	PASS

FINAL TEST RESULTS

Parameter	Measured Value	Specification	Status
Supply Current, Nom	24.9 mA	< 75 mA	PASS
Supply Current, Max	112.6 mA	< 194 mA	PASS
Output Resistance	20 ohms	< 55 ohms	PASS
Exc. Voltage	3.333 V	3.333+/-.002 V	PASS
Exc. Load Reg.	-18 ppm/mA	+/- 36 ppm/mA	PASS
Vout Reg. w/ Load	-0.04 %	+/- .1 %	PASS
Exc. Current Limit	41.6 mA	< 47 mA	PASS
Linearity	0.004 %	+/- .03 %	PASS
Accuracy	0.055 %	+/- .08 %	PASS
Supply Sensitivity	1.1 uV/%	+/- 2 uV/%	PASS
Frequency Response	30.8 dB	34+/- 7 dB	PASS
Output Noise	933 uVrms	< 6000 uVrms	PASS
240 VAC Withstand			PASS
Hi-Pot			PASS

Check List

Module Appearance: ✓ Mounting Screw: ✓

Pins Straight: ✓ Module Header: ✓

Tested by: BW QC: QC 13

It is hereby certified that the above product is in conformance with all requirements to the extent specified. This product is not authorized or warranted for use in life support devices and/or systems.

* NIST traceable calibration certificates support Measured Value data. Calibration services are available through ANSI/NCSL Z540-1 and ISO Guide 25 Certified Metrology Labs.

Figure 7.14: Calibration record for channel Strain gauge rosette, SGR-2-Z

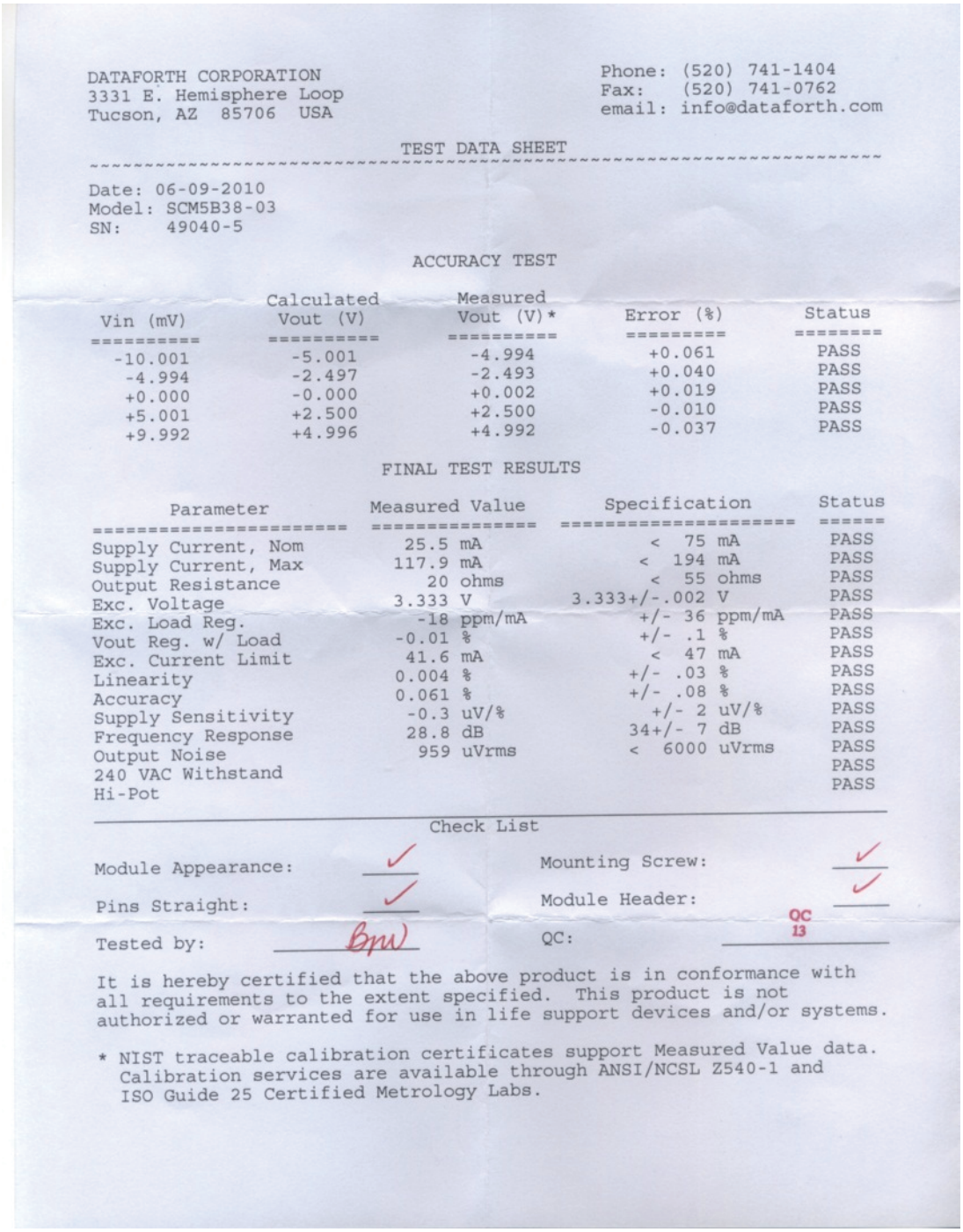

DATAFORTH CORPORATION
3331 E. Hemisphere Loop
Tucson, AZ 85706 USA

Phone: (520) 741-1404
Fax: (520) 741-0762
email: info@dataforth.com

TEST DATA SHEET

Date: 06-09-2010
Model: SCM5B38-03
SN: 49040-5

ACCURACY TEST

Vin (mV)	Calculated Vout (V)	Measured Vout (V)*	Error (%)	Status
-10.001	-5.001	-4.994	+0.061	PASS
-4.994	-2.497	-2.493	+0.040	PASS
+0.000	-0.000	+0.002	+0.019	PASS
+5.001	+2.500	+2.500	-0.010	PASS
+9.992	+4.996	+4.992	-0.037	PASS

FINAL TEST RESULTS

Parameter	Measured Value	Specification	Status
Supply Current, Nom	25.5 mA	< 75 mA	PASS
Supply Current, Max	117.9 mA	< 194 mA	PASS
Output Resistance	20 ohms	< 55 ohms	PASS
Exc. Voltage	3.333 V	3.333+/-.002 V	PASS
Exc. Load Reg.	-18 ppm/mA	+/- 36 ppm/mA	PASS
Vout Reg. w/ Load	-0.01 %	+/- .1 %	PASS
Exc. Current Limit	41.6 mA	< 47 mA	PASS
Linearity	0.004 %	+/- .03 %	PASS
Accuracy	0.061 %	+/- .08 %	PASS
Supply Sensitivity	-0.3 uV/%	+/- 2 uV/%	PASS
Frequency Response	28.8 dB	34+/- 7 dB	PASS
Output Noise	959 uVrms	< 6000 uVrms	PASS
240 VAC Withstand			PASS
Hi-Pot			PASS

Check List

Module Appearance: ✓ Mounting Screw: ✓

Pins Straight: ✓ Module Header: ✓

Tested by: BPW QC: QC 13

It is hereby certified that the above product is in conformance with all requirements to the extent specified. This product is not authorized or warranted for use in life support devices and/or systems.

* NIST traceable calibration certificates support Measured Value data. Calibration services are available through ANSI/NCSL Z540-1 and ISO Guide 25 Certified Metrology Labs.

Figure 7.15: Calibration record for channel Strain gauge rosette, SGR-3-X

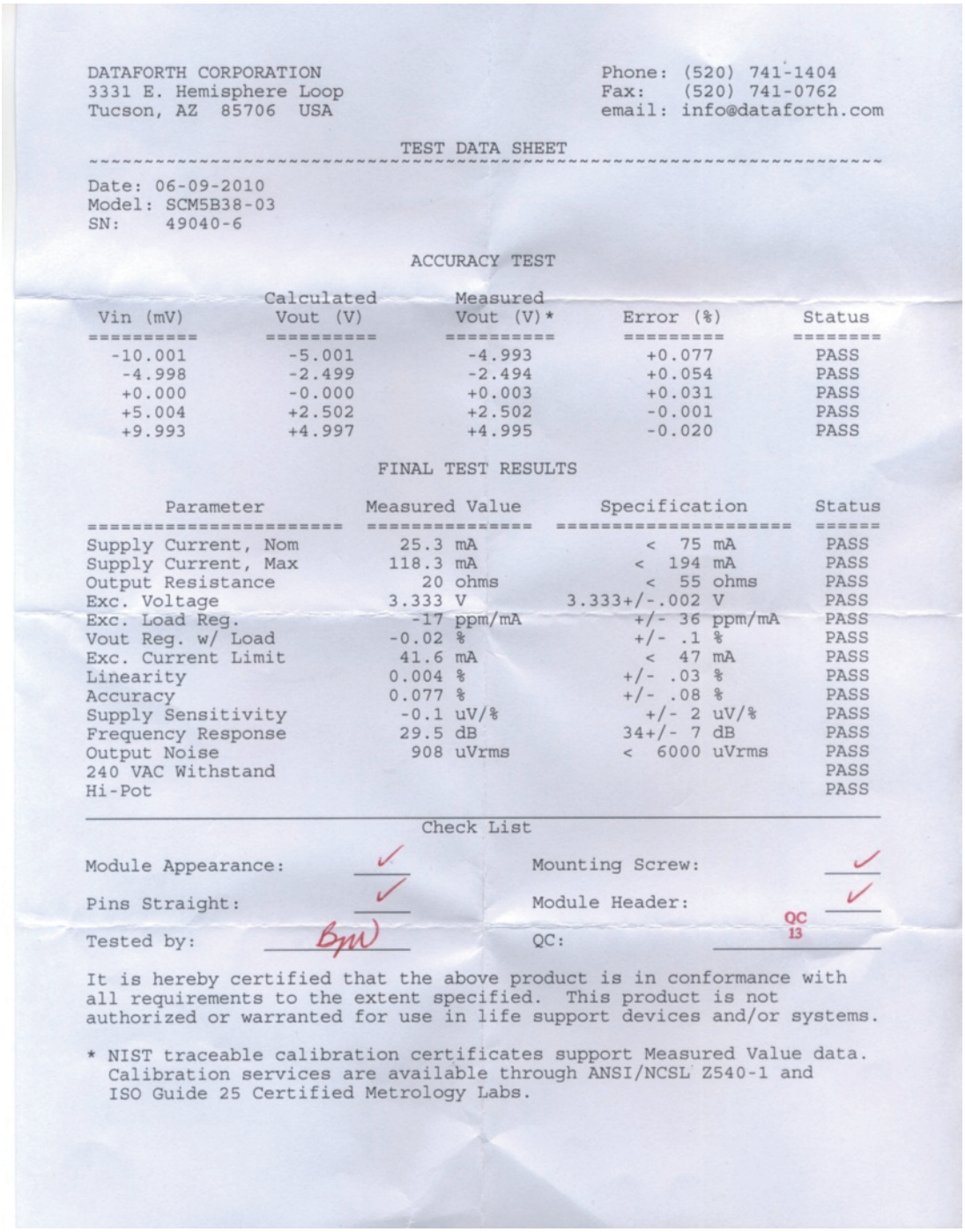

DATAFORTH CORPORATION
3331 E. Hemisphere Loop
Tucson, AZ 85706 USA

Phone: (520) 741-1404
Fax: (520) 741-0762
email: info@dataforth.com

TEST DATA SHEET

Date: 06-09-2010
Model: SCM5B38-03
SN: 49040-6

ACCURACY TEST

Vin (mV)	Calculated Vout (V)	Measured Vout (V)*	Error (%)	Status
-10.001	-5.001	-4.993	+0.077	PASS
-4.998	-2.499	-2.494	+0.054	PASS
+0.000	-0.000	+0.003	+0.031	PASS
+5.004	+2.502	+2.502	-0.001	PASS
+9.993	+4.997	+4.995	-0.020	PASS

FINAL TEST RESULTS

Parameter	Measured Value	Specification	Status
Supply Current, Nom	25.3 mA	< 75 mA	PASS
Supply Current, Max	118.3 mA	< 194 mA	PASS
Output Resistance	20 ohms	< 55 ohms	PASS
Exc. Voltage	3.333 V	3.333+/-.002 V	PASS
Exc. Load Reg.	-17 ppm/mA	+/- 36 ppm/mA	PASS
Vout Reg. w/ Load	-0.02 %	+/- .1 %	PASS
Exc. Current Limit	41.6 mA	< 47 mA	PASS
Linearity	0.004 %	+/- .03 %	PASS
Accuracy	0.077 %	+/- .08 %	PASS
Supply Sensitivity	-0.1 uV/%	+/- 2 uV/%	PASS
Frequency Response	29.5 dB	34+/- 7 dB	PASS
Output Noise	908 uVrms	< 6000 uVrms	PASS
240 VAC Withstand			PASS
Hi-Pot			PASS

Check List

Module Appearance: ✓ Mounting Screw: ✓

Pins Straight: ✓ Module Header: ✓

Tested by: BW QC: QC 13

It is hereby certified that the above product is in conformance with all requirements to the extent specified. This product is not authorized or warranted for use in life support devices and/or systems.

* NIST traceable calibration certificates support Measured Value data. Calibration services are available through ANSI/NCSL Z540-1 and ISO Guide 25 Certified Metrology Labs.

Figure 7.16: Calibration record for channel Strain gauge rosette, SGR-3-Y

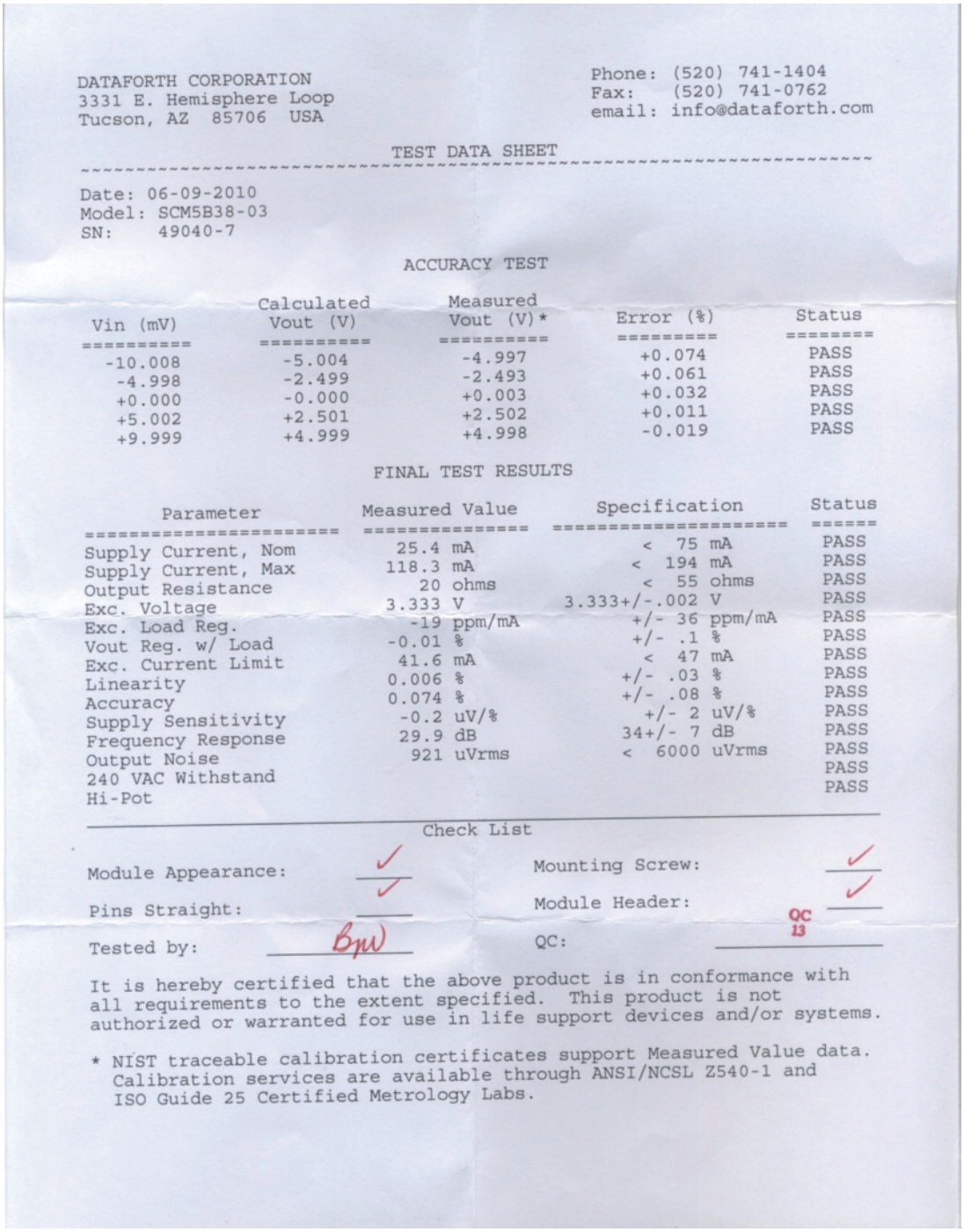

DATAFORTH CORPORATION
3331 E. Hemisphere Loop
Tucson, AZ 85706 USA

Phone: (520) 741-1404
Fax: (520) 741-0762
email: info@dataforth.com

TEST DATA SHEET

Date: 06-09-2010
Model: SCM5B38-03
SN: 49040-7

ACCURACY TEST

Vin (mV)	Calculated Vout (V)	Measured Vout (V)*	Error (%)	Status
-10.008	-5.004	-4.997	+0.074	PASS
-4.998	-2.499	-2.493	+0.061	PASS
+0.000	-0.000	+0.003	+0.032	PASS
+5.002	+2.501	+2.502	+0.011	PASS
+9.999	+4.999	+4.998	-0.019	PASS

FINAL TEST RESULTS

Parameter	Measured Value	Specification	Status
Supply Current, Nom	25.4 mA	< 75 mA	PASS
Supply Current, Max	118.3 mA	< 194 mA	PASS
Output Resistance	20 ohms	< 55 ohms	PASS
Exc. Voltage	3.333 V	3.333+/-.002 V	PASS
Exc. Load Reg.	-19 ppm/mA	+/- 36 ppm/mA	PASS
Vout Reg. w/ Load	-0.01 %	+/- .1 %	PASS
Exc. Current Limit	41.6 mA	< 47 mA	PASS
Linearity	0.006 %	+/- .03 %	PASS
Accuracy	0.074 %	+/- .08 %	PASS
Supply Sensitivity	-0.2 uV/%	+/- 2 uV/%	PASS
Frequency Response	29.9 dB	34+/- 7 dB	PASS
Output Noise	921 uVrms	< 6000 uVrms	PASS
240 VAC Withstand			PASS
Hi-Pot			PASS

Check List

Module Appearance: ✓
Mounting Screw: ✓
Pins Straight: ✓
Module Header: ✓
Tested by: BW
QC: QC 13

It is hereby certified that the above product is in conformance with all requirements to the extent specified. This product is not authorized or warranted for use in life support devices and/or systems.

* NIST traceable calibration certificates support Measured Value data. Calibration services are available through ANSI/NCSL Z540-1 and ISO Guide 25 Certified Metrology Labs.

Figure 7.17: Calibration record for channel Strain gauge rosette, SGR-3-Z

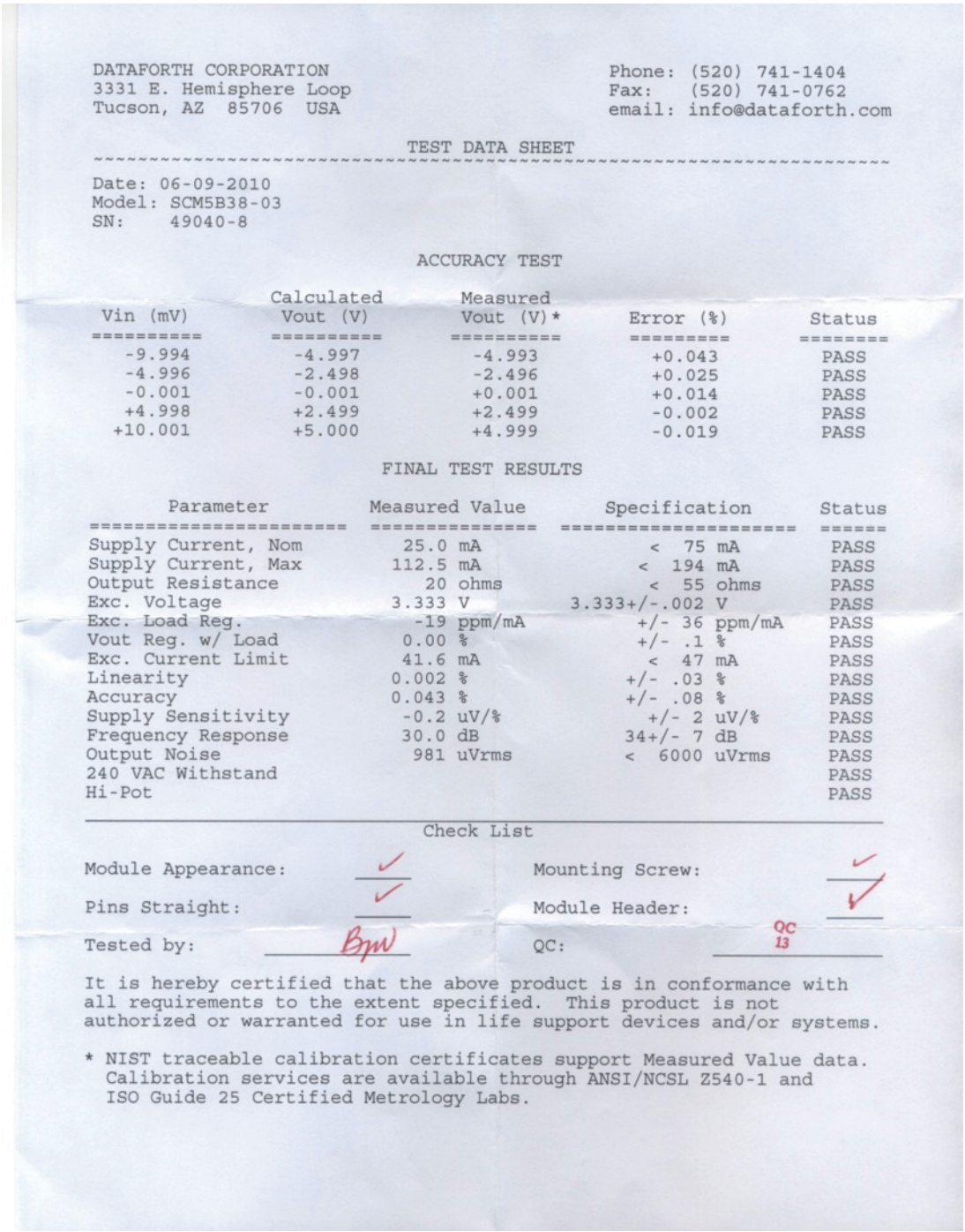

DATAFORTH CORPORATION
3331 E. Hemisphere Loop
Tucson, AZ 85706 USA

Phone: (520) 741-1404
Fax: (520) 741-0762
email: info@dataforth.com

TEST DATA SHEET

Date: 06-09-2010
Model: SCM5B38-03
SN: 49040-8

ACCURACY TEST

Vin (mV)	Calculated Vout (V)	Measured Vout (V)*	Error (%)	Status
-9.994	-4.997	-4.993	+0.043	PASS
-4.996	-2.498	-2.496	+0.025	PASS
-0.001	-0.001	+0.001	+0.014	PASS
+4.998	+2.499	+2.499	-0.002	PASS
+10.001	+5.000	+4.999	-0.019	PASS

FINAL TEST RESULTS

Parameter	Measured Value	Specification	Status
Supply Current, Nom	25.0 mA	< 75 mA	PASS
Supply Current, Max	112.5 mA	< 194 mA	PASS
Output Resistance	20 ohms	< 55 ohms	PASS
Exc. Voltage	3.333 V	3.333+/-.002 V	PASS
Exc. Load Reg.	-19 ppm/mA	+/- 36 ppm/mA	PASS
Vout Reg. w/ Load	0.00 %	+/- .1 %	PASS
Exc. Current Limit	41.6 mA	< 47 mA	PASS
Linearity	0.002 %	+/- .03 %	PASS
Accuracy	0.043 %	+/- .08 %	PASS
Supply Sensitivity	-0.2 uV/%	+/- 2 uV/%	PASS
Frequency Response	30.0 dB	34+/- 7 dB	PASS
Output Noise	981 uVrms	< 6000 uVrms	PASS
240 VAC Withstand			PASS
Hi-Pot			PASS

Check List

Module Appearance: ✓ Mounting Screw: ✓

Pins Straight: ✓ Module Header: ✓

Tested by: BJW QC: QC 13

It is hereby certified that the above product is in conformance with all requirements to the extent specified. This product is not authorized or warranted for use in life support devices and/or systems.

* NIST traceable calibration certificates support Measured Value data. Calibration services are available through ANSI/NCSL Z540-1 and ISO Guide 25 Certified Metrology Labs.

Figure 7.18: Calibration record for channel Strain gauge rosette, SGR-4-X

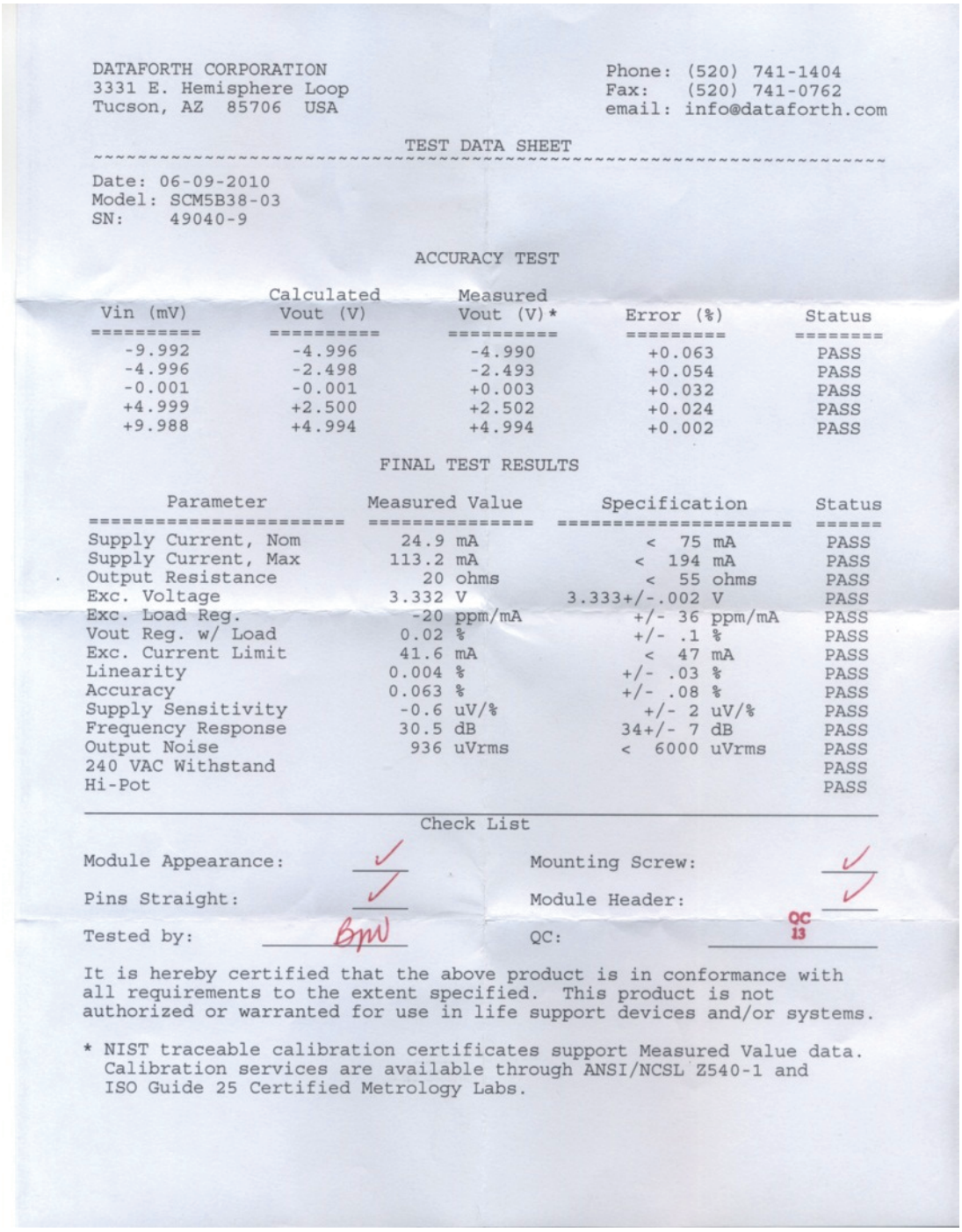

DATAFORTH CORPORATION
3331 E. Hemisphere Loop
Tucson, AZ 85706 USA

Phone: (520) 741-1404
Fax: (520) 741-0762
email: info@dataforth.com

TEST DATA SHEET

Date: 06-09-2010
Model: SCM5B38-03
SN: 49040-9

ACCURACY TEST

Vin (mV)	Calculated Vout (V)	Measured Vout (V)*	Error (%)	Status
-9.992	-4.996	-4.990	+0.063	PASS
-4.996	-2.498	-2.493	+0.054	PASS
-0.001	-0.001	+0.003	+0.032	PASS
+4.999	+2.500	+2.502	+0.024	PASS
+9.988	+4.994	+4.994	+0.002	PASS

FINAL TEST RESULTS

Parameter	Measured Value	Specification	Status
Supply Current, Nom	24.9 mA	< 75 mA	PASS
Supply Current, Max	113.2 mA	< 194 mA	PASS
Output Resistance	20 ohms	< 55 ohms	PASS
Exc. Voltage	3.332 V	3.333+/-.002 V	PASS
Exc. Load Reg.	-20 ppm/mA	+/- 36 ppm/mA	PASS
Vout Reg. w/ Load	0.02 %	+/- .1 %	PASS
Exc. Current Limit	41.6 mA	< 47 mA	PASS
Linearity	0.004 %	+/- .03 %	PASS
Accuracy	0.063 %	+/- .08 %	PASS
Supply Sensitivity	-0.6 uV/%	+/- 2 uV/%	PASS
Frequency Response	30.5 dB	34+/- 7 dB	PASS
Output Noise	936 uVrms	< 6000 uVrms	PASS
240 VAC Withstand			PASS
Hi-Pot			PASS

Check List

Module Appearance: ✓ Mounting Screw: ✓

Pins Straight: ✓ Module Header: ✓

Tested by: BW QC: QC 13

It is hereby certified that the above product is in conformance with all requirements to the extent specified. This product is not authorized or warranted for use in life support devices and/or systems.

* NIST traceable calibration certificates support Measured Value data. Calibration services are available through ANSI/NCSL Z540-1 and ISO Guide 25 Certified Metrology Labs.

Figure 7.19: Calibration record for channel Strain gauge rosette, SGR-4-Y

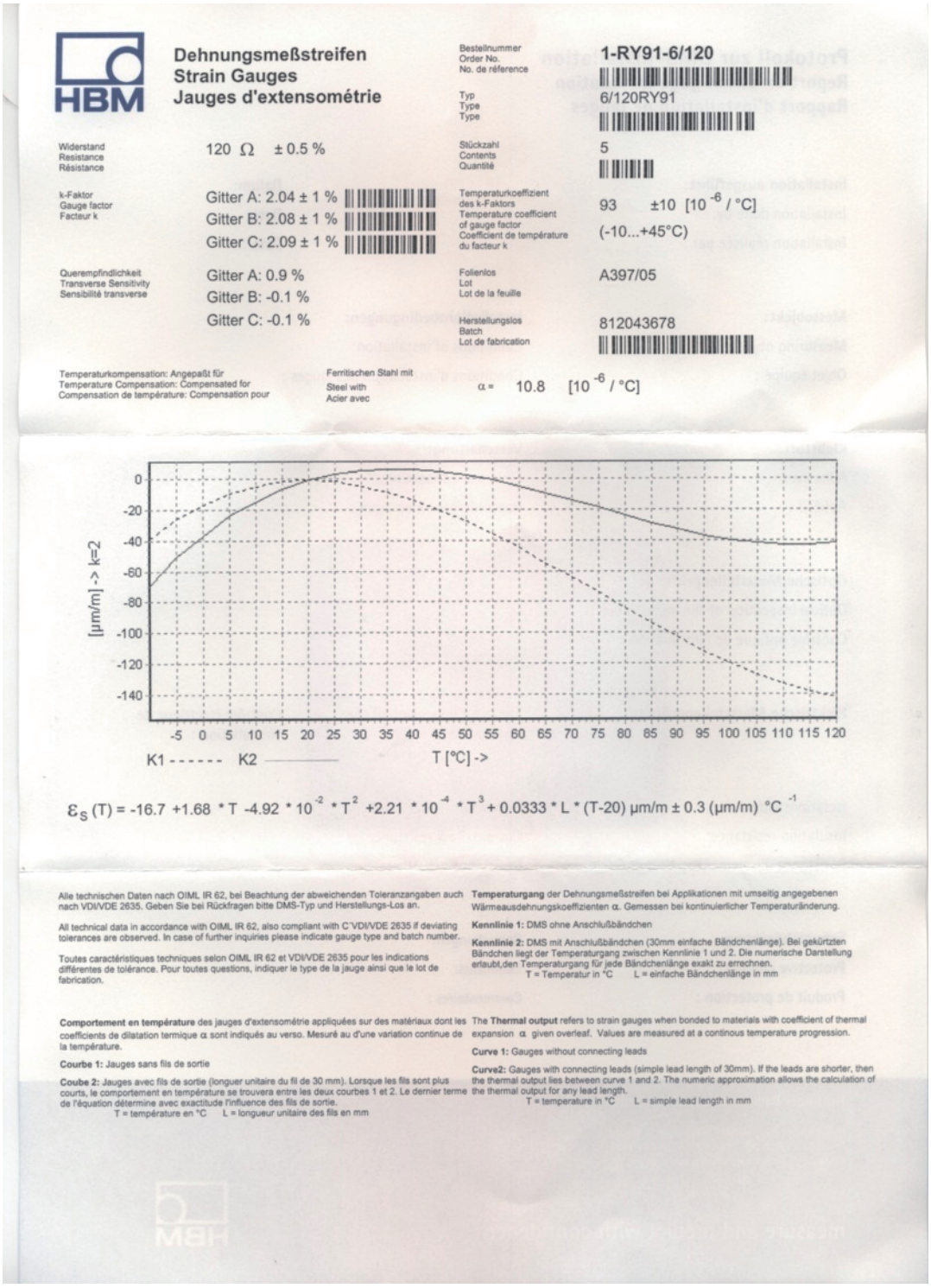

Figure 7.20: Calibration record for strain gauge rosette, SGR in terms of temperature

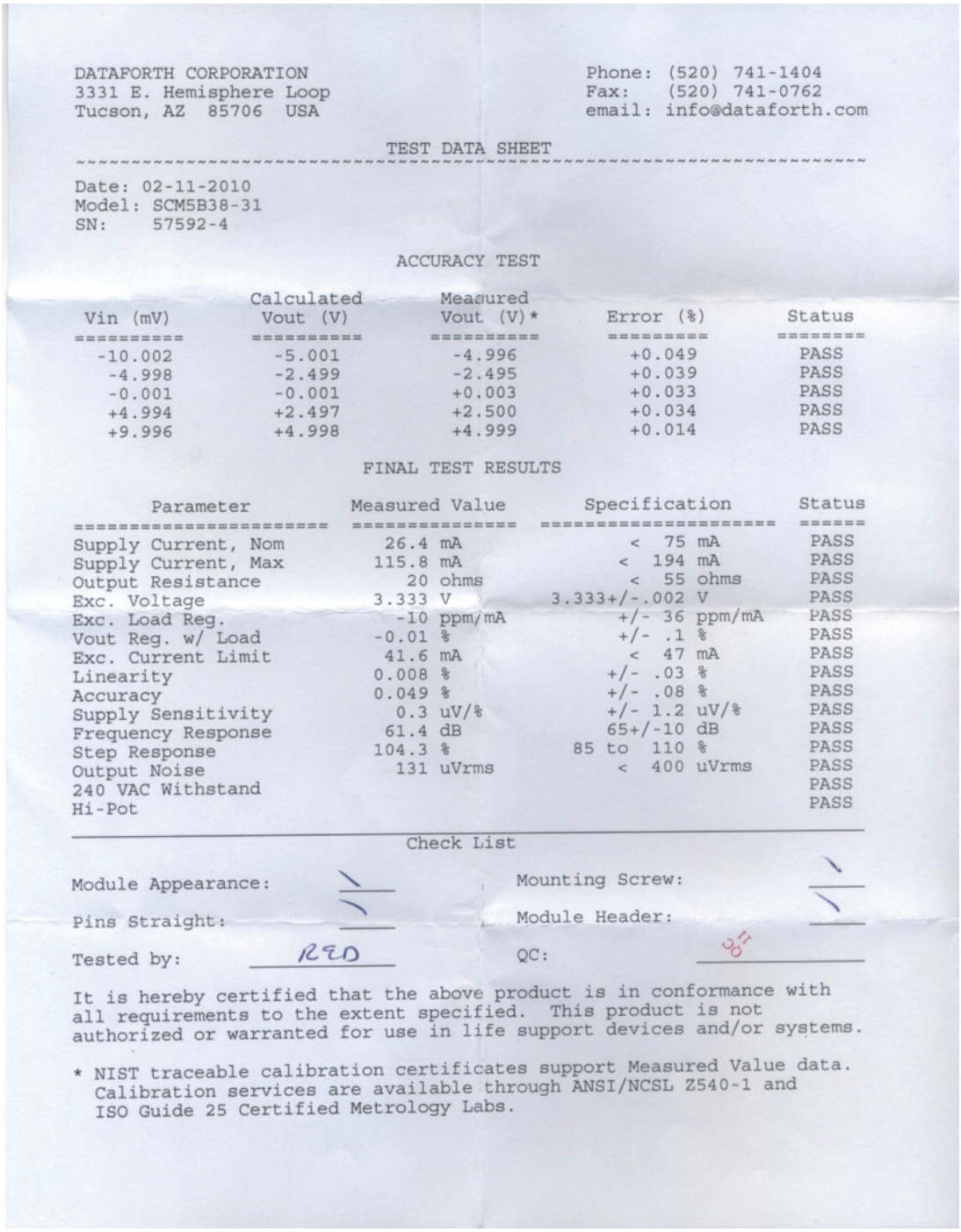

DATAFORTH CORPORATION
3331 E. Hemisphere Loop
Tucson, AZ 85706 USA

Phone: (520) 741-1404
Fax: (520) 741-0762
email: info@dataforth.com

TEST DATA SHEET

Date: 02-11-2010
Model: SCM5B38-31
SN: 57592-4

ACCURACY TEST

Vin (mV)	Calculated Vout (V)	Measured Vout (V)*	Error (%)	Status
-10.002	-5.001	-4.996	+0.049	PASS
-4.998	-2.499	-2.495	+0.039	PASS
-0.001	-0.001	+0.003	+0.033	PASS
+4.994	+2.497	+2.500	+0.034	PASS
+9.996	+4.998	+4.999	+0.014	PASS

FINAL TEST RESULTS

Parameter	Measured Value	Specification	Status
Supply Current, Nom	26.4 mA	< 75 mA	PASS
Supply Current, Max	115.8 mA	< 194 mA	PASS
Output Resistance	20 ohms	< 55 ohms	PASS
Exc. Voltage	3.333 V	3.333+/-.002 V	PASS
Exc. Load Reg.	-10 ppm/mA	+/- 36 ppm/mA	PASS
Vout Reg. w/ Load	-0.01 %	+/- .1 %	PASS
Exc. Current Limit	41.6 mA	< 47 mA	PASS
Linearity	0.008 %	+/- .03 %	PASS
Accuracy	0.049 %	+/- .08 %	PASS
Supply Sensitivity	0.3 uV/%	+/- 1.2 uV/%	PASS
Frequency Response	61.4 dB	65+/-10 dB	PASS
Step Response	104.3 %	85 to 110 %	PASS
Output Noise	131 uVrms	< 400 uVrms	PASS
240 VAC Withstand			PASS
Hi-Pot			PASS

Check List

Module Appearance: ✓ Mounting Screw: ✓

Pins Straight: ✓ Module Header: ✓

Tested by: REO QC: 2/11

It is hereby certified that the above product is in conformance with all requirements to the extent specified. This product is not authorized or warranted for use in life support devices and/or systems.

* NIST traceable calibration certificates support Measured Value data. Calibration services are available through ANSI/NCSL Z540-1 and ISO Guide 25 Certified Metrology Labs.

Figure 7.21: Calibration record for channel axial strain gauge, SG-01

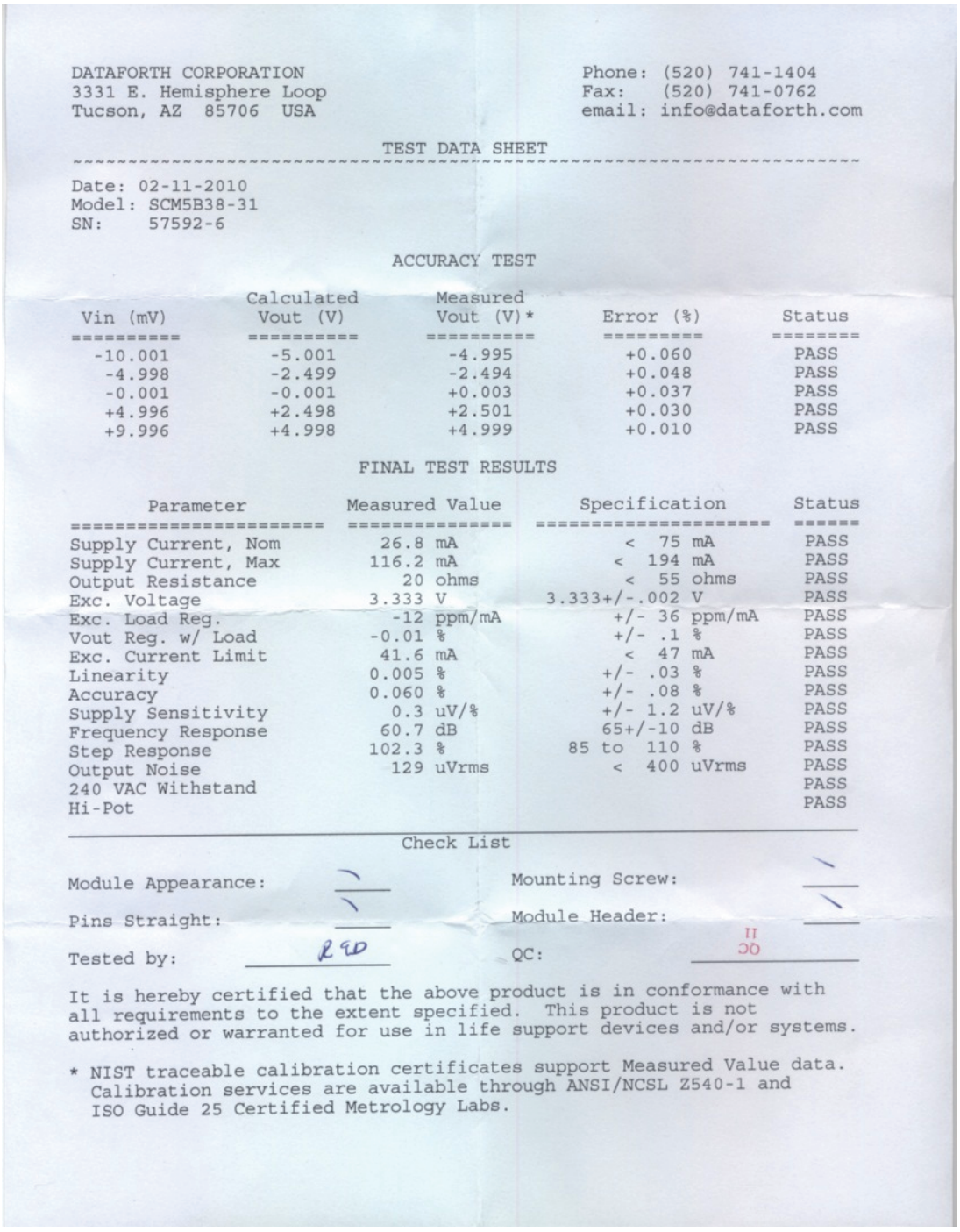

DATAFORTH CORPORATION
3331 E. Hemisphere Loop
Tucson, AZ 85706 USA

Phone: (520) 741-1404
Fax: (520) 741-0762
email: info@dataforth.com

TEST DATA SHEET

Date: 02-11-2010
Model: SCM5B38-31
SN: 57592-6

ACCURACY TEST

Vin (mV)	Calculated Vout (V)	Measured Vout (V)*	Error (%)	Status
-10.001	-5.001	-4.995	+0.060	PASS
-4.998	-2.499	-2.494	+0.048	PASS
-0.001	-0.001	+0.003	+0.037	PASS
+4.996	+2.498	+2.501	+0.030	PASS
+9.996	+4.998	+4.999	+0.010	PASS

FINAL TEST RESULTS

Parameter	Measured Value	Specification	Status
Supply Current, Nom	26.8 mA	< 75 mA	PASS
Supply Current, Max	116.2 mA	< 194 mA	PASS
Output Resistance	20 ohms	< 55 ohms	PASS
Exc. Voltage	3.333 V	3.333+/-.002 V	PASS
Exc. Load Reg.	-12 ppm/mA	+/- 36 ppm/mA	PASS
Vout Reg. w/ Load	-0.01 %	+/- .1 %	PASS
Exc. Current Limit	41.6 mA	< 47 mA	PASS
Linearity	0.005 %	+/- .03 %	PASS
Accuracy	0.060 %	+/- .08 %	PASS
Supply Sensitivity	0.3 uV/%	+/- 1.2 uV/%	PASS
Frequency Response	60.7 dB	65+/-10 dB	PASS
Step Response	102.3 %	85 to 110 %	PASS
Output Noise	129 uVrms	< 400 uVrms	PASS
240 VAC Withstand			PASS
Hi-Pot			PASS

Check List

Module Appearance: ✓ Mounting Screw: ✓

Pins Straight: ✓ Module Header: ✓

Tested by: RGD QC: JO

It is hereby certified that the above product is in conformance with all requirements to the extent specified. This product is not authorized or warranted for use in life support devices and/or systems.

* NIST traceable calibration certificates support Measured Value data. Calibration services are available through ANSI/NCSL Z540-1 and ISO Guide 25 Certified Metrology Labs.

Figure 7.22: Calibration record for channel axial strain gauge, SG-02